LIFE SCIENCE PHD MEETING 2026

08.–10. April

Meeting Organization

This meeting is organized by:

Lena Denk, Konstantin Siegmann, Maria Troppmair

Jan Frederik Ahrend, Magdalena Fickl, Malou Hanisch, Martina Höllwarth, Adriana Knoll, Maria Peteinareli, Mitja Amon Posch, Eva Rauch, Norbert Redlinger, Jakob Scheler, Francesca Silvagni

Design by Hannah Pirchl

Mission Statement

The Life Science PhD Meeting provides a platform for the whole Life Science community, from undergraduate students up to PIs, to share their knowledge, experience and critical thinking. Furthermore, we want to encourage all students to present their research to train this important skill for international conferences.

We are proud to present excellent scientific work from numerous fields, which is only possible due to the huge variety of scientific interests of the groups represented in the meeting. Therefore, the organizing committee would like to take the opportunity to thank the research programs and their coordinators making it possible to organize this meeting for all the Life Scientists in Innsbruck:

- MCBD (Matthias Erlacher, Natascha Kleiter, Guido Wollmann)
- Clinical PhD program (Bernhard Glodny)
- Neuroscience PhD Program (Christoph Schwarzer, Kai Kummer)
- CavX (Petronel Tuluc)
- IGDT (Wolfgang Freyrsinger, Elke Gizewski, Clemens Decristoforo)
- IIT & MYCOS (Timon Adolph, Michaela Lackner)

Promega

Measure Cell **Proliferation** with Confidence

Lumit® hKi-67 Immunoassay

Tired of proliferation assays influenced by metabolic changes or complex wash steps? The Lumit® hKi-67 Immunoassay enables precise, metabolism-independent measurement of cell proliferation by directly detecting hKi-67 expression.

Why Lumit® hKi-67 Immunoassay for Cell Proliferation?

- Well-established Ki-67 marker for true proliferation readout
- Metabolism-independent
- Simple, no-wash add-and-read workflow
- Reliably distinguish antiproliferative effects from cell death
- Earlier readout for faster decision-making

Scan for more Info

Visit us at the booth to learn more
www.promega.com/Lumit-hKi-67

Contents

6-7	Program
8	Keynote Speaker
10-11	Selected Short Talks
13-39	Short Talk Abstracts
41-220	Poster Abstracts

Schon gehört? MED-EL sucht Sie.

MED-EL ermöglicht Menschen, das Leben wieder zu hören. Werden Sie Teil dieses weltweit tätigen Hörtechnologie-Unternehmens! Bewerben Sie sich jetzt unter jobs.medel.com

hearLIFE

MED-EL Medical Electronics
Fürstenweg 77a, 6020 Innsbruck | Austria

medel.com

*Registrations open on April 7th and 8th (9am-12pm on both days)

Wednesday April 8th

09:00 - 13:00	M.EG. 180	Imaging Seminar Series		

Thursday April 9th

08:30 - 10:30	M.EG. 180	Opening Day 2		
	M.EG. 180	**Short talk session 1**	Luca Szabó Angelina Ananich	Chair
	L.EG. 220	Project Presentations I Clinical PhD	Maria Troppmair	Chair
10:30 - 11:00	Aula	Coffee break with snacks		
11:00 - 11:45	M.EG. 180	Anna Heidbreder – Promoting Brain Health Through Sleep	Lena Denk Maria Troppmair	Chair
11:45 - 13:30	M.EG. 180	**Short talk session 2**	Ryoichi Taguchi Ervin Alcanzo	Chair
13:30 - 15:30	Aula	Poster session I (even numbers)		
15:30 - 16:00	Aula	Coffee break with snacks		
16:00 - 17:15	M.EG. 180	Charna Dibner – The Art of Being Rhythmic: Circadian Timing in Human Physiology and Health	Ryoichi Taguchi	Chair
	M.EG. 180	MedLife Lab Innovation		
17:15 - 17:30	M.EG. 180	Closing remarks – Microscopy and Imaging Award		
17:30 - 19:30	Aula	Drinks and snacks		

Friday April 10th

08:30 - 10:30	M.EG. 180	Opening Day 3		
	M.EG. 180	**Short talk session 3**	Felix Eichin Ferenc Török	Chair
	L.EG. 220	Project Presentations II Clinical PhD	Lena Denk	Chair
10:30 - 11:00	Aula	Coffee break with snacks		

11:00 - 11:45	M.EG. 180	**Anna Beyeler** – Contributions of the insular cortex to anxiety: from dopamine modulation to psychedelic anxiolysis		
11:45 - 13:30	M.EG. 180	**Short talk session 4**	Martina A. Höllwarth Maria Peteinareli	Chair
13:30 - 15:30	Aula	**Poster session II** (uneven numbers)		
15:30 - 16:00	Aula	Coffee break with snacks		
16:00 - 17:30	M.EG. 180	**Riina Richardson** – A deeper look into superficial Candida infections	Jakob Scheler	Chair
	M.EG. 180	**Clemens Diwoky** – Imaging Metabolism: New Horizons for MRI in Basic Research	Adriana Knoll	Chair
17:30 - 17:45	M.EG. 180	**Closing remarks – MUI PhD Awards**		
18:00 - 22:00	Aula	Come together with dinner and drinks on the second floor		

Short talk sessions

Session 1

1. Hannah Biermann
2. Lukas Müller
3. Chendo Dieleman
4. David Eisele
5. Janine Vierthaler
6. Andreas Aufschnaiter

Session 2

1. Beatriz López-Amo Calvo
2. Francesca Silvagni
3. Jan Frederik Ahrend
4. Elisa Roth
5. Matthias Ganglberger
6. Mitja Amon Posch

Session 3

1. Alexander Plesche
2. Natalia Melo Santos
3. Nikolas Marchet
4. Baris Bekdas
5. Maria Peteinareli
6. Laura Häfele

Session 4

1. Luca Szabó
2. Lucija Kucej
3. Simon Aschenwald
4. Pere Patón González
5. Adam Pollio
6. Alexander Stürz

LIFE SCIENCE PHD MEETING 2026

08.-10. April

OUR KEYNOTE SPEAKERS

Anna Heidbreder
„Promoting Brain Health Through Sleep“

Charna Dibner
„The Art of Being Rhythmic: Circadian Timing in Human Physiology and Health„

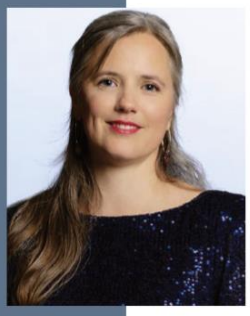

Anna Beyeler
„Contributions of the insular cortex to anxiety: from dopamine modulation to psychedelic anxiolysis„

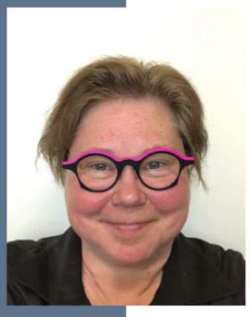

Riina Richardson
„A deeper look into superficial Candida infections“

Clemens Diwoky
„Imaging Metabolism: New Horizons for MRI in Basic Research“

From Eye to Insight

Leica MICROSYSTEMS

Step into the Microhub era.
Mica. The world Xs first Microhub.

Mica. This changes everything.

> Access for all
  > Over 85% fewer setup steps, making it ideal for all users
  > 1/3 less time to generate the first image
  > 1/2 the training time compared with other systems

> No constraints
  > Simultaneous 4 label imaging in widefield using Leica Qs patented FluoSync technology
  > 4 times more data with 100% correlation
  > Seamless switching from widefield to confocal without moving the sample

> Radically simplified workflows
  > Over 60% reduction in process steps required to perform specialist microscopy
  > 100% reproducibility and repeatability throughout the experiment

Selected Short Talks

Session	Order	Speaker	Title
1	1	Hannah Biermann	Scavenger receptor class B type I supports alphavirus infection
	2	Lukas Müller	Loss of myeloid GPX4 promotes Salmonella enterica serovar Typhimurium infection through ferroptosis-associated cell death
	3	Chendo Dieleman	Exploring Efflux Pump–Mediated Azole Resistance in Aspergillus fumigatus
	4	David Eisele	FungAI Using machine learning for the identification of fungi in patient isolates
	5	Janine Vierthaler	Who am I? CD64+cDC2 Identity Crisis: Unmasking Melanoma's Mysterious Antigen
	6	Andreas Aufschnaiter	Modifying oncolytic virus – induced cell death
2	1	Beatriz López-Amo Calvo	Neural progenitors adjust cell cycle speeds and cell-cell communication to ensure normal brain development
	2	Francesca Silvagni	Neuronal correlates of Salience Processing
	3	Jan Frederik Ahrend	From sound to movement: The neural backbone of the acoustic startle reflex
	4	Elisa Roth	Characterization of voltage-gated calcium currents in rod bipolar cells of mutant Cav1.x mouse models
	5	Matthias Ganglberger	Cell-Type-Specific Molecular Changes in Photoreceptors by a Cav1.4 C-Terminal truncation variant causing CSNB2
	6	Mitja Amon Posch	Unequal pairs: DREADDs do not mimic their "parents" signaling

Session	Order	Speaker	Title
3	1	Alexander Plesche	Effects of Mechanical Stress on the Lipid Homeostasis of the Endoplasmic Reticulum
	2	Natalia Melo Santos	Cancer cell metabolism during contact guidance migration
	3	Nikolas Marchet	TXNIP mediated LAT1/SLC7A5 endocytosis limits amino acid uptake and ensures cell survival in quiescence
	4	Baris Bekdas	A potential mighty captain in “lipid” ocean
	5	Maria Peteinareli	MicroRNA-Dependent Regulation of Neurite Outgrowth and Peripheral Nerve Regeneration
	6	Laura Häfele	Role of Stac2 adaptor protein on membrane excitability and hormone secretion of endocrine cells
4	1	Luca Szabó	The Role of the Retriever in Polarized Plasma Membrane Recycling
	2	Lucija Kucej	Identification of Golgi quality control systems in human cells
	3	Simon Aschenwald	Dual function of ERH in primary miRNA biogenesis
	4	Pere Patón González	Migration and Contact Guidance in cancer cells
	5	Adam Pollio	Pediatric microbiome: neonates to adulthood
	6	Alexander Stürz	Assessing brain magnetic microstructure in aceruloplasminemia using quantitative MRI

UltraMicroscope Blaze

Light sheet microscopy made fast and easy
3D imaging at cellular resolution of large samples-even multiple at once.

▶ miltenyibiotec.com

Miltenyi Biotec B.V. & Co. KG | Friedrich-Ebert-Straße 68 | 51429 Bergisch Gladbach | Germany | Phone +49 2204 8306-0 | Fax +49 2204 85197 | macsde@miltenyi.com | www.miltenyibiotec.com

Miltenyi Biotec provides products and services worldwide.
Visit www.miltenyibiotec.com/local to find your nearest Miltenyi Biotec contact.

Miltenyi Biotec

Scavenger receptor class B type I supports alphavirus infection

Hannah Biermann[1], Lisa Lasswitz[2], Gisa Gerold[1]

[1] Institute of Virology, Medical University Innsbruck, Innsbruck, Austria.
[2] Institute of Biochemistry & Research Center for Emerging Infections and Zoonoses (RIZ), University of Veterinary Medicine Hanover, Hanover, Germany.

Chikungunya virus (CHIKV), a re-emerging mosquito-borne alphavirus, replicates its positive-sense single-stranded RNA genome within cholesterol-rich, plasma membrane-derived spherules. These spherules incorporate both viral non-structural and host proteins. The cellular proteins that support replication within these compartments have not yet been fully characterized.
Previously, we identified the transmembrane protein CD81 as an essential host factor that colocalizes with replicating viral RNA at the plasma membrane. As a member of the tetraspanin family, CD81 coordinates the assembly of other proteins and lipids within tetraspanin-enriched microdomains. In this study, an siRNA-based screen of CD81 interactors identified the high-density lipoprotein receptor scavenger receptor class B type I (SR-BI) as a putative host factor involved in CHIKV infection.
Using SR-BI knock-out (KO) cells, we observed a marked reduction in CHIKV permissivity, which was further enhanced by concurrent knockdown of CD81, suggesting additive contributions of both host factors. These effects were not due to altered cell surface expression, with CD81 levels comparable in SR-BI KO cells and SR-BI expression unaffected by the loss of CD81. Functional analyses using lentiviral particles pseudotyped with CHIKV glycoproteins demonstrated that SR-BI is dispensable for viral entry. In contrast, electroporation of CHIKV replicon RNA revealed a strong reduction in genome replication in SR-BI KO cells, indicating that SR-BI acts as a replication-supporting factor.
Notably, SR-BI deficiency also decreased infection by other alphaviruses, including Semliki Forest virus, Ross River virus and Venezuelan equine encephalitis virus, highlighting its role as a pan-alphavirus host factor.
Collectively, these findings identify SR-BI as a critical host factor supporting CHIKV replication and pan-alphavirus infection.

Loss of myeloid GPX4 promotes *Salmonella enterica* serovar Typhimurium infection through ferroptosis-associated cell death

Lukas Müller, Egon Demetz, Nidhi Srinivasan, Monika Bauer, Natascha Brigo, Christa Pfeifhofer-Obermair, Markus Seifert, Chiara Volani, Günter Weiss, David Haschka
Medical University of Innsbruck, Department of Internal Medicine II, Innsbruck, Austria.

Glutathione peroxidase 4 (GPX4) is a central regulator of lipid peroxidation and ferroptosis in mammalian cells, yet its role in myeloid cell–dependent antibacterial defense remains poorly understood. Here, we identify GPX4 as a key regulator of myeloid cell–mediated control of Salmonella enterica serovar Typhimurium (S. tm) infection in mice.
Myeloid GPX4 deficiency resulted in impaired infection control in mice, characterized by increased bacterial burdens in tissues and blood and significantly accelerated mortality.
Using bone marrow–derived macrophages (BMDMs) and peritoneal macrophages (PMs), we observed enhanced intracellular bacterial replication and increased cell death, both of which were reversed by the ferroptosis inhibitor ferrostatin-1, indicating ferroptotic cell death as a key mechanism. GPX4 loss was further associated with altered macrophage polarization, metabolic reprogramming, and disrupted iron homeostasis, including an expanded labile iron pool and altered expression of key iron-regulatory proteins such as transferrin receptor 1, ferroportin and ferritin, all reversible upon ferrostatin-1 treatment.

In vivo, GPX4 deficiency led to elevated lipid peroxidation in infected organs, increased bacterial loads, and enhanced myeloid cell infiltration, as assessed by both colony-forming unit plating and image-based cytometry of infected tissue sections.

Collectively, these findings identify GPX4 as a critical determinant of myeloid cell viability and antibacterial defense, preserving host control of S. tm infection by limiting lipid peroxidation and ferroptosis, thereby restricting bacterial dissemination and tissue damage during systemic infection.

Exploring Efflux Pump–Mediated Azole Resistance in *Aspergillus fumigatus*

Chendo Dieleman

Aspergillus fumigatus is a major fungal pathogen and poses a substantial burden in clinical settings due to its high annual death toll. As the management of A. fumigatus-caused aspergillosis becomes more challenging due to rising antifungal resistance, studying the underlying mechanisms to better understand the development of antifungal resistance is pressing.
While mutations in the cyp51A gene are well-characterized drivers of azole resistance, the resistant phenotype in many azole-resistant A. fumigatus isolates is not attributable to mutations related to this gene alone. Non-cyp51A resistance mechanisms remain understudied, and their contribution to overall azole resistance is poorly understood. Among these understudied mechanisms are ATP-binding cassette (ABC)-transporters, only a handful of which have been characterized. In this study, we investigate the role of both known and previously uncharacterized ABC transporters in A. fumigatus azole resistance.
To elucidate the function of these ABC-transporters, we first checked the gene annotation and, where necessary, corrected the annotation of all ABC transporter-encoding genes in the A. fumigatus genome. Using protoplast-mediated CRISPR/Cas9 transformation, we generated strains with inducible overexpression of each putative transporter. These mutant strains were screened for altered azole resistance phenotypes through spot assays. Strains showing increased susceptibility or resistance were further analyzed by broth microdilution to quantify the impact of ABC transporter overexpression on azole resistance.
Using our approach. we identified 11 ABC transporters – including the well-described Cdr1B and AtrF – that affected azole susceptibility upon overexpression, four of which were previously uncharacterized. Interestingly, one uncharacterized transporter conferred cross resistance to all tested azoles, indicating that its overexpression mediates resistance to azoles with both clinical and agricultural relevance.
In conclusion, our work demonstrates that previously undescribed ABC transporters contribute to A. fumigatus azole resistance. These transporters may confer specificity for a particular azoles or broader cross-resistance. Although speculative, mutations leading to overexpression of ABC-transporters may act independently or synergistically with cyp51A-associated mutations, potentially contributing to the emergence of unique azole resistance phenotypes in both clinical and environmental contexts.

FungAI - Using machine learning for the identification of fungi in patient isolates

David Eisele[1], Angelika Bauer[1], Ronald Gstir[1], Werner Ruppitsch[1], Cornelia Lass-Flörl[1]
[1]Institute of Hygiene and Medical Microbiology, Medical University of Innsbruck, Innsbruck, Austria

Purpose: This project aimed to train specialized artificial intelligence (AI) models to enable a high confidence genus-level discrimination of fluorescence microscopy images of two clinically important fungal pathogens, Aspergillus spp. and Candida spp.. It is well known that quick identification is essential to treat invasive fungal infections and improve survival rates. Currently, morphological identification of fungi relies on expert knowledge and many traditional methods are time-consuming. Molecular methods allow for faster identification with rapid throughput but are typically associated with higher cost. AI image classification offers the advantage of being lower in cost while still having high throughput.

Methods: We adapted pre-trained convolutional neural networks (CNNs), including DenseNet161, DenseNet169 and ConvNeXt Small, for the identification of fluorescence microscopy images acquired by using a 100x oil-immersion objective. Fungal elements in patient samples were stained using Calcofluor White. Original patient material containing these fungi was stored at -80°C between 2018 and 2025, and retrospectively analysed by acquiring fluorescence microscopy images for this project. Aspergillus spp. and Candida spp. both possess specific characteristics: Aspergillus spp. typically form septate hyphae and mycelia while Candida spp. grow as yeast cells and may form pseudohyphae. 2006 images of 61 Aspergillus spp. isolates and 1095 images of 59 Candida spp. isolates were split into training, validation and test sets.

Results: The trained models achieved high quality genus-level distinction of Aspergillus spp. and Candida spp.. The DenseNet161 based classifier correctly identified 88% (929/1060) of the Aspergillus spp. images and 79% (121/153) of the Candida spp. images in the test set, the DenseNet169 based classifier correctly identified 85% of Aspergillus spp. (899/1060) and 85% of Candida spp. (130/153) and the ConvNeXt Small based classifier, correctly identified 85% of Aspergillus spp. (897/1060) and 88% of Candida spp. (135/153). When combining the output of the three models into a simple majority vote classifier, 90% of Aspergillus spp. and 88% of Candida spp. in the test set were correctly identified. Misidentified images typically had a lower probability score (mean < 80%) than correctly identified isolates (mean > 90%).

Conclusion: CNNs enable reliable genus-level discrimination between Aspergillus spp. and Candida spp. on genus-level. The primary challenges for AI based classification of images was reliably distinguishing septate hyphae from pseudohyphae and the identification of small fungus elements with few classifiable features. Majority vote to combine the output of several classifiers appears promising for improving classification accuracy. Additionally, classifiers had lower average confidence in wrong calls than correct calls meaning that errors primarily occur when the model is uncertain.

Outlook: The future aim is the training of new models to achieve species-level classification. The main challenges are the smaller morphological differences of species within the same genus and the limited availability of less prevalent species for the training set.

Who am I? CD64+cDC2 Identity Crisis: Unmasking Melanoma's Mysterious Antigen Presenter

Janine Vierthaler

Our research has identified a distinct cDC2 phenotype in melanoma mouse models, characterized by FcγRI/CD64 expression - typically associated with monocytes and macrophages rather than DC. CD64+cDC2 are abundant in tumors and tumor-draining lymph nodes but are rarely found in lymph nodes of tumor-free mice. CD64+cDC2 express both activation (CD40) and inhibitory (PD-L1, PD-L2) markers, suggesting their involvement in initiating and regulating effector T cell responses. Interestingly, some CD64+cDC2 lack the DC-lineage marker Zbtb46, as shown by a Zbtb46-GFP DC-reporter mouse strain, suggesting that CD64+cDC2 originate from both pre-DC and monocytes.

We have shown that CD64+cDC2 expand in response to FLT3L, a driver of DC differentiation and proliferation, indicating a possible pre-DC origin. Using dual DC- and monocyte-reporter mouse models, we now demonstrated that CD64+cDC2 arise predominantly from DC-lineage progenitors, although a fraction originated from monocytes that acquire a DC-like phenotype within the TME. Functionally, studies employing a ZsGreen-expressing melanoma model revealed that CD64+cDC2 are highly efficient in tumor antigen uptake and trafficking to tumor-draining lymph nodes. However, CD64 expression on cDC2 did not influence CD4+ T cell polarization in in vitro T cell assays.

Our ongoing research aims to elucidate the precise developmental origin and functional specification of CD64+cDC2 in tumor immunity and explore whether CD64 serves as a biomarker of antigen-experienced DC. Understanding the biology of this CD64+cDC2 population may reveal new opportunities for DC-targeted immunotherapy in melanoma and other cancers.

Modifying oncolytic virus – induced cell death

Andreas Aufschnaiter

Oncolytic virotherapy (OV) is a therapeutic concept in which a replication-competent virus with a lytic life cycle clears cancer cells via preferential infection and/or replication, while sparing normal tissue. VSV-GP is a chimeric oncolytic vesicular stomatitis virus (VSV) with the glycoprotein of lymphocytic choriomeningitis virus (LCMV-GP), which shows abrogated neurotoxicity compared to parental VSV. Infection of cancer cells with VSV usually induces apoptosis resulting in effective tumor control in vitro and in vivo in susceptible syngeneic mouse tumor models. In some models, however, rechallenge with the same tumor type leads to outgrowth, suggesting an insufficient or no activation of anti-tumor immunity. Here we show three concepts to modify VSV-GP – induced cell death facilitating molecular characteristics of necroptosis, an immune system activating, regulated cell death modality. VSV-GP armed with necroptosis-inducing transgenic cargos show superior killing potency in a screen of murine and human cancer cell lines. Additionally, this optimized cell death after infection correlates with plasma membrane lysis and DAMP (damage-associated molecular pattern) release, a hallmark of immunogenic cell death (ICD). Furthermore, we identified a murine cancer cell line (KPC3), which resists parental VSV-GP – induced cell death, yet shows complete susceptibility to cell death-modified VSV-GP. This could translate into enhanced stimulation of anti-tumor immune responses in vivo.

MACHEREY-NAGEL

RNA Promotion 2026

Scan for promo

Bioanalysis

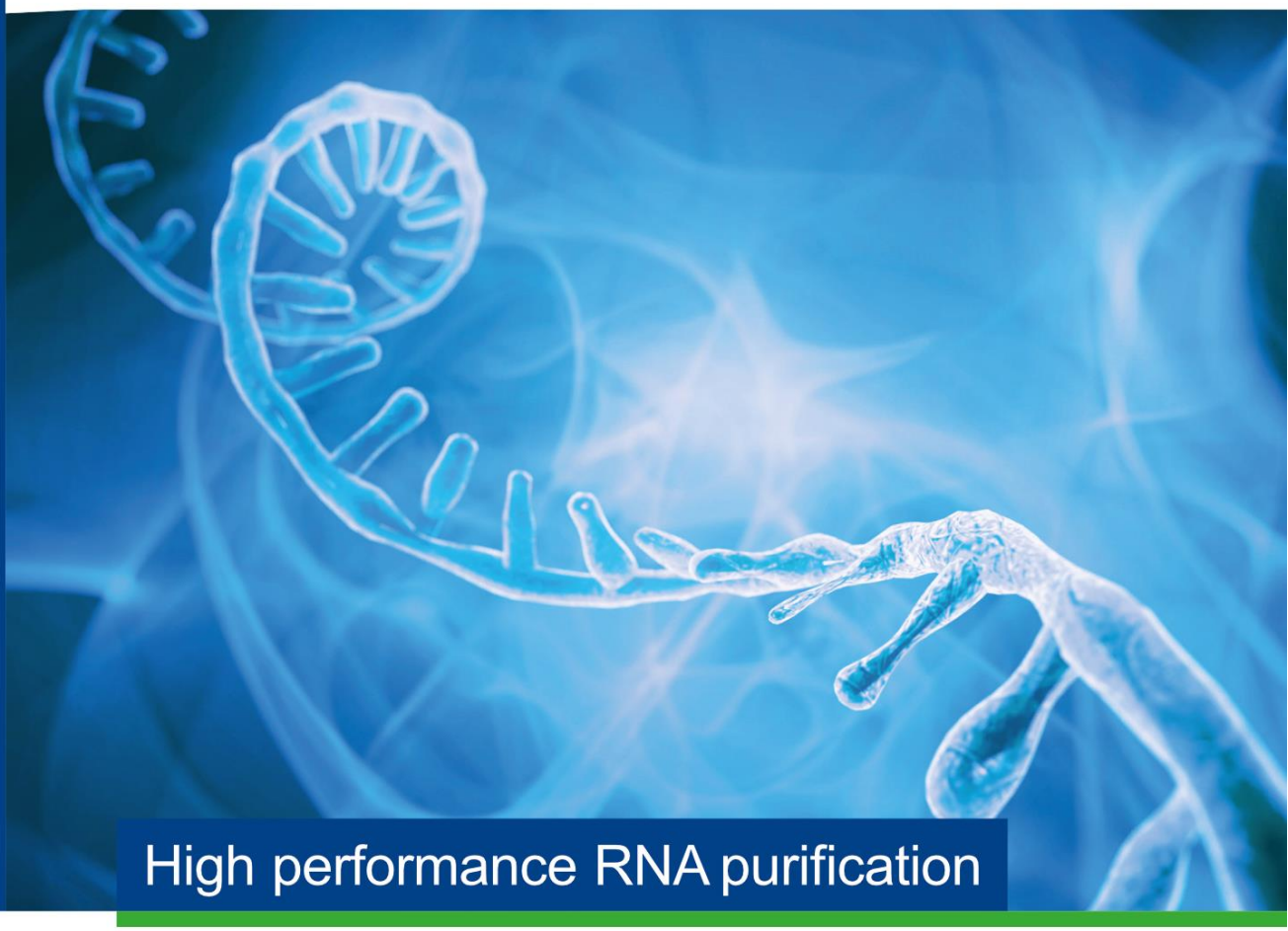

High performance RNA purification

- NEW! NucleoMag® RNA/DNA Pro
- NEW! NucleoSpin® 96 RNA Plant and Fungi
- NEW! Current comparative data NucleoSpin® RNA and QIAGEN RNeasy®[1)]
- Developed and produced in Germany

[1)]Qiagen, RNeasy® Mini Kit (50), REF 74104

Neural progenitors adjust cell cycle speeds and cell-cell communication to ensure normal brain development

Beatriz López-Amo Calvo

During brain development, neural stem cells (NSCs) initially expand by symmetric cell divisions before transitioning to asymmetric cell divisions to generate neurons while sustaining the NSC pool. The timing and regulation of this transition vary across species, with human neurogenesis being particularly heterogenous. Furthermore, human NSCs can adjust progeny output in response to tissue perturbation, but the processes that enable this replenishment remain unclear. Here, using a human chimeric brain organoid paradigm with controlled and targeted tissue loss, we show that neural progenitors mount a compensatory response to tissue damage by rewiring their cell-cell communication program and accelerating their cell cycle. Combining microscopy, flow cytometry, time-resolved transcriptomics and lineage-resolved scRNA-sequencing, we demonstrate that tissue-perturbed organoids maintain overall cell type composition, yet exhibit a striking expansion of fast-growing lineages within ten days. This response is accompanied by an elevated cell cycle and increased signalling through developmental and extracellular matrix ligand–receptor pathways. These findings reveal a compensatory strategy in which neural progenitors restore tissue homeostasis not via bulk self-expansion, but by transiently increasing mitotic speed while preserving lineage identity. These insights provide a framework for understanding tissue-mediated growth control and how human neural tissue withstands and repairs structural disruption, with implications for regenerative strategies and models of developmental neurobiology.

Neuronal correlates of Salience Processing

Silvagni Francesca[1], Kobakhidze Nino[2], Gorkiewicz Sarah[3], Matulewicz Pawel[1], Ramos-Prats Arnau[4], Sartori Simone B.[2], Singewald Nicolas[2], Novarino Gaia[3], Ferraguti Francesco[1], Schmuckermair Claudia[1].

Affiliations:
[1] Institute of Pharmacology, Medical University of Innsbruck, Innsbruck, Austria.
[2] Department of Pharmacology and Toxicology, University of Innsbruck, Innsbruck, Austria.
[3] Institute of Science and Technology Austria (ISTA), Klosterneuburg, Austria.
[4] Friedrich Miescher Institute for Biomedical Research, Basel, Switzerland.

Dysfunctional salience processing is observed across a spectrum of psychiatric conditions, including schizophrenia, autism spectrum disorder, anxiety disorders, depression, and dementia. Although human fMRI work has delineated large-scale networks and key nodes involved in salience detection, such as the insular cortex for passive processing and the cingulate cortex for active oddball detection, the precise neuronal computations that support these processes remain unclear. To address this, we employ a multidimensional passive auditory oddball paradigm in mice, integrating pupillometry as an objective readout of arousal with in vivo calcium imaging of excitatory and inhibitory neuronal subpopulations in the anterior insular cortex (aIC). We further use optogenetic manipulations to probe the causal contributions of defined circuits. Our preliminary results show that optogenetic activation of CamK2+ excitatory neurons in the aIC is sufficient to increase arousal, evidenced by pronounced pupil dilation. Auditory oddball stimuli reliably trigger pupil dilation in both male and female mice, validating the paradigm as a sensitive measure of salience-related arousal. Importantly, we identify a distinct cohort of neurons within the aIC that is selectively recruited during oddball events, indicating selective encoding of salience in this region. This integrated approach links cellular-level activity and circuit dynamics with behavioral and physiological markers of salience detection. By connecting animal-model mechanisms with human imaging findings, these studies aim to advance mechanistic insight into salience processing and its disruption across psychiatric conditions.

From sound to movement: The neural backbone of the acoustic startle reflex

Jan Frederik Ahrend

The acoustic startle reflex (ASR) is a fast, reactive body movement in response to a loud and unexpected auditory stimulus that has been observed in all mammalian species. In rats, cochlear root neurons (CRNs) – located between auditory periphery and cochlear nucleus (CN) – have been identified as the first neural substrate of the underlying reflex circuit. CRNs receive excitatory input from primary afferent spiral ganglion neurons (SGNs). Their axons mainly target neurons of the contralateral pontine reticular nucleus (PnC) formation, which project onto motor neurons. CRNs are subject to diverse modulatory inputs from higher brain areas. Despite their central role in a reflex circuit directly implicated with individual survival, CRNs are poorly characterized in regards to their cellular excitability and activity patterns, as well as their molecular composition and morphology in situ. Therefore, we set out to characterize CRNs in different species regarding their morphology, their pattern and identity of afferent as well as efferent somatic innervation, as well as their counts and spatial distribution between modiolar base and CN. For these purposes, we combined immunofluorescent labelings with either whole cochlea tissue clearing or high-resolution confocal microscopy using a novel intact cochlea+CN preparation. We further employed genetic reporter mice, neuronal tracer dyes, and immunohistochemical stainings to visualize the afferent and efferent functional inputs onto CRNs soma. Finally, we are currently establishing tissue preparations for functional analyses. In this way, we hope to shed light onto the primary neural base of the ASR.

Characterization of voltage-gated calcium currents in rod bipolar cells of mutant Cav1.x mouse models

Elisa Roth[1], Matthias Ganglberger[1], Lucia Zanetti[1], Nadine J. Ortner[1], Georgios Fotakis[2], Zlatko Trajanoski[2], Hartwig Seitter[1] and Alexandra Koschak[1]
[1]University of Innsbruck, Institute of Pharmacy, Pharmacology & Toxicology unit, Innsbruck, Austria
[2]Medical University, Institute of Bioinformatics, Innsbruck, Austria

Retinal ribbon synapses provide sustained glutamatergic transmitter release that, in photoreceptors, is controlled by Cav1.4 L-type calcium channels (LTCCs). In contrast, the role of Cav1.4 in rod bipolar cells (RBCs) is less understood. Pathogenic Cav1.4 variants, such as the R1827X truncation that induced calcium dependent inactivation (CDI) and the I745T variant displayed gain-of-function characteristics in heterologous expression systems. In humans, these variants cause congenital stationary night blindness type 2 (CSNB2). However, it has not been reported how these functional phenotypes manifest in photoreceptors and/or bipolar cells yet. To address this, we first investigated the expression and the role of voltage-gated calcium channels (VGCCs) in wild-type (WT) RBCs, given that the VGCC composition in RBCs still remains elusive.

qPCR-experiments in FACS-sorted RBCs showed transcripts for β2, α2δ-4, various Cav1.3 splice variants, Cav1.4, Cav3.2 and a C-terminal Cav1.1 splice variant. Whole-cell patch-clamp recordings in WT-RBCs revealed a sustained high-voltage activated (HVA) and a transient, low-voltage activated calcium current. Despite substantial Cav1.4 transcript in RBCs, a HVA calcium current persisted in Cav1.4KO RBCs. Using the LTCC modulators Isradipine (10µM) and Bay-K (10µM), we confirmed the L-type nature of the remaining current. To assess a possible Cav1.3 component, we used Cav1.3KO and CavAG mice; the latter shows a gain-of-function phenotype with a left-shift in the voltage dependence of activation in heterologous expression systems. While we observed no significant difference in the activation properties, CavAG RBCs exhibited a hyperpolarizing shift of the reversal potential and a trend towards a slower inactivation during a 500ms testpulse to Vmax, suggesting only a minor contribution of Cav1.3 channels to WT RBC HVA currents. Of note, western-blot analyses detected residual Cav1.3 expression in Cav1.3KO retinas, which may explain why calcium currents in Cav1.3KO and WT RBCs were similar.

Despite this compensatory HVA calcium current, Cav1.4KO-RBCs exhibited a substantial reduction in overall calcium currents, highlighting a critical role of Cav1.4 channels in RBCs and thus enabling the characterization of its pathogenic variants RX and IT within these cells. Notably, both variants exhibited phenotypes distinct from those previously observed in heterologous expression systems, possibly due to compensatory by Cav1.3 and T-type channels. Reduced current influx was observed for both variants, with the RX also showing faster inactivation kinetics during a 5s test pulse to Vmax from a holding potential of -100mV, but not -50mV, pointing towards an increased T-type contribution.

So far, it seems that Cav1.3 and Cav1.4 channels are able to uphold L-type calcium currents in RBCs, suggesting that CSNB2-phenotypes may be caused solely by mutant Cav1.4 channels in photoreceptors. Further characterization of pathogenic Cav1.4 variants will also facilitate the design of personalized gene therapy interventions.

Cell-Type-Specific Molecular Changes in Photoreceptors by a Cav1.4 C-Terminal truncation variant causing CSNB2

Matthias Ganglberger

Pathogenic variants in the CACNA1F gene, encoding the Cav1.4 L-type calcium channel, cause congenital stationary night blindness type 2 (CSNB2) in humans. Our lab recently published a mouse model carrying the R1827X (RX) truncation variant, which lacks the C-terminal modulatory domain. In these mice, the rod pathway is functionally and morphologically disrupted, as evidenced by altered synaptic ribbon architecture and pronounced sprouting primarily in rod bipolar cells. The rod pathway impairment is corroborated by electroretinography showing specific deficits in rod-mediated responses while cone pathways remained unaffected. However, electron microscopy revealed ultrastructural deficits in both rod and cone photoreceptors, including floating ribbons causing ribbon-less active zones. Despite these synaptic alterations in cones, no functional phenotype was observed, prompting the hypothesis that cones possess compensatory mechanisms at the molecular level to maintain function.
To investigate this differential molecular response, we established a low-cell-input proteomics pipeline optimized for FACS-sorted rods and cones from RX mutant and control retinas. This platform enabled robust detection of low-abundance synaptic proteins, including the Cav1.4 channel complex and associated interactors. Proteomic analysis uncovered decreased Cav1.4 protein levels in both cell types. Interestingly, rods showed additional altered protein involved in the vesicle release machinery, such as vGlut1 and SV2a.
These initial findings point to divergent molecular changes in rods versus cones to Cav1.4 RX dysfunction, suggesting at potential compensatory mechanisms in cones that warrant further validation. Future studies will focus on validating these mechanisms and exploring their therapeutic potential for CSNB2.

Funding: FWF: DOC 30-B30, P36262 to AK, TWF: F52779 to MG, the LFU Innsbruck and the CMBI.

Unequal pairs: DREADDs do not mimic their "parents" signaling

Mitja Amon Posch, Sarah Seidel, Leandra Abt, Olga Trovato, and Andreas Lieb

Institute of Pharmacology, Medical University Innsbruck, Innsbruck, Austria

Designer Receptors Exclusively Activated by Designer Drugs (DREADDs) are mutated human muscarinic acetylcholine receptors (hM) that can be potently activated by synthetic compounds but not by their native ligand. The most widely used DREADDs, hM3D (excitatory) and hM4D (inhibitory), are frequently used to modulate cellular excitability and are preclinically explored for therapy development. While their selective hM4D- and hM3D-dependent inhibition or excitation is well established, recent data have challenged this concept. Here, we systematically analyzed the signaling profiles of hM3/4 and their respective DREADDs. We find that hM3D shows increased specificity for excitatory Gaq/11 signaling cascades, whereas hM4D displays more promiscuous coupling, engaging additional non-Gai/o signaling such as Gaq/11. These differences extend to altered Ca^{2+} and cAMP responses, as well as changed β-arrestin 2 recruitment. Evaluation of the two point mutations underlying DREADD generation identified the molecular basis for these signaling alterations. Together, our findings reveal that hM4D acquires additional signaling properties while hM3D becomes more selective, emphasizing that DREADDs do not fully mimic their wild-type receptor counterparts and results generated in vivo should be interpreted with caution.

THP MEDICAL PRODUCTS

YOUR N°1LIFE SCIENCE SUPPLIER

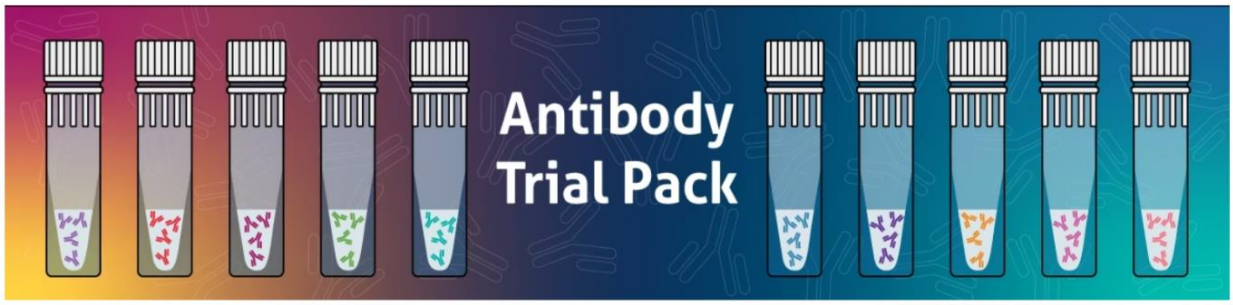

proteintech® Antibodies | ELISA kits | Proteins

Bioss ANTIBODIES

RayBiotech Empowering your proteomics

PAN™ BIOTECH

MCE® MedChem Express

horizon INSPIRED CELL SOLUTIONS

CAPRICORN SCIENTIFIC

BioAssay Systems Solutions for Research and Analysis

Vazyme

ACTIVE MOTIF

CELL BIOLABS, INC. Creating Solutions for Life Science Research

TargetMol® YOUR TARGET MOLECULES

GeneCopoeia™ Expressway to Discovery

FAVORGEN® BIOTECH CORP.

BIOSYSTEMS Acro

Bio SB BIOSCIENCE FOR THE WORLD

Life Science Shop

Visit *lifescience.thp.at*

- 2.3+ Mio Products
- User Friendly Product Search
- Easy Ordering

Our Services & Your Support:

- Product Search & Comparison
- Scientific Project Support
- On-Site Tech Support
- Smart Shopping Support
- Quality & Cost Optimization

Visit our booth or contact us:

P: +43 1 292 82 80
E: orders.lsr@thp.at

Effects of Mechanical Stress on the Lipid Homeostasis of the Endoplasmic Reticulum

Alexander Plesche

In living organisms, cells are constantly exposed to mechanical stimuli and stresses. The cellular responses and their adaptations to these mechanical cues are only beginning to be unraveled, in particular those of intracellular organelles beyond the nucleus. We are using cell confinement to a defined height of 3 µm to study the effects of mechanical stress on the endoplasmic reticulum (ER). Our study identified the ER-resident protein phosphatidylethanolamine-N-methyltransferase (PEMT) as a regulator of both the lipidome and ER morphology following mechanical stimulation.

When cells are confined to a height of 3 µm, lipidomics analysis revealed an increase in the ratio of phosphatidylcholine (PC) to phosphatidylethanolamine (PE). This mechanically induced alteration of the lipid composition is mediated by a direct conversion of PE to PC by the PEMT enzyme, as small-interfering-RNA-mediated knockdown of PEMT abolishes the phenotype. This change in the two most abundant phospholipid groups of the cellular membranes has a profound impact on the morphological appearance of the ER: sheet-like structures are strongly expanded at the expense of the peripheral tubular network during cell confinement. Given the cylindrical geometry of PC lipids, their enrichment likely facilitates the formation of the extended planar sheet structures, which is supported by the sensitivity of this phenotype to the presence of PEMT. As a functional consequence, the lipid remodeling affects the response of ER exit sites (ERES) to mechanical stress. Whereas under normal conditions the number of ERES is elevated following confinement, this increase disappears if PEMT is not present.

Future experiments will investigate whether PEMT itself is directly or indirectly regulated by mechanical stress. Furthermore, the reason for the PEMT-induced ER morphology under mechanical stress needs to be clarified, with possible roles in overall mechanical stability, secretion or calcium homeostasis.

Cancer cell metabolism during contact guidance migration

Natalia Melo Santos

In 3D tumour environments, cancer cells navigate the extracellular matrix (ECM) by exploiting its heterogeneous topography through a process called contact guidance. This migration strategy, driven by physical cues such as substrate stiffness and topography, is still poorly understood at the molecular level. Due to their plasticity, cancer cells can switch between distinct migratory modes — such as mesenchymal or amoeboid modes — depending on the physical properties of the substrate. In mesenchymal migration, focal adhesions (FAs) play a central role by linking the actin cytoskeleton to the ECM and transmitting contractile forces, making this process highly energy demanding. We hypothesized that FA-independent contact guidance might be energetically more efficient, and aim to understand how energy production adapts during this migration mode. Using metastatic breast cancer MDA-MB-231 cells depleted of Talin1, a key FA component, we found that FAs are dispensable for this type of migration. To test our hypothesis, we cultured cells on polydimethylsiloxane (PDMS) substrates engineered with ridge-like topographies functionalized with collagen. Preliminary analysis shows that MDA-MB-231 cells migrating along ridges maintain ATP levels while there is a reduction in mitochondrial membrane potential ($\Delta\Psi m$) and increase in mitochondrial number and elongation — suggesting mitochondrial remodelling and a potential shift toward glycolytic metabolism. Interestingly, FA-deficient cells exhibited no change in mitochondrial number or $\Delta\Psi m$ but presented a significant drop in ATP levels when exposed to ridges. These findings suggest that although FAs are not essential for contact guidance per se, they might play an important role for sustaining the metabolic flexibility required for this type of migration. Collectively, our results could indicate that contact guidance induces a topography-dependent metabolic adaptation.

TXNIP mediated LAT1/SLC7A5 endocytosis limits amino acid uptake and ensures cell survival in quiescence

Nikolas Marchet

Entry into and exit from cellular quiescence require dynamic regulation of nutrient uptake; however, the mechanisms by which quiescent cells suppress amino acid (AA) transport remain largely unknown. Here, we show that cells entering quiescence selectively target plasma membrane–resident AA transporters for endocytosis and lysosomal degradation, thereby aligning AA uptake with reduced translational demand. We identified the a-arrestin TXNIP as a key regulator for this metabolic adaptation, as it regulates the endocytic degradation of the heterodimeric AA transporter SLC7A5–SLC3A2 (LAT1–4F2hc) upon reduced AKT signaling. Mechanistically, we demonstrate that a single PPCY motif in TXNIP is required for SLC7A5–SLC3A2 downregulation and is essential for TXNIP interaction with members of the HECT-type ubiquitin ligase family.

Under growth conditions, active AKT phosphorylates TXNIP at S308, thereby inhibiting its function. In contrast, during quiescence, diminished AKT signaling permits TXNIP-dependent endocytosis of SLC7A5–SLC3A2, resulting in reduced AA uptake. Loss of TXNIP leads to dysregulated AA transport, enhanced mTORC1 signaling, increased protein synthesis, and accelerated exit from quiescence with increased proliferation. Conversely, during prolonged quiescence, TXNIP-mediated endocytic removal of SLC7A5–SLC3A2 becomes essential for cell survival. Quiescent cells in which SLC7A5–SLC3A2 endocytosis is disrupted, continue to acquire AA leading to severe metabolic imbalance. We speculate that this metabolic imbalance finally results in cell death.

Supporting this role in nutrient homeostasis, we identify a novel loss-of-function TXNIP mutation in a patient with severe metabolic disease, underscoring the importance of TXNIP in human health. Together, these findings establish TXNIP as a key regulator of SLC7A5–SLC3A2–mediated AA acquisition, with broad implications for metabolism (Kahlhofer J., Marchet N., 2025, EMBO J). Building on these findings, we now aim to elucidate how SLC7A5–SLC3A2-dependent AA transport integrates with metabolic signaling to regulate translation, proliferation, and to define in molecular detail how TXNIP mediated SLC7A5–SLC3A2 endocytic degradation ensures survival in quiescence.

A potential mighty captain in "lipid" ocean

Baris Bekdas

Sphingolipids (SLs) play a crucial role in maintaining membrane integrity and function, and their derivatives, e.g. ceramides, act as signalling molecules involved in cell proliferation, apoptosis, and stress responses. However, excessive accumulation of SL intermediates causes cytotoxicity, necessitating a tight regulation. Evolutionary conserved ORMDL family proteins - Orm1 and Orm2 in budding yeast - control SL homeostasis by inhibiting serine-palmitoyl-CoA transferase (SPT), a key enzyme of de novo SL biosynthesis. Under conditions of low SL levels or membrane stress, Orm1 and Orm2 dissociate from the complex, thereby activating SPT.
Mass spectrometry–based interactome analyses verified by reciprocal co-immunoprecipitations indicate that Orm2 also interacts with multiple ER-resident enzymes involved in the biosynthesis of ergosterol, the fungal analogon of cholesterol. The phosphorylation status of Orm2, which regulates its binding to SPT, has little effect on these interactions. Binding requirements of Orm2 for Erg enzymes are different, with some requiring Orm2 to be bound to the SPT and others not. Hence, Orm2 apparently binds several smaller Erg complexes rather than a large single entity, which we are currently aiming to characterize.
Moreover, Orm2 mutants with low SPT activity show increased levels of ergosterol metabolites, whereas they are mildly decreased in cells with elevated SPT activity. Although SL and sterol biosynthetic pathways are thought to be co-regulated, the underlying molecular mechanisms are not well defined. We propose that Orm2 might be a key factor for mediating this cross-talk.

MicroRNA-Dependent Regulation of Neurite Outgrowth and Peripheral Nerve Regeneration

Maria Peteinareli
Maria Peteinareli[1], Michaela Kress[1], Theodora Kalpachidou[1]
[1] Institute of Physiology, Medical University of Innsbruck, Innsbruck, Austria

MicroRNAs (miRNAs) are short non-coding RNA molecules that regulate gene expression and are increasingly recognized as key modulators of diverse biological functions, including injury-induced neuropathic pain and neuronal repair. Following injury, alterations in miRNA expression suggest that these regulators orchestrate complex molecular programs that control axonal remodelling, cytoskeletal dynamics, and regenerative capacity. However, the specific contribution of individual miRNAs to peripheral nerve regeneration, independent of nociceptive processes, remains incompletely understood. In this study, we investigated the role of a specific miRNA using a knockout (KO) mouse model in combination with behavioural, anatomical, and transcriptomic approaches following spared nerve injury (SNI). Additionally, ex vivo dorsal root ganglia (DRG) explant cultures and in vitro neurite outgrowth assays were performed. Sensorimotor behavioural testing demonstrated normal development of SNI-induced pain-like behaviours in KO mice. In contrast, anatomical analysis using whole-mount staining revealed significantly reduced sciatic nerve fiber sprouting seven days after injury in the KO sciatic nerves. RNA sequencing of KO DRG uncovered widespread changes in gene networks related to axonal growth, cytoskeletal organization, and epigenetic regulation. In line with these findings, KO DRG explants and cultured neurons displayed diminished intrinsic outgrowth capacity. Collectively, these data support a selective role for this miRNA in axonal remodelling rather than nociceptive processing, identifying it as an important regulator of regenerative signalling pathways that contribute to peripheral nerve repair and neurite growth. Ongoing work will determine whether similar regulatory mechanisms operate in other sensory ganglia and evaluate the relevance of this miRNA in the central nervous system. Elucidating these shared pathways may provide broader insight into miRNA-mediated control of neuronal growth and repair.

Role of Stac2 adaptor protein on membrane excitability and hormone secretion of endocrine cells

Laura E. Häfele[1], Noelia Jacobo-Piqueras[1], Ryoichi S. Taguchi[1], Marta Campiglio[2], Stefanie M. Geisler[1], Petronel Tuluc[1]

[1] Leopold-Franzens University of Innsbruck

[2] Medical University of Innsbruck

Introduction: Stac adaptor proteins (Stac1-Stac3) have been identified as novel regulators of L-type voltage gated Ca2+ channel (CaV) expression and biophysical properties. Functionally, it has only been shown in heterologous cell systems or cultured hippocampal neurons that Stac2 overexpression abolishes L-type CaV channel voltage-dependent inactivation.
Aims: Here we set to investigate if genetic ablation of the endogenous Stac2 protein alters mouse chromaffin cells (MCCs) or pancreatic β-cells CaV channels biophysical properties, membrane excitability, and hormone release.
Methods: For this we used a combination of voltage-clamp, current-clamp, capacitance measurements, calcium imaging and glucose-induced dynamic insulin release.
Results: In MCCs, Stac2 deletion did not alter whole-cell calcium currents amplitude or inactivation kinetics but significantly shifted the voltage-dependence of activation to more hyperpolarized potentials. Stac2-/- MCCs did not show altered resting membrane potential or spontaneous action potential (AP) firing frequency. However, the AP depolarization threshold was significantly reduced and step current injection elicited APs with higher initial firing frequency in Stac2-/- compared to WT. Interestingly, Stac2 deletion impaired the time course of MCCs vesicle exocytosis. In pancreatic β-cells, Stac2 deletion caused a significant increase in glucose-induced membrane depolarization. While the AP-train duration and frequency were not affected, the AP threshold was significantly higher in Stac2-/- compared to WT. In lower glucose concentrations (5 mM and 7.5 mM) Stac2-/- exhibits an increased insulin secretion in comparison to the WT.
Conclusion: Cumulative we show that Stac2 is an important regulator of endocrine MCCs and β-cell excitability and vesicle exocytosis.

The Role of the Retriever in Polarized Plasma Membrane Recycling

Luca Szabó

The Retriever complex, a trimeric assembly of vps29, vps35l and dscr3, shares a similar structure and function with the Retromer as they have a common subunit (vps29). Both recycle proteins from endosomes towards the plasma membrane (PM) or Golgi. Crucial difference, however, is that they recognize a different subset of cargoes through different adaptor proteins. In non-polarized cells the cargo adaptor of the Retriever is snx17. It forms the Commander complex together with the COMMD/CCDC22/CCDC93 (CCC) complex. Up to date, the Retriever complex has not been studied in the context of epithelial polarity, in particular apical and basolateral Retriever cargo segregation.
To address this, we used the epithelial polarity model Madin-Darby Canine Kidney (MDCK) cells and generated WT, VPS35L knock-out (KO), SNX17 KO and CCDC22 KO lines. To study PM cargo recycling, we implemented an unbiased approach where we compared polarized WT and KO clones by selectively biotinylating apical and basolateral PM proteins and identified Retriever-dependent PM cargoes by quantitative mass spectrometry in combination with tandem mass tag (TMT)-labeling. We have found previously established snx17 cargoes as well as several others (e.g., lrp1, integrin β1, integrin α2) among the proteins that were regulated in our KO clones based on mass spectrometry measurements. We have shown that the Retriever crucially regulates basolateral integrin recycling affecting polarized functions, such as 3D cyst formation or collective cell migration.
Overall, the project aims to provide a comprehensive understanding of Retriever-dependent plasma membrane cargo recycling in polarized epithelial cells.

Identification of Golgi quality control systems in human cells

Lucija Kucej

Protein homeostasis, or proteostasis, is a hallmark of all healthy cells. Maintaining proteostasis involves protein synthesis, folding, modification, sorting, and degradation. Disruption of any of these steps leads to the mis-folding or mis-localization of proteins, which can contribute to various diseases (e.g. neurodegeneration, cancer, etc.). To prevent these issues, cells use proteostasis networks within organelles that detect and selectively degrade misfolded membrane proteins or orphaned membrane proteins (those that cannot integrate into protein complexes or fail to reach their correct destinations).

While the protein quality control functions of the ER, lysosomes, and mitochondria are well characterized, the Golgi apparatus is often overlooked, despite its crucial role in protein sorting and modification. Given its sorting capabilities, the Golgi presents an ideal site for detecting misfolded proteins that have escaped the ER, or orphaned proteins.

The Teis lab has recently identified the Dsc ubiquitin ligase complex and Rer1 protein as essential components of a multi-layered Golgi quality control network in budding yeast S. cerevisae for the degradation of orphaned proteins. Their absence leads to Golgi collapse and cellular death.

In mammalian cells, the molecular mechanism underlying Golgi quality control are only partially understood. Yet, RER1 is a highly conserved protein also found in the early Golgi of mammalian cells. There, it retrieves orphaned membrane proteins (typically unassembled subunits of multimeric protein complexes) from the early Golgi back to the ER. Dysregulation of the RER1 pathway has been linked to prevalent neurodegenerative diseases (e.g. Alzheimer's and Parkinson's) and cancer.

In this project, we aim to identify additional Golgi-resident proteins, including specific ubiquitin ligases, that cooperate with RER1 in Golgi quality control, thereby preventing the accumulation of orphaned proteins. So far, we have successfully generated RER1 knockout (RER1KO) cell lines in Hap1, HEK293T, and HeLa cells, along with their corresponding rescue cell lines. We have identified two novel potential RER1 cargoes, and our findings suggest that loss of RER1 leads to elevated proteostasis stress, indicating a role of the Golgi apparatus in protein quality control.

To further address, these questions, we plan to perform mass spectrometry-based immunoprecipitation of tagged RER1 to identify additional cargo proteins and potential interacting partners involved in Golgi associated proteostasis. In parallel, we will conduct a CRISPR-Cas9 KO screen targeting ubiquitin ligases to uncover key regulatory factors contributing to Golgi quality control. These approaches will be complemented by molecular cloning, confocal microscopy, and a range of biochemical assays to dissect the mechanisms underlying Golgi-mediated protein surveillance.

Together, this project aims not only to enhance our understanding of protein quality control mechanisms in the Golgi apparatus but also to elucidate their broader implications for cellular health and disease.

Dual function of ERH in primary miRNA biogenesis

Simon Aschenwald

MicroRNAs are small non-coding RNAs that mediate post-transcriptional silencing of most mammalian genes. They are generated in a multi-step process initiated by the Microprocessor, a protein complex composed of DROSHA and DGCR8. Recent studies have described the phenomenon of "cluster assistance", in which a prototypic primary miRNA hairpin can license the Microprocessor-mediated processing of a clustered suboptimal hairpin in cis. Genetic screening and mechanistic analyses led to the identification of two critical factors for this process, SAFB2 (scaffold attachment factor B2) and ERH (enhancer of rudimentary homolog), which have been shown to associate with the N-termini of DROSHA and DGCR8, respectively, but also form a complex with each other. However, it remains unclear how SAFB2 and ERH can alter the Microprocessor substrate specificity, and whether the described protein-protein interactions are required for cluster assistance.

We focused on the role of ERH and show that its loss largely phenocopies the effect of SAFB1/2 deletion on the miRNA transcriptome, suggesting that both factors are involved in the same processes of primary miRNA biogenesis. In this context, our data demonstrate that both SAFB1/2 and ERH are required for efficient Microprocessor feedback regulation via processing of pri-miR-1306, uncovering a clear physiological function of cluster assistance. Mechanistically, our data show that ERH-mediated cluster assistance depends neither on its direct association with SAFB2 nor on its described interaction with DGCR8. In contrast, disrupting the ERH binding site within DGCR8 drives the processing of a subset of cluster assistance-unrelated pri-miRNAs. Thus, our study reveals dual roles of ERH in primary miRNA biogenesis, a largely suppressive one driven by its direct binding to DGCR8, and the other in cluster assistance that does not require DGCR8 binding.

Migration and Contact Guidance in cancer cells

Pere Patón González

Metastases are the leading cause of cancer-related mortality, yet no therapies specifically target cancer cell dissemination. Radially aligned collagen fibres are often observed around tumours that have started to spread. Cancer cells invade along those fibres in a process known as contact guidance. Although this process has been recognized for decades, its underlying mechanism remains unclear. To investigate this process, we developed a soft lithography method to generate transparent nanocurvatures that recapitulate aligned collagen fibres. We then optimized an automated workflow to track cell migration along nanocurvatures using phase contrast imaging. This allowed us to observe that metastatic breast cancer cells (MDA-MB-231) exhibit strong contact guidance.

We reasoned that adhesion and force transmission are key for contact guidance. Focal adhesions (FAs) typically mediate adhesive migration by connecting the extracellular matrix to the cytoskeleton, enabling force transmission. Talin1 is a key protein for FA assembly. To assess the role of FA in contact guidance, we generated Talin1-deficient clones (MDA dTLN1). Surprisingly, dTLN1 cells retained their ability to undergo contact guidance, suggesting an alternative mechanism for topography sensing. To further explore force transmission in contact guidance, we performed a small-scale drug screen targeting the actin and microtubule cytoskeleton using topographical migration as a readout. Our results indicate a critical role for microtubules in contact guidance, while at the same time confirming that actin and focal adhesions are dispensable.

In search for alternative adhesions that might play a role in contact guidance, we investigated Cortical Microtubule Stabilizing Complexes (CMSCs), which tether microtubules to the plasma membrane and adhesion structures. We observed that two structural components of the CMSCs, Liprin-a1 and CLASP1, are required for contact guidance. Future studies will focus on defining more in depth the function of CMSCs in topography sensing. Unravelling this mechanism may open the door to new anti-metastatic therapies.

Pediatric microbiome: neonates to adulthood

Adam Pollio

The human microbiome is a dynamic pseudo-organ that has a key role in digestion, disease, and development. The gut microbiome has been shown to be a tool for evaluating disease at a more macro scale in pediatric patients. It has also been shown to act through the gut-brain axis to predict psychological development. It has more recently been shown that viral and fungal communities also play a key role in the changes that occur overtime within the microbial community. Here, we evaluate the maturation of microbial communities from birth through adulthood in humans. We used a systematic literature search to identify papers with pediatric cohorts and shotgun metagenomic data. Inclusion criteria were pediatric patients paired with metadata (date of birth, geographic region, diet, etc). We split the data into 5 tranches by age A (0-1 years), B (1-2 years), C (3-13 years), D (13-18 years), E (adult-control). We ran each group through a uniform bioinformatic pipeline for trimming qc e=referenced based taxonomy analysis (MetaPhlan 4). We have identified 7856 individuals from a total of 77 studies. We had over 3000 individuals sampled in each of the first two groups. Data in older age groups are limited within the scope of our search strategy. Prevalence and abundance data will be used to identify core microbiomes for the age groups as well as for geographic groups. Unsurpervised clustering and supervised machine learning algorithms will be used to group geographic populations and identify discriminating factors between cohorts. Additionally, we will establish the viriome and the mycobiome based on a similar methodology using Kraken2 and Kaiju databases. Lastly, we will make de-novo assembled MAGs (metagenomic-assembled genomes) to compare the viral-host relationships during gut microbiome maturation.

Assessing brain magnetic microstructure in aceruloplasminemia using quantitative MRI

Alexander Stürz[1], Marlene Panzer[2,3], Elke R. Gizewski[1,4], Heinz Zoller[2,3], Christoph Birkl*[1,4]

[1] Department of Radiology, Medical University of Innsbruck, Innsbruck, Austria
[2] Department of Internal Medicine I, Medical University of Innsbruck, Innsbruck, Austria
[3] Christian Doppler Laboratory on Iron and Phosphate Biology, Innsbruck, Austria
[4] Neuroimaging Research Core Facility, Medical University of Innsbruck, Innsbruck, Austria
* Corresponding author: christoph.birkl@i-med.ac.at

INTRODUCTION
Quantifying brain microstructure using magnetic resonance imaging (MRI) is essential for a wide range of medical applications. Although transverse relaxation and Larmor frequency shifts provide access to magnetic microstructure, their interpretation is still largely empirical. Obtaining precise biophysical models is challenging due to the complexity of biological tissue and the involvement of physical processes across multiple length scales.
In this work, we employ a biophysical model that explicitly links magnetic microstructure to measurable macroscopic MRI parameters. We used our biophysical model to study tissue microstructure in patients with aceruloplasminemia (ACP), a rare pathology characterized by extreme iron accumulation and enlarged iron-loaded cells.

METHODS
Quantitative brain MRI of three patients with ACP and three matched healthy controls was acquired in vivo on a 3 Tesla system. Transverse relaxation rates (R2*, R2) and magnetic susceptibility maps (QSM) were derived from the measured data and interpreted within a biophysical framework supported by theoretical considerations and Monte Carlo simulations.

RESULTS
Across deep gray matter brain regions, patients exhibited higher R2* and R2 values compared to controls, accompanied by markedly increased R2*/R2 ratios. Monte Carlo simulations of spherical magnetic inclusions predicted the same behavior, showing an increase of the R2*/R2 ratio with inclusion size. Analysis of the relationship between R2* and bulk magnetic susceptibility further revealed a substantially steeper susceptibility-dependent relaxation slope in patients (295.93 Hz/ppm) compared to controls (162.25 Hz/ppm). For reference, theory predicts a slope of 324.4 Hz/ppm.

CONCLUSION
The observed in vivo relaxation and susceptibility behavior was consistent with theoretical predictions and Monte Carlo simulations. The microstructural characteristics are in agreement with reported histopathological findings in ACP. Together, these results demonstrate that a multiparametric qMRI approach combining relaxometry and QSM enables a detailed assessment of tissue magnetic microstructure and provides sensitivity not only to increase in iron concentration but also to size differences of magnetic inclusions in vivo.

Nikon

Experience effortless, high-performance imaging

ECLIPSE Ji with AX

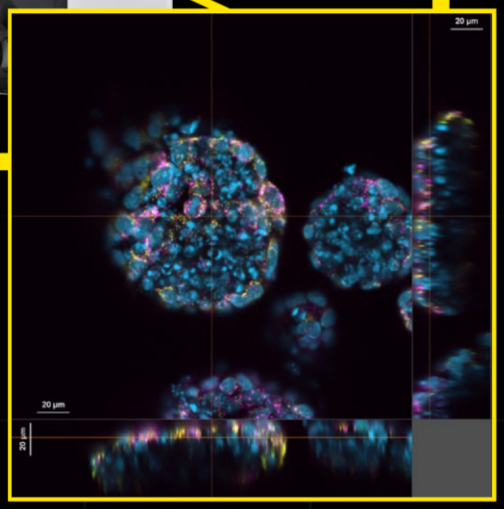

Fully automated platform featuring cutting-edge confocal capabilities

ECLIPSE Ji

- Robust and minimal training required
- User friendly with automated sample detection and simple navigation

ECLIPSE Ji with **AX**

AX

- High confocal image quality
- High resolution across the entire objective range without sacrificing the field of view
- Excellent imaging in depth

NIS.ai **Maximize reproducible** scientific results with **minimal** manual intervention

Single automated instrument which seamlessly integrates **widefield** and **confocal imaging**

Are you looking for…

- From whole organism to subcellular imaging
- Future proof & upgradable as your needs evolve
- Accommodating different sample types
- Easy for daily use with built-in flexibility

Contact us for the offer details:

For more information contact:

marko.pende@nikon.com

VISIT OUR WEBSITE

LEARN MORE

Poster overview

Even numbers on Thursday, odd numbers on Friday

Hanna Huvaiz	Day 2	Poster Nr.1
Divyadharshini Sakthivel	Day 1	Poster Nr.2
Fabian Rabensteiner	Day 2	Poster Nr.3
Sree Jeevitha Parameswaran	Day 1	Poster Nr.4
Amelie Schurer	Day 1	Poster Nr.6
Alexeja Kleiter	Day 1	Poster Nr.8
Magdalena Wildt	Day 2	Poster Nr.9
Lara Harringer	Day 1	Poster Nr.10
Nino Kobakhidze	Day 2	Poster Nr.11
Rotraud Hirschberger	Day 1	Poster Nr.12
Pauline Bicker	Day 2	Poster Nr.13
Benedikt Kindl	Day 1	Poster Nr.14
Carolin Becker	Day 2	Poster Nr.15
Lorena Neurauter	Day 1	Poster Nr.16
Stefan Salzmann	Day 2	Poster Nr.17
Michael Vogetseder	Day 1	Poster Nr.18
Christopher Hettegger	Day 2	Poster Nr.19
Michael Swoboda	Day 1	Poster Nr.20
Anna Verena Roth	Day 2	Poster Nr.21
Lorenzo Merotto	Day 1	Poster Nr.22
Felix Petschko	Day 2	Poster Nr.23
Clemens Untersulzner	Day 1	Poster Nr.24
Irene Rigato	Day 2	Poster Nr.25

Leonie Wolf	Day 1	Poster Nr.26
Matthias Groell	Day 2	Poster Nr.27
Johannes Bereiter-Payr	Day 1	Poster Nr.28
Erica Alfonsi	Day 2	Poster Nr.29
Alexandra Fritz	Day 1	Poster Nr.30
Clancy Cerejo	Day 2	Poster Nr.31
Eva Rauch	Day 1	Poster Nr.32
Tariq Oluwakunmi Agbabiaka	Day 2	Poster Nr.33
Turkhan Mehdiyev	Day 1	Poster Nr.34
Angelina Ananich	Day 2	Poster Nr.35
Isabell Gonnella	Day 1	Poster Nr.36
Alina Nowak-Rainer	Day 2	Poster Nr.37
Michaela Mayr	Day 1	Poster Nr.38
Victoria Schön	Day 2	Poster Nr.39
Lea Dümpelmann	Day 1	Poster Nr.40
Horia C. Hermenean	Day 2	Poster Nr.41
Janik Kokot	Day 1	Poster Nr.42
Hamed Wafa	Day 2	Poster Nr.43
Jennifer Birke	Day 1	Poster Nr.44
Lukas Vergeiner	Day 2	Poster Nr.45
Sebastian von der Emde	Day 1	Poster Nr.46
Volker Schaefer	Day 1	Poster Nr.48
Wolfgang Straka	Day 2	Poster Nr.49
Petr Simurda	Day 1	Poster Nr.50
Alberto Galimberti	Day 2	Poster Nr.51

Magdalena Matić	Day 1	Poster Nr.52
Felix Melchior	Day 2	Poster Nr.53
Judith Stefanie Söller	Day 1	Poster Nr.54
Simon Leiter	Day 1	Poster Nr.56
Philipp Fischer	Day 2	Poster Nr.57
Anita Sandor	Day 1	Poster Nr.58
Lina Schwaighofer	Day 2	Poster Nr.59
Samuel Pröll	Day 1	Poster Nr.60
Vanessa Heim	Day 1	Poster Nr.62
Florian Vogetseder	Day 2	Poster Nr.63
Celina Wilgermein	Day 1	Poster Nr.64
Isabella Weisleitner	Day 2	Poster Nr.65
Martina A. Höllwarth	Day 1	Poster Nr.66
Nicolas Melcher	Day 2	Poster Nr.67
Sophie Ann Erckert	Day 1	Poster Nr.68
Nastasiia Artamonova	Day 2	Poster Nr.69
Jonas Eder	Day 1	Poster Nr.70
Noelia Peña Arauzo	Day 2	Poster Nr.71
Thanida Laopanupong	Day 2	Poster Nr.73
Betül Sari	Day 1	Poster Nr.74
Alexandra Ioannou	Day 2	Poster Nr.75
Maria Ioannou-Nikolaidou	Day 1	Poster Nr.76
Katharina Thaler	Day 2	Poster Nr.77
Lukas Prüfer	Day 1	Poster Nr.78
Doris Stepić	Day 2	Poster Nr.79

Sebastian Schauflinger	Day 1	Poster Nr.80
Martina Saretto	Day 2	Poster Nr.81
Katja Rungger	Day 2	Poster Nr.83
Meike Terwort	Day 1	Poster Nr.84
Franziska Reier	Day 2	Poster Nr.85
Julia Rudek	Day 1	Poster Nr.86
Jonas Dunz	Day 2	Poster Nr.87
Kristina Jasmin Grassl	Day 2	Poster Nr.89
Christoph Frisch	Day 2	Poster Nr.91
Felix Puster	Day 2	Poster Nr.93
Greta Hemicker	Day 1	Poster Nr.94
Caren Agreiter	Day 2	Poster Nr.95
Kamila Saramak	Day 1	Poster Nr.96
Tendral Sekar	Day 1	Poster Nr.98
Martina Steinlechner	Day 2	Poster Nr.99
Christopher Schaar	Day 2	Poster Nr.101
Aldrien Ryan Naces Reynaldo	Day 1	Poster Nr.102
Riccardo Lunelli	Day 1	Poster Nr.104
Antonia Degen	Day 1	Poster Nr.106
Nidhi Srinivasan	Day 2	Poster Nr.107
Isidor Happacher	Day 1	Poster Nr.108
Frederik Eisendle	Day 2	Poster Nr.109
Lynn Muller	Day 2	Poster Nr.111
Lukas Hallbrucker	Day 1	Poster Nr.112
Ulrich Sturm	Day 2	Poster Nr.113

David Wippel	Day 1	Poster Nr.114
Alexander Tilg	Day 1	Poster Nr.116
Abdallah Abdalhady	Day 2	Poster Nr.117
Alessia Rossi	Day 1	Poster Nr.118
Pallavi Saxena	Day 2	Poster Nr.119
Elena Mayer	Day 1	Poster Nr.120
Carina Spitzauer-Perger	Day 2	Poster Nr.121
Matthias Demetz	Day 1	Poster Nr.122
Ryoichi Taguchi	Day 2	Poster Nr.123
Erika Kvalem	Day 1	Poster Nr.124
Niklas Schomisch	Day 2	Poster Nr.125
Lisa Waltle	Day 1	Poster Nr.126
Alice Vincenzi	Day 2	Poster Nr.127
Katarína Schwarzová	Day 1	Poster Nr.128
Julian Fenkart	Day 2	Poster Nr.129
Marta Konopka	Day 1	Poster Nr.130
Manuela Ranalter	Day 1	Poster Nr.132
Lukas Scherer	Day 2	Poster Nr.133
Lukas Kampik	Day 1	Poster Nr.134
Maximilian Lutz	Day 2	Poster Nr.135
Cristina Alomar Domínguez	Day 1	Poster Nr.136
Laura Sammarco	Day 2	Poster Nr.137
Fabio Fugger	Day 1	Poster Nr.138
Samuel Vorbach	Day 2	Poster Nr.139
Lena Gatterer	Day 1	Poster Nr.140

Philipp Geiger	Day 2	Poster Nr.141
Verena Sturmlehner	Day 1	Poster Nr.142
Ronja Lohmann	Day 2	Poster Nr.143
Philipp Deisl	Day 1	Poster Nr.144
Anto Abramovic	Day 2	Poster Nr.145
Daniel Pavluk	Day 1	Poster Nr.146
Alex Kaser	Day 2	Poster Nr.147
Pauline Alton	Day 1	Poster Nr.148
Mateus Enzenberg	Day 2	Poster Nr.149
Dagmar Morell Hofert	Day 1	Poster Nr.150
Emanuel Vogel	Day 2	Poster Nr.151
Lena Gufler	Day 1	Poster Nr.152
Paul Petermann	Day 2	Poster Nr.153
Robert Barket	Day 1	Poster Nr.154
Luisa Delazer	Day 2	Poster Nr.155
Katharina Wagner	Day 1	Poster Nr.156
Stefan Hardy Lung	Day 1	Poster Nr.158
Lena Denk	Day 2	Poster Nr.159
Olayinka Ruth Bamidele	Day 2	Poster Nr. 163

Sample
to Insight

QIAGEN

Transforming the PCRexperience

Fully integrated nanoplate-based digital PCRsystemfor absolute quantification

- Superior partitioning for high accuracy and sensitivity
- Advanced multiplexing for simultaneous multiple target detection
- Walk-away workflow automation for faster time to results
- Flexible and scalable instruments for various throughput needs

Visitwww.qiagen.com/dPCR for more information or scan the QRcode

Poster abstracts

Day 2 Poster Nr. 1

Hanna Huvaiz

The pancreatic β cell plays a central role in glucose homeostasis by secreting insulin in response to elevated blood glucose levels. This process relies on a tightly regulated sequence of insulin granule docking, priming, and exocytosis. A key feature of β-cell physiology is the precise spatial and temporal control of calcium influx, which links electrical activity to insulin secretion. Voltage-gated calcium channels (VGCCs), particularly the L-type channels CaV1.2 and CaV1.3, represent the main pathway for calcium entry during membrane depolarization and serve as the principal trigger for exocytosis.

Importantly, calcium signaling in β cells is highly localized. Instead of acting globally, calcium entry forms microdomains near docked insulin granules, enabling rapid and efficient exocytosis. Previous studies have shown that insulin release occurs preferentially at membrane sites enriched in L-type Ca^{2+} channels and scaffolding proteins such as Munc13, suggesting that spatial coupling between calcium channels and granules is essential for efficient secretion. Disruption of this coupling has been implicated in type 2 diabetes (T2D), where insulin secretion becomes impaired despite relatively preserved calcium influx.

This project aims to investigate how L-type calcium channels are recruited and stabilized at insulin granule release sites in pancreatic β cells. Using advanced imaging approaches and quantitative analysis of channel–granule organization, we will examine the spatial relationship between VGCC clusters and insulin granules under physiological and disease-relevant conditions. By characterizing the mechanisms that regulate channel–granule coupling, this work seeks to provide new insights into the molecular organization of insulin secretion and its disruption in T2D.

CaV1.2-dependent δ-cell activity coordinates β-cell function and glucose homeostasis

Divyadharshini Sakthivel

Divyadharshini Sakthivel, Rosalie Dittrich, Dominik Regele, Sonja Töchterle & Dirk Meyer

Institute for Molecular Biology, University of Innsbruck.

Abstract:

Pancreatic islet function depends on coordinated interactions among β-, α-, and δ-cells to maintain glucose homeostasis. While β cells are the primary source of insulin, increasing evidence indicates that non-β endocrine cells critically shape β-cell excitability and hormone secretion. However, the mechanisms by which δ cells regulate β-cell function remain poorly understood.

Here, we investigate intra-islet communication using a zebrafish model lacking the L-type calcium channel CaV1.2, which exhibits severe hyperglycemia and disrupted islet calcium dynamics. Using in vivo and ex vivo calcium imaging, we show that δ cells in wild-type islets display rhythmic calcium oscillations consistent with pulsatile somatostatin signaling. In contrast, CaV1.2-deficient δ cells are calcium-silent, indicating a loss of δ-cell activity.

Notably, targeted ablation of δ cells in CaV1.2 mutants unexpectedly rescued the hyperglycemic phenotype, despite the absence of detectable δ-cell calcium activity. This finding reveals that dysfunctional δ cells retain a regulatory influence over β-cell–dependent glucose homeostasis and that their removal alleviates islet dysfunction.

Together, our results identify CaV1.2 as a critical regulator of δ-cell activity and uncover a previously unappreciated role for δ cells in shaping β-cell function through non-cell-autonomous mechanisms. These findings highlight the importance of intra-islet communication in glucose regulation and provide new insight into how disruption of δ-cell function contributes to metabolic dysregulation.

Keywords: CaV1.2, pancreatic islets, glucose homeostasis, calcium signaling, zebrafish

Fabian Rabensteiner

Gastrulation with the formation of the three germ layers followed by a step by step fate determination forms a keystone in the development of multicellular organisms. During this early process, cells undergo extensive chromatin remodelling which alters its structure and regulates gene transcription. FoxH1 is a known major key transcription factor which, during this early embryotic development, controls and fine tunes regulatory gene programs involved in mesoendoderm induction and left-right patterning. Recent studies further suggest FoxH1 as a potential pioneer-transcription-factor with more general function in chromatin remodelling during transition during early cell specification. Recent work from our group in zebrafish revealed interaction of FoxH1 with various DNA-sites lacking the FoxH1 consensus motif, suggesting that FoxH1 might indirectly influence the chromatin state as part of a bigger protein complex. However, how FoxH1 contributes to loci targeting, with which proteins it is interacting and the underlying kinetics during this early remodelling is still unknown. To address these questions, a set of human iPSC cell lines with domain-specific FOXH1 mutations was established. The DNA recognizing FH domain as well as the protein interacting SI domain are thought to be essential for chromatin remodelling events and available data suggests that the absence of either one of them will interfere with FoxH1's function of chromatin-looping. By the usage of these cell lines, the specific functions of each domain can be identified. Additionally, the lines are tagged with a 3xTY1 epitope, which will further be used for a molecular characterization of direct targets.

Frequency-Specific Neural Degeneration in the Aging Cochlea

Sree Jeevitha Parameswaran

The cochlea encodes sound through a precise tonotopic organization, with specific frequencies mapped to distinct locations along its length, spanning approximately 1 kHz to 100 kHz in mice. To enable frequency-specific analysis in thin plastic sections, we generated a three-dimensional cochlear frequency map using high-resolution micro-CT datasets combined with the Greenwood function. Given the minimal anatomical variation in inbred mouse strains, this approach provides a standardized reference for accurate frequency localization.

Age-related auditory nerve degeneration influences cochlear implant outcomes, with strain-dependent, frequency-specific patterns of selective nerve fiber loss and preservation that directly affect hearing function. By integrating frequency-specific auditory brainstem response (ABR) audiometry with precise anatomical mapping, we correlated physiological measurements with nerve fiber morphometry. Manual segmentation of the basilar membrane at the level of inner hair cells enabled spatial mapping of nerve fibers into an atlas dataset, allowing accurate registration of thin sections within the micro-CT framework for frequency-correlated morphological analysis.

Automated segmentation and g-ratio quantification using deep learning algorithms provide an objective assessment of nerve fiber integrity across defined frequency regions. By correlating ABR parameters, including hearing thresholds and latencies in young and aged mice, this approach refines our understanding of frequency-specific neural degeneration. These insights into cochlear pathology may support optimized cochlear implant electrode placement and stimulation strategies aimed at preserving and enhancing neural function in critical frequency regions.

PRTG as a novel key regulator of human neurodevelopment

Amelie Schurer

Amelie Schurer, Angeliki Spathopoulou, Travis Spitzock, Marcel Tisch, Katharina Günther, Marta Suarez Cubero, Julianne Beirute, Christopher Esk, Frank Edenhofer

Institute of Molecular Biology, Department Genomics, Stem Cell Biology & Regenerative Medicine, Leopold-Franzens-University Innsbruck, Innsbruck, Austria

To model earliest developmental processes, we previously established an embryonic tissue-derived system for early human neurodevelopment. These monoclonally expandable, naïve, and pre-polarized embryonic neural stem/progenitor cells (eNSPCs) are characterized by high PAX2/PAX6 and low OCT4 expression. Transcriptomic profiling and immunocytochemistry revealed Protogenin (encoded by PRTG), a member of the immunoglobulin superfamily, as highly expressed in eNSPCs and downregulated during later developmental stages. We found that Protogenin exhibits an uniformal distribution in eNSPCs, indicating a pre-polarized phenotype. In mouse, PRTG is highly expressed between E7–E9.5, overlapping with rising SOX2 and declining Oct4 expression. As PRTG and SOX2 persist, neuronal markers (Nestin, ASCL1, Tubb3) emerge, defining a distinct stage of neural tube development in mice. PRTG knockdown in chicken neural tube induces premature neuronal differentiation marked by a SOX2- and TUBB3high expression profile compared to wildtype (Wong et al., 2010). PRTG-/- mice show decreased survival of rostral cephalic neural crest cells during early development caused by decreased interaction of Protogenin with Radil, inducing decreased cell migration and increased apoptosis (Wang et al., 2013). More recently, PRTG has been reported to modulate GDF11/SMAD2 signaling in mouse neural tube patterning (Hung et al., 2024). The underlying hypothesis of our study is that PRTG functions as a key regulator during early human neurodevelopment, particularly in the transition from pluripotency to neuronal commitment and in subsequent processes such as neural tube formation and patterning. Employing siRNA and CRISPRi-mediated PRTG knockdown in iPSC-derived neuronal differentiation systems we show revealed impaired rosette formation, characterized by increased rosette numbers and overall smaller lumen diameters. These findings point to an essential role of PRTG modulating human neural tube formation and patterning. To further investigate the role of PRTG, we are generating PRTG knockout and inducible overexpression lines to examine effects on progenitor identity, apicobasal polarity, adhesion, and differentiation dynamics. Complementary approaches, including ATAC-seq and in silico analysis of the PRTG genomic locus, will identify its upstream regulatory landscape. Additionally, characterization of PRTG-perturbed populations will uncover downstream targets and unravel gene regulatory networks. In summary, we aim to define PRTG's functional and regulatory role during neurodevelopment, to contribute to a better understanding of human specific early neurodevelopment in physiological and pathological conditions.

Development of an immunocompetent 3D bioprinted melanoma-on-chip model

Alexeja Kleiter

Melanoma remains one of the most aggressive skin cancers, and understanding tumor cell interactions with the immune system is crucial for developing effective treatments. However, tumor immunology research relies heavily on mouse models, but translating these findings to patients is challenging. To address this, we focus on developing a human 3D bioprinted melanoma-on-chip model.
As part of this effort, we printed in microfluidic chips and evaluated fibroblast viability, keratinocyte differentiation (confirmed by cytokeratin 1/10 staining), and overall tissue integrity.
In parallel, melanoma cell lines (MugMel 2, MugMel 3, and A375) were tested for their growth properties and spheroid formation potential. These spheroids were then incorporated into the 3D bioprinted skin model to establish a 3D melanoma-on-chip model.
To incorporate human DC, protocols to differentiate cDC1, cDC2, and pDC from CD34+ hematopoietic stem cells were established. Overall, we confirmed that human cDC1 and cDC2 generated from CD34+ precursors are valuable substitutes for blood DC subtypes to generate bioprinted immunocompetent models. Therefore, we will incorporate them into our 3D bioprinted melanoma-on-chip model and study the interactions between melanoma cells and DC.
Further, protocols for generating Langerhans cells (LC) from CD34+ progenitors are currentlytested, and markers CD1a and Langerin are evaluated on LC.
Including immune cells and melanoma cells in the 3D bioprinted skin will be a significant step forward in the study of skin immunology and melanoma, offering new opportunities for investigating tumor-immune dynamics and testing therapeutic approaches.

Slowing cognitive decline in alpha-synucleinopathies by enhancing physical activity: ALPHA-FIT study protocol and gender aspects

Magdalena Wildt

Introduction

Yearly phenoconversion rates of isolated REM sleep behavior disorder (iRBD), an early stage alpha-synucleinopathy (Högl et al. 2017), are estimated at 6.25% (Postuma et al. 2019), reaching 96.6% at 14 years (Galbiati et al. 2019). Prevalence of iRBD is between 1.06-1.34% in adults and older adults (AASM, 2023, 3rd edition), and higher prevalence in males compared to females is reported. In younger patients, sex differences are less pronounced (AASM 2023, 3rd edition, Rodriguez et al. 2017). Hormonal factors have been proposed to explain higher prevalence in male population, but data did not support this hypothesis (Iranzo et al. 2007). Phenoconversion-risk is sex-independent (Li et al. 2023). Increased physical activity has been correlated with a decreased risk to develop Parkinson's Disease (Fang et al. 2018) and showed positive effects on cognitive functions in Parkinson's Disease patients (Kim et al. 2023).

Methods

This double-blind, placebo-controlled study is conducted at Center for Sleep Medicine, Department of Neurology, Medical University Innsbruck, Austria, at the Department of Parkinson, Sleep and Movement Disorders, University Hospital Bonn, Germany, and at the Radboudumc Center of Expertise for Parkinson & Movement Disorders, Department of Neurology, Radboud University Medical Center, Nijmegen, Netherlands. 270 iRBD-patients and 100 controls (age-/sex-matched) aged 50-75 years will be included. Exclusion criteria are daily physical activity over 120 minutes or over 10.000 steps during the four-week eligibility period, relevant cardiovascular diseases and impaired fine motor skills or cognitive ability. Participants over one year will gradually increase their physical activity by 100% (intervention) or 10% (control group) compared to baseline. This will be done in an individually tailored fashion by using a motivational smartphone-app connected to a Fitbit. Neurocognitive tests, brain MRI, movement analysis and different questionnaires will be administered and blood samples drawn in six-months intervals. In between, participants will complete a self-administered cognitive test battery using the Neuronation app bi-weekly.

Endpoints

Primary endpoint is to investigate the effects of increased physical activity on non-motor, in particular cognitive, and motor changes. Changes from baseline to follow-up will be compared between intervention and control-group among iRBD-patients, and between iRBD-patients and healthy controls within the two groups. Brain MRI and blood markers of brain-ageing will be evaluated as secondary endpoints. Sex differences will be investigated.

Conclusion

This study could offer valuable novel neuroprotective non-pharmacological interventions for iRBD-patients if physical activity will be shown to improve cognitive and motor function, and to reduce the risk of phenoconversion. The intervention is easily administrable, broadly applicable and cost-effective.

Not only the higher prevalence of iRBD in male (Innsbruck-Databank 85.21% male) but also (socio-) cultural/language aspects are a challenge in the execution of this study as cognitive tests used for the evaluation of the primary endpoint are language dependent and educational background has impact on performance. All these aspects will be taken into account.

Lara Harringer

During brain development neural stem cells initially expand through symmetric cell division before transitioning to asymmetric cell division to maintain neural stem cells while producing differentiated cell types. The exact timing of this transition to asymmetric division of neural stem cells and the generation of more committed cell types varies between species, resulting in lineage size heterogeneity. Cortical organoids are a valuable 3D in vitro model to study human brain development since they mimic many aspects of in vivo development. While organoid lineage tracing and computational modelling have demonstrated that organoid development follows a dynamic growth pattern, individual lineages vary in size and large lineages maintain a pool of symmetrically dividing cells long after onset of neurogenesis. Growth perturbation experiments in chimeric organoids indicated that cells are capable of compensating for a remarkable degree of tissue insults. This suggests that neural stem cell fate is plastic and human brain development is governed by tissue-mediated growth control. Ablation assays in chimeric organoids were performed to characterize the compensatory growth capacity of neural stem cells during development. Microscopy- and flow cytometry-based assays revealed nearly complete phenotype rescue of organoids four weeks after cell perturbation, starting on day 16, while earlier induction resulted in complete rescue. Immunohistochemistry analysis showed replenishing organoids maintaining similar progenitor-to-neuron ratios compared to controls, indicating cell fate maintenance throughout compensation stages. Flow-cytometry, transcriptomic, and image-based analyses revealed changes in cell cycle dynamics in ablated organoids instead, indicating adaptive cell cycle control as a major driver in tissue-mediated growth control.

Oroboros MitoAnalytics

Präzise mitochondriale Analyse

Entdecken Sie die **Energie** Ihrer Zellen

Warum sind **Mitochondrien** wichtig?

- Mitochondrien sind die **Kraftwerke der Zellen**. Sie wirken als mikroskopisch kleine Elektromotoren des Lebens.
- Die Mitochondrien verbrennen bei der **Zellatmung** die Kalorien unserer Nahrung und erzeugen nutzbare Energie.
- **Sauerstoffverbrauch** der Mitochondrien ist ein Schlüssel zu **gesundem Altern**. Bewegung, Sport in der Natur – besonders in alpiner Höhe – sind die beste **Medizin für die Mitochondrien**.
- Regelmäßige **Analysen der Zellatmung** zeigen, wie sich Ernährung, Bewegung und Therapie auf Ihre Zellenergie auswirken – und schaffen die Grundlage für individuelle, gezielte Optimierungen.

©Oroboros Instruments

Warum **Oroboros** MitoAnalytics?

Unsere hohen **Qualitätsstandards** resultieren aus der engen Verbindung von Forschung und klinischer Praxis.

Dieses Zusammenspiel eröffnet neue diagnostische und therapeutische Perspektiven für eine **personalisierte medizinische Versorgung.**

Einblicke in die **Funktion Ihrer Mitochondrien**

Fortschritt wird messbar: Wie hoch ist die Leistungsfähigkeit Ihrer Mitochondrien?

©Shutterstock

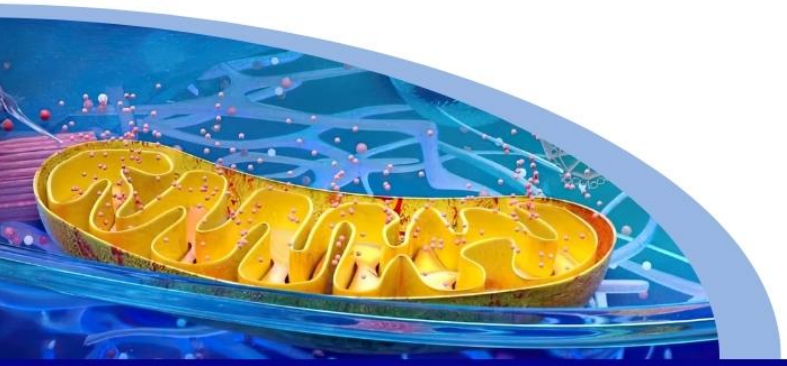

Einfache **Schritte**

1. Kontaktieren Sie uns: MitoAnalytics@oroboros.at
2. Vereinbaren Sie einen Termin für die Blutabnahme.
3. Wir testen die Zellatmung Ihrer Blutprobe und erstellen den wissenschaftlichen Befund zur mitochondrialen Leistungsfähigkeit.
4. Ihr:e Ärzt:in entwickelt die ganzheitliche Diagnose und bespricht sie mit Ihnen.

Oroboros MitoAnalytics
Schöpfstraße 18
6020 Innsbruck
www.oroboros-mitoanalytics.at

MitoAnalytics@oroboros.at
Tel +43 512 566 796-29

Enhanced carbon dioxide (CO_2) sensitivity and dysregulated interoceptive threat processing in a mouse model of high trait anxiety

Nino Kobakhidze

Nino Kobakhidze1, Sadegh Rahimi2, Francesca Silvagni2, Claudia Schmuckermair2, Pawel M. Matulewicz2, Arnau Ramos-Prats4, Sarah Gorkiewicz3 Gaia Novarino3, Francesco Ferraguti2, Nicolas Singewald1, Simone B. Sartori1
1Department of Pharmacology and Toxicology, Institute of Pharmacy and Center for Molecular Biosciences Innsbruck (CMBI), University of Innsbruck, Innrain 80-82/III, A-6020, Innsbruck, Austria.
2Institute of Pharmacology, Medical University of Innsbruck, Peter-May-Strasse 1a – 6020, Innsbruck, Austria.
3Institute of Science and Technology (IST) Austria, Klosterneuburg, Austria.
4Friedrich Miescher Institute for Biomedical Research, Basel, Switzerland.

Individuals diagnosed with anxiety disorders frequently exhibit disrupted perception and evaluation of internal bodily signals. Although altered interoception is increasingly recognized as a core component of anxiety pathology, the neural mechanisms underlying this dysfunction remain insufficiently characterized. In the present study, we investigated whether trait anxiety levels modulate the recruitment of anxiety-related neural circuits during CO_2 exposure, a well-established translational model for probing interoception-driven negative valence states.

To this end, mice selectively bred for high anxiety-related behavior (HAB) and normal anxiety-related behavior (NAB) were exposed to 10% CO_2-enriched air. Behavioral and physiological parameters were recorded to assess anxiogenic and autonomic responses. CO_2 exposure induced robust anxiety-like behavior in both lines; however, HAB mice displayed significantly stronger behavioral and autonomic responses compared to NAB controls, indicating enhanced CO_2 sensitivity in animals with high trait anxiety. To map neuronal activation patterns, c-Fos immunohistochemistry was performed as a marker of neuronal activity. Across experimental conditions, HAB mice exhibited hyperactivity in multiple limbic, hypothalamic, and brainstem regions implicated in stress and anxiety processing relative to NAB mice. Importantly, CO_2 exposure robustly activated the paraventricular nucleus (PVN) of the hypothalamus in both lines, with a significantly greater response observed in HAB animals, suggesting exaggerated hypothalamic stress recruitment in high trait anxiety.

Region-specific differences were also observed within the amygdala and insular cortex. In HAB mice, CO_2 inhalation selectively increased c-Fos–positive cells in the lateral amygdala, whereas no significant increase was detected in basal amygdalar or insular subregions. In contrast, NAB mice exhibited CO_2-induced increases in c-Fos expression within basal amygdalar and insular areas, indicating differential circuit engagement between anxiety phenotypes. These findings suggest that high trait anxiety is associated with a shift in interoceptive threat processing toward distinct amygdalar pathways, accompanied by altered cortical integration.

Ongoing experiments aim to further characterize the neuronal identity and molecular profile of CO_2-responsive insular neurons to better understand the cellular substrates underlying altered interoceptive processing. Collectively, our findings demonstrate that high-trait anxiety is associated with enhanced CO_2 sensitivity and dysregulated

recruitment of classical stress-related and interoceptive threat-processing circuits. These alterations mirror key features of anxiety disorders and support the validity of HAB mice as a translational model for investigating the neurobiological basis of interoception-triggered hypersensitivity in high-trait anxiety.

Defining the Substrate Specificity of Caspase-2

Rotraud Hirschberger

Authors: Rotraud Hirschberger1, Raed Shalaby2, Ana Garcia-Saez2, Andreas Villunger1

Affiliation: 1 Institute for Developmental Immunology, Biocenter, Medical University of

Innsbruck; 2 Institute for Genetics, CECAD, University of Cologne

Proteases are enzymes balancing activation and degradation of proteins in living organisms. One class of proteases – caspases – are a collection of cysteine-dependent aspartate-specific proteases that regulate cell death, inflammation, cell cycle progression and differentiation.

Caspases are categorized into three major groups differentiated by their structure and function: initiator-, effector- or inflammatory caspases. Focusing on initiator-caspases it has been shown that they have a long pro-domain, allowing interaction with adapter proteins, as well as a large and a small subunit. For activation initiator caspases, such as caspase-1, 2, or -9, rely on auto-processing aided by their recruitment to activation

platforms like the inflammasome, the PIDDosome, or the apoptosome, respectively.

The PIDDosome assembles in response to supernumerary centrosomes resulting in the activation of caspase-2. Active caspase-2 can cleave two critical substrates, MDM2 and BID, leading to cell cycle arrest or cell death.

Recent data highlights differences in cell fate dependent on the cell type, i.e., cell cycle arrest in epithelial tissue vs. apoptosis in hematopoietic cells. This leads to questions for the cellular contexts influencing substrate preference and the mode of operation of caspase-2 affecting decision-making. To address these questions we started to compare the substrate processing activity of caspase-2 in vitro using purified proteins and to study its subcellularly localization via immunofluorescence in resting and activated cells exploiting endogenous protein tagging, to understand how caspase-2 can control cell fate in different cell types.

Pauline Bicker

Diabetic retinopathy (DR) is a major complication of diabetes characterized by vascular and neuronal damage in the retina. Retinal neurodegeneration has been hypothesized to contribute to DR pathogenesis either independently or as a consequence of vascular injury. Inflammatory processes regulated by matrix metalloproteinases (Mmps) are central to both tissue injury and regeneration, and emerging evidence implicates Mmps in DR-related tissue damage as well as in photoreceptor (PR) regeneration. Although hyperglycaemia affects both vascular and neuronal cells, the molecular mediators involved—particularly the role and activity of Mmps—remain poorly defined. Moreover, heat shock protein 70 (Hsp70), a key regulator of cellular stress responses and proteostasis, was suggested to interact with activated Mmp9 contribute to mitochondrial injury. We currently examine the expression, activity, and interplay of Mmp9 and Hsp70 in an established zebrafish model of DR. Unlike humans, zebrafish can regenerate retinal neurons, and PR restoration occurs alongside vascular damage and neurodegeneration. Early results show that hsp70 and mmp9 proteins localize to the retinal photoreceptor layer, in proximity to mitochondria. Methods for detecting mmp9 protein activity in situ are being developed and applied. Western blot analysis is being used for comparison of protein levels between affected samples and controls. Protein localization and quantification in diabetic retina will provide new insights into the role of Mmps and Hsp70 in DR. Understanding how Mmps and Hsp70 contribute to both degeneration and repair will clarify their role in maintaining retinal homeostasis during diabetes. This can lead to identification of new molecular targets for mitigating neurodegeneration and promoting retinal regeneration in DR.

Digital secondary prevention after acute coronary syndrome: Design and rationale of the randomized TELE Alpine trial

Benedikt Kindl

Kindl B1, Schreinlechner M1, Mauracher D1, Baron D[3], Lederle-Kranzler S[3], Pusl T[2], Pavluk D1,

Raake P[2], Hinterseer M[3], Bauer A1, Reinstadler SJ1

1University Clinic of Internal Medicine III/ Cardiology and Angiology – Innsbruck, Austria

[2]University Clinic of Internal Medicin I/ Cardiology – Augsburg, Germany

[3]Medical Clinic of Internal Medicin – Füssen, Germany

Research Question:

Patients after acute coronary syndrome (ACS) frequently fail to achieve guideline-recommended targets for cardiovascular secondary prevention in routine clinical care. Digital health applications and structured telemedical support may help to improve guideline-directed goals in secondary prevention after ACS. This study aims to investigate whether app-based digital follow-up strategies, with or without digital consultations, improve fulfilment of guideline-defined secondary prevention targets at 12 months after ACS compared with usual care.

Material and Methods:

TELE-Alpine is a prospective, multicenter, open-label, randomized, three-arm superiority trial. A total of 351 patients with ST-elevation or non–ST-elevation myocardial infarction (STEMI/NSTEMI) following invasive management are randomized 1:1:1 to (1) non-digital usual care, (2) usual care plus a mobile health application or (3) usual care plus a mobile health application and structured digital consultations. Randomization is stratified by center and ACS subtype.

The primary endpoint is the modified INTERASPIRE guideline target score after 12 months, a 10-point composite measure capturing attainment of lifestyle, risk factor, and pharmacological treatment goals according to ACS guidelines. Secondary endpoints include individual score components, health-related quality of life (HeartQoL), adherence and digital engagement metrics, biosignal monitoring profiles, health care utilization, unplanned cardiovascular readmissions and major adverse cardiovascular events (MACE). The primary analysis follows the intention-to-treat principle using pairwise comparisons of mean scores between groups.

Expected Results:

This trial will start in Q3 2026 and is designed to evaluate the effectiveness of digital-augmented follow-up strategies after ACS. It is hypothesized that both digitally supported strategies will result in higher modified INTERASPIRE guideline target scores at 12 months than non-digital usual care, with the greatest improvement expected in the arm including structured digital consultations.

Funding: Interreg Bayern Österreich (Grant Number: BA0100299)

Human CACNA1D variant lines for comparative brain development phenotyping

Carolin Becker

Authors: Carolin Becker, Amelie Schurer, Verena Roth, Angeliki Spathopoulou, Beatriz Lopez-Amo Calvo, Prof. Frank Edenhofer, Christopher Esk

Calcium signalling plays a central role in brain development, regulating processes such as neuronal differentiation, migration, network formation and activity. Tight control of intracellular calcium homeostasis is therefore essential. One key regulator of calcium influx is the Cav1.3 L-type voltage-gated calcium channel, encoded by CACNA1D. Pathogenic variants in CACNA1D have been associated with a broad spectrum of clinical symptoms, including autism spectrum disorder or developmental delay, yet the developmental consequences of distinct patient variants remain poorly understood. 3D-models such as cerebral organoids offer valuable insight into early brain development and enable the investigation of gene–disease relationships in a human context.

This study aims to assess CACNA1D patient variants on brain development. To this end we generated human induced pluripotent stem cell (hiPSC) lines carrying different patient-derived CACNA1D variants which will be differentiated into cerebral organoids for analysis in isogenic backgrounds. To generate gene-modified human iPSC lines, a prime-editing workflow was established. Prime editing requires a pegRNA that identifies the target DNA sequence and encodes the intended edit, as well as a reverse transcriptase fused to an engineered Cas9 protein. Optimized conditions using stabilized epegRNA designs, La, a small RNA-binding protein, and a dominant-negative hMLH1 (hMLH1dn) were used to improve pegRNA stability and suppress mismatch repair activity, respectively. Gene editing was performed on 2 different cell lines (one male, one female) using Lipofection, followed by single-cell FACS sort, monoclonal expansion in 96-well plates and multiplexed NGS-based genotyping readouts of several hundred clones. Using this approach, 14 independent hiPSC lines carrying four different mutations were successfully generated. The cell lines are currently being stabilized, and differentiation into cerebral organoids will follow.

Modelling human tissue ageing in vitro: A comparative analysis of cortical brain organoids and heart organoids

Lorena Neurauter

Lorena Neurauter1, Theresa Lindlbauer1,2, Elisa Gabassi1, Marta Suárez-Cubero1, Frank Edenhofer1

1Department of Genomics, Stem Cell Biology and Regenerative Medicine, University Innsbruck, Innsbruck, Austria

2VASCage—Centre on Clinical StrokeResearch, Innsbruck, Austria

Ageing is a major risk factor for various chronic diseases such as stroke, neurodegeneration, and cardiovascular disease. It is characterized by a set of interconnected biological hallmarks including genomic instability, epigenetic alterations and mitochondrial dysfunction. While these processes have been extensively studied in animal models, their manifestation across distinct human tissues remains incompletely understood. This project aimed to investigate and compare ageing phenotypes in two human in vitro systems. To this end, induced pluripotent stem cell (iPSC)-derived cortical brain organoids (cBOs) and human heart organoids (hHOs) were artificially aged via doxycycline (DOX) -inducible progerin overexpression. Age-associated cellular changes were assessed by immunohistochemistry (IHC), including markers for genomic instability (γH2AX), epigenetic alterations (H3K9me), and nuclear lamina architecture (LMNA). Mitochondrial respiration was evaluated using high-resolution respirometry (Oroboros O2k) to assess bioenergetic consequences of ageing. As part of this work, the hHO protocol was further optimized to improve long-term culture conditions and robust progerin overexpression. Progerin overexpression induced key hallmarks of ageing in both organoid systems. In hHOs, DOX-treated organoids showed a significant increase in nuclei with γH2AX foci, indicating elevated genomic instability, while no differences in H3K9me levels or mitochondrial respiration were observed. Nuclear lamina abnormalities, including increased folding in progerin-overexpressed cells was observed. In contrast, cBOs exhibited changes across multiple hallmarks of ageing, including increased genomic instability, decreased levels of heterochromatin marker H3K9me and impaired mitochondrial function. Mitochondrial respiration measurements showed significant changes between aged and control organoids after prolonged progerin overexpression, with lower electron transfer (ET) capacity and reserve capacity in aged organoids. Together, these findings indicate that genomic instability is a shared feature of progerin-induced ageing in both organoids systems, while heterochromatin changes could only be observed in cBO. Mitochondrial dysfunction appears to represent a later or downstream consequence of the ageing process.

The PHF2–ZNF93 Axis Controls LINE-1 Dynamics and Genome Stability in Age-Induced Human Brain Organoids

Stefan Salzmann

S. Salzmann (1), E. Gabassi (1), S. Campagnol (1), C. Esk (1,2), F. Edenhofer (1)

(1) Department of Genomics, Stem Cell Biology and Regenerative Medicine, Institute of Molecular Biology & CMBI, University of Innsbruck, Austria

(2) Institute of Molecular Biotechnology of the Austrian Academy of Science (IMBA), Vienna, Austria

Abstract

Ageing of the human brain is characterized by progressive epigenetic remodelling, genomic instability, and loss of transcriptional control. However, in vitro model systems that faithfully recapitulate these ageing-associated processes in the human brain remain limited. Previous work carried out in our group showed that progerin-overexpressing human brain organoids recapitulate key molecular hallmarks of ageing, including heterochromatin loss, mitochondrial dysfunction, cellular senescence and DNA damage accumulation, making them a robust model to study age-associated chromatin alterations.

The histone demethylase PHF2 represents an interesting candidate gene for its role in regulating chromatin state and DNA damage repair. PHF2 binds to genes involved in neuronal function and neurodegeneration, many of which are enriched for DNA repair hotspots (DRHs). Our previous data showed that PHF2 expression declines in progerin-overexpressing organoids and in aged-human postmortem brain tissue, suggesting that reduced PHF2 levels may compromise genome integrity. ChIP-seq further revealed enrichment for the ZNF93 binding motif – a zinc-finger protein known to repress LINE-1 retrotransposons. This raises the possibility of a functional axis linking PHF2 to transposable element control during neuronal ageing.

To address this, we investigated the localization and expression of PHF2, ZNF93, and LINE-1 in human neural progenitor cells and brain organoids under progerin-induced ageing conditions using immunofluorescence microscopy. We observed an average 59% increase in LINE-1 signal intensity upon progerin overexpression, suggesting an enhanced TE activation in aged-like cells. Furthermore, ZNF93 displayed reduced nuclear localization and a more diffuse cellular distribution, suggesting impaired chromatin association and diminished repression of LINE-1. These changes correlate with reduced PHF2 levels, supporting a model in which age-associated PHF2 decline weakens ZNF93-mediated retrotransposon control, thereby promoting LINE-1 de-repression and genomic instability.

Together, our data identify a putative chromatin regulatory axis linking PHF2, ZNF93, and LINE-1 activity during neuronal ageing. Ongoing studies aim to dissect the mechanistic relationship between PHF2 and ZNF93 through a shRNA-mediated knockdown in 2D and 3D systems, protein-protein interaction and extended transposable element profiling. By investigating how chromatin regulators safeguard genome integrity in ageing neurons, this work provides foundational insight into epigenetic drivers of ageing and neurodegeneration.

Sex- and age-related effects on Kappa Free Light Chain index in Multiple Sclerosis

Michael Vogetseder

Introduction:

Incidence and disease course differ between female and male patients with multiple sclerosis (1-4). This is partially explained by genetic, lifestyle and hormonal factors (5, 6). In recent years, the kappa free light chain (kFLC) index has emerged as new diagnostic and prognostic biomarker in patients with early multiple sclerosis and is part of the revised McDonald criteria 2024 (7-9). On the path towards a more individualised approach, we aimed to investigate the effect of sex and age on the kFLC index.

Objectives:

The main objective was to investigate a potential difference in the kFLC index between female and male patients with multiple sclerosis, and to assess whether kFLC index changes with age.

Methods:

A total of 240 prospectively recruited patients with early multiple sclerosis throughout Austria, Swiss and Italy were included. kFLC index was calculated as (CSF kFLC/serum kFLC)/albumin quotient. Mann-Whitney U test and Spearman correlation was used for the statistical analysis. Multivariate analyses involving disease activity parameters such as MRI data are yet to be performed.

Results:

One-hundred-fifty-six /240 (65%) of patients were female, the median age was 31.3 (25.4-39.8) years. The median kFLC-index was significantly higher in female patients (47.4, 25th-75th percentile: 19.9-112.9) than in male patients (26.1, 13.4-105.2; p=0.028). There was no statistically significant difference in absolute cerebrospinal or blood kFLC concentrations or in the quotient of the kFLC concentrations. The albumin quotient was significantly higher in male patients with a median of 5.2 (3.9-7.1) compared to female patients with a median of 4.4 (3.6-5.6; p=0.003). There was no correlation between age and the kFLC index (ρ -0.027, p=0.328).

Conclusion:

We demonstrated a significantly higher kFLC index in female patients compared to male patients with early multiple sclerosis. This effect may be due to lower albumin quotient in female patients. No correlation was found between age and kFLC index.

Christopher Hettegger

Substance dependence is a global challenge with far-reaching consequences affecting social, individual and economic dimensions. These are accompanied by changes at the molecular level in the brains of affected patients, but to date there are no biomarkers that can detect these substance-induced adaptations. Due to their ability to cross the blood-brain barrier and their neuronal enrichment by the marker L1CAM, neuronal extracellular vesicles (NEVs) from peripheral blood offer a minimally invasive way of visualising neuron-specific changes caused by substance use.

In this study, blood samples from patients with cocaine dependence or alcohol dependence, each with comorbid nicotine consumption, were analysed. Healthy non-smokers and healthy smokers served as control groups to rule out potential effects of nicotine consumption on protein expression. After immunoprecipitation of L1CAM-positive NEVs, group-specific differences in protein expression were analysed using proteomics.

Our findings reveal both distinct and shared proteomic signatures in NEVs between the alcohol and cocaine dependence groups. The altered proteins are associated with cellular stress, neuroinflammation and synaptic functions.

Our results suggest that substance-induced changes can be detected by NEV-based biomarkers, thereby offering a way to identify neural changes at an early stage and potentially use them for diagnostic or therapeutic approaches.

As a leading medical technology company, we want to advance a world in which breakthroughs in healthcare create new possibilities sustainably. We've been pushing the boundaries in medical technology for more than 125 years. Today, we are active in imaging, diagnostics, cancer care, and minimally invasive therapies – augmented by digital technologies and artificial intelligence.

With our unique combination of strengths in Patient Twinning[1], Precision Therapy, and Healthcare AI, we take on the greatest challenges in healthcare. We help improve access to healthcare for underserved communities worldwide and overcome the most threatening diseases: Neuro-degenerative and cardiovascular diseases, stroke, and cancer. We partner with healthcare providers to address their most pressing challenges so that they can deliver high-quality, patient-centered care, efficiently.

Motivated by our purpose and guided by our values, we foster an inclusive and innovative workplace for our diverse and engaged teams globally. We are a team of around 74,000 Healthineers in over 70 countries passionately pushing the boundaries of what is possible in healthcare so that patients can live with hope, not fear of disease.

[1] *Early detection, accurate diagnosis, individualized therapy selection, simulation and planning, continuous monitoring, and aftercare.*

SIEMENS Healthineers

Real-time virtual Ultrasound (RVS) using prone Position Breast-MRI: Technical Feasibility and Accuracy in locating 125 Breast Lesions following a Landmark-based Approach.

Michael Swoboda

Background:

This study evaluates the feasibility and technical success rate of real-time virtual sonography (RVS) of the breast using prone contrast-enhanced MRI sequences during second-look examinations. Usually, additional supine MRI sequences are acquired for co-registration.

Methods:

This single-centre retrospective study was performed in a cohort of female patients who underwent contrast-enhanced prone breast MRI followed by second-look ultrasound for MRI-detected incidental lesions. RVS was used to co-register supine ultrasound and prone MRI data without requiring additional supine MRI studies. Lesion localization success as well as lesion visibility, fusion quality, and histopathological correlation through ultrasound-guided biopsy were assessed. A covariate analysis of factors affecting lesion localization was performed.

Results:

A total of 103 female patients (mean age 48.3 ± 11.0 years) with 125 MRI-detected breast lesions were included. Of the lesions, 91.2% were successfully localized using RVS including a high proportion of non-mass enhancements (41.6%). Ultrasound-guided biopsy was performed in 42.4% of cases, confirming malignancy in 31.9%. Covariate analysis identified higher breast volume as the only factor significantly associated with reduced RVS co-registration success (OR 0.993, $p = 0.035$).

Conclusion:

RVS represent an advanced imaging approach in breast diagnostics, offering a promising solution to overcome the limitations of standalone modalities and potentially enhance diagnostic accuracy. We showed that prone MRI studies may

be sufficient for RVS-based co-registration of breast lesions, potentially rendering additional supine MRI acquisitions unnecessary.

Human brain organoids with controlled ageing and rejuvenation capacities

Anna Verena Roth

Authors: Verena Roth, Carolin Becker, Beatriz López-Amo Calvo, Angeliki Spathopoulou,

Frank Edenhofer, Christopher Esk

Studying the human brain remains challenging. Animal models and conventional 2D tissue cultures each offer advantages but fail to capture the full complexity of the human brain. To address this limitation, we employ 3D tissue cultures — brain organoids — as an improved model system. Human brain organoid models based on pluripotent stem cell technology enable the study of neurodevelopment as well as neurodevelopmental disorders in a physiologically relevant context. Aging, defined by several "hallmarks of aging," is a major driver of neurodegenerative diseases affecting post-mitotic neurons. To better understand aging mechanisms in the human brain, this project aims to model brain aging in human brain organoids.

We generated and characterized pluripotent stem cell lines that allow inducible and reversible progerin expression. Expression of progerin, a mutant form of Lamin A, causes premature aging and causes Hutchinson Gilford Progeria syndrome in patients. We established a robust workflow for gene-engineering pluripotent stem cell cultures starting with three pluripotent stem cell lines that were transfected with expression-controlled transgenic GFP-Progerin. Positively transfected cells were selected via FACS and monoclones were sorted into 96-well plates. Challenges like cell death of single cells were overcome during this process. Handling cells in a 96-well format, including splitting, freezing and thawing was established during the cell line generation. DNA was extracted from all monoclones to test their correct genotype, and positive clones have been expanded further. Following this established workflow, aging-capable pluripotent stem cell lines from multiple donors were generated and will be differentiated into brain organoids for 30, 60, and 90 days. Subsequent characterization under aging and control conditions will be performed using microscopy, flow cytometry, and transcriptional analyses. Together our data will provide details on the formation of neuronal tissue in the context of aging in a 3D-model.

omnideconv: a novel framework for single-cell-informed deconvolution of bulk transcriptomic data

Lorenzo Merotto

Computational deconvolution techniques enable the estimation of cell-type proportions from bulk RNA-seq data by leveraging reference transcriptomic profiles. As bulk transcriptomics remains widely used due to its cost-effectiveness, scalability, and compatibility with large clinical cohorts, accurate deconvolution is essential for resolving cellular heterogeneity in complex tissues. In recent years, a new generation of deconvolution methods has emerged that directly leverages annotated single-cell RNA-seq (scRNA-seq) datasets. By learning cell-type-specific expression signatures from single-cell data, these approaches extend applicability across diverse tissues, experimental platforms, and even species. However, this increased flexibility introduces new challenges: method selection becomes more complex, benchmarking is non-trivial, and performance may vary substantially depending on data characteristics such as batch effects, annotation resolution, RNA bias, or unknown cellular content.

To support the systematic development, application, and evaluation of single-cell-informed deconvolution methods, we introduce omnideconv (omnideconv.org), a comprehensive and modular ecosystem of tools and resources designed to unify access, enhance usability, and enable reproducible benchmarking. The omnideconv framework integrates five complementary components. (1) omnideconv, an R package that provides a standardized interface to multiple state-of-the-art deconvolution methods, harmonizing input formats and simplifying method comparison. (2) deconvExplorer, an interactive web-based application for intuitive visualization and comparative exploration of deconvolution results. (3) deconvData, a curated collection of bulk and matched single-cell validation datasets spanning multiple tissues and organisms. (4) SimBu, a flexible simulator for generating pseudo-bulk RNA-seq data from single-cell datasets, enabling controlled performance assessment under defined ground-truth scenarios. (5) deconvBench, a fully reproducible Nextflow-based benchmarking pipeline for systematic large-scale method evaluation.

Using this ecosystem, we performed a comprehensive benchmarking study of eight state-of-the-art deconvolution methods across multiple biologically relevant scenarios. We systematically evaluated the influence of RNA composition bias, varying levels of cell-type annotation granularity, presence of unknown or missing cell populations, and batch effects between training and testing datasets. Our analyses reveal substantial variability in method performance depending on the evaluation setting, highlighting that no single method consistently outperforms others across all scenarios. Instead, performance is strongly context-dependent, underscoring the importance of informed method selection and parameter optimization.

By lowering technical barriers, standardizing evaluation procedures, and providing curated resources for validation, omnideconv facilitates transparent comparison and robust optimization of deconvolution methods. Ultimately, this framework supports broader adoption and refinement of single-cell-informed deconvolution approaches across diverse biological and clinical research contexts.

Scirpy enables immune-cell receptor analysis in millions of single cells

Felix Petschko

Authors: Felix Petschko, Antonio Rodríguez-Sánchez, Gregor Sturm, Francesca Finotello

Scirpy is a popular Python tool for single-cell analysis of adaptive immune receptor repertoires, which was previously used in large-scale studies like the Tabula Sapiens. With the rapid growth of data size driven by advancements in single-cell technologies, scalability has become a central challenge. The analysis of larger datasets enables more detailed and robust insights into immune repertoires. More performant solutions reduce hardware cost and accelerate the discovery of biological insights.

A key functionality of Scirpy is clonotype analysis, which enables the identification of T or B cells likely to recognize the same antigen or share a common ancestor. This analysis consists of two crucial steps: 1) computing distances between complementarity-determining region 3 (CDR3) sequences based on a similarity metric; 2) identifying cell clusters based on the computed CDR3 similarity and V/J gene usage. These two major steps proved to be performance bottlenecks for Scirpy analysis of large datasets, alongside secondary limitations like result graph visualization and result storage.

For distance computation, we focused on two widely-used metrics: the sequence distance metric TCRdist based on a substitution matrix for T cell receptors (TCR), and Hamming distance for B cell receptors (BCR). We integrated tcrdist3, an accelerated CPU implementation of the TCRdist metric, further optimized it by supporting sparse matrices, and added a CuPy-based GPU implementation. For the Hamming distance, we created a CPU implementation with Numba and a GPU version with CuPy. For the clustering step, we reimplemented Scirpy's existing algorithms to optimize sparse matrix operations. We added result graph filtering for better readability and efficiency, and changed the output data format to accelerate result storage.

For 1.5 million T cells with 64 CPU cores, the improved CPU version of the Hamming distance calculation achieved a speedup of ~15.6 (92.5s vs. 1440.3s). This calculation took 468.2s with the TCRdist method. The Hamming distance GPU implementation achieved an additional speedup of 9.2 (43.7s vs. 402.2s) over the improved CPU version on a laptop. The improved CPU version of the cluster identification achieved a speedup of ~127.7 (57.5s vs. 7345.4s) for 1 million cells with 64 CPU cores. We successfully tested the improved CPU versions on up to 8 million T cells, which was previously infeasible due to memory or runtime constraints.

These enhancements significantly improve Scirpy's capability to analyze growing single-cell RNA sequencing data, facilitating continued usability in large-scale immune repertoire analysis.

Retrospective analysis of clinical parameters and trajectories of kidney function in patients with ADPKD

Clemens Untersulzner

Abstract:

Background:

Autosomal dominant polycystic kidney disease (ADPKD) is the most common rare genetic cause of kidney failure. It leads to the formation of kidney cysts, which progressively impair kidney function over time. Various factors, such as genetics, comorbidities, and laboratory parameters, influence the progression of this disease.

Objective:

The aim of this study was to investigate the relationship between clinical and laboratory parameters and the annual decline in eGFR in ADPKD patients. Parameters such as age, gender, arterial hypertension, diabetes mellitus, BMI, CRP, protein-to-creatinine ratio, albumin-to-creatinine ratio, RAAS blockers, Tolvaptan, genetic findings, and Mayo classification were considered.

Methods:

In this retrospective cohort study, 137 ADPKD patients from the Department of Internal Medicine IV at Innsbruck University Hospital, who were treated between 2002 and 2022, were analyzed. Patients were categorized into three groups based on their annual eGFR decline: rapid, moderate, and slow eGFR decline. Differences in clinical parameters and laboratory values between these groups were statistically evaluated.

Results:

Significant differences were observed in proteinuria ($p = 0.007$), albuminuria ($p < 0.001$), BMI ($p = 0.047$), and the use of RAAS blockers ($p = 0.003$) as well as Tolvaptan ($p = 0.001$). No significant difference was found in the distribution of Mayo classifications and genetic findings.

Conclusion:

Elevated protein and albumin levels, as well as higher BMI, are associated with a more rapid decline in kidney function. RAAS blockers and Tolvaptan may positively influence the course of the disease and should be considered in risk stratification and therapy planning.

Irene rigato

Dissecting molecular rewiring in cancer requires analytical strategies that move beyond the simple analysis of differential gene expression and enable functional interpretation at the regulatory and signalling level. Footprint-based computational approaches partially overcome this limitation by inferring regulator activity from the expression patterns of transcription factor (TF) targets and pathway (PW)-responsive genes. However, they do not explicitly reconstruct the signalling context in which these regulators operate. Network-based approaches can address this limitation by coupling prior biological knowledge information with context-specific transcriptomic data to infer condition-specific signalling programs. However, accurate inference across multiple conditions is not trivial and requires careful tuning of sparsity parameters that control the trade-off between network size, similarity, and false-positive interactions.

Here, we present an integrated framework for context-specific signalling network inference based on CORNETO, a context-specific multi-condition network inference method that leverages prior knowledge and omics data simultaneously. CORNETO identifies shared signalling mechanisms while preserving condition-specific differences, with the balance between these objectives controlled by a regularization parameter (λ). We developed a framework to efficiently explore the λ parameter space using adaptive sampling guided by network topology changes. This approach helps users identify the optimal parameter setting for a given dataset and analysis. The selection is supported by the computation and visualization of metrics that quantify network size, transcription factor recovery, and cross-condition network similarity, thereby enabling informed and data-driven decisions. Furthermore, we implemented a novel visualization strategy that enables direct comparison of networks across conditions, facilitating rapid identification of shared and distinct subnetworks and TF activity regulatory patterns.

We applied this workflow to bulk RNA-seq data generated from murine models of B-cell leukaemia lymphomagenesis to investigate signalling rewiring associated with Tet2 deletion in premalignant and malignant conditions. Using the CORNETO-powered framework, we inferred condition-specific signalling networks that reveal both shared and differential regulatory programs in premalignant and malignant murine models subjected to Tet2 deletion, which converge onto different TF mediators. These results demonstrate that adaptive context-specific network inference enables systematic characterization of signalling rewiring from transcriptomic data potentially revealing mechanisms that are not apparent with gene-centred approaches

20-colour spectral flow cytometry panel for the characterisation of mouse antigen-specific CD8 T cell subsets

Leonie Wolf

Leonie Wolf, Lea Sadurski, Brigitte Müllauer, Gisa Gerold and Zoltán Bánki

Institute of Virology, Medical University of Innsbruck, Innsbruck, Austria

Comprehensive phenotyping of antigen-specific T cell responses is essential for understanding immune mechanisms following infection or vaccination. Conventional flow cytometry is often constrained by spectral overlap and available detectors, thereby restricting parameter capacity. This limits the simultaneous use of markers for assessing T cell phenotype, activation and differentiation states. Spectral flow cytometry overcomes these limitations by capturing the full emission spectra of fluorophores, thus enabling high-dimensional immune profiling within a single staining.

Here, we utilised the Sony ID7000 to develop and optimise a 20-colour spectral flow cytometry panel for comprehensive CD8 T cell analysis in immunised mice. The purpose of the panel was to identify antigen-specific populations of major CD8 T cell subsets, their activation and differentiation states within murine lymphoid and non-lymphoid tissues. Multiple markers enabled the delineation of CD8 T cell memory subsets (TEM, TCM, and TRM) and various effector CD8 T cell subsets. In addition, dextramer staining was employed to define CD8 T cell specificity.

Overall, this 20-colour spectral flow cytometry panel provides a powerful and flexible tool for in-depth analysis of T cell responses with a particular focus on antigen-specific CD8 T cells. The strategy can be easily adapted to other antigens, thereby facilitating comprehensive immune monitoring.

Automated Segmentation of Extracranial Arteries in Contrast-Enhanced MRI Using nnU-Net: Performance in Healthy and Dissection Patients

Matthias Groell

Background: Accurate segmentation of extracranial arteries in contrast-enhanced magnetic resonance imaging (CE-MRI) is essential for quantitative vascular assessment and the evaluation of vascular pathology. Manual delineation is time-consuming and subject to inter-observer variability. Deep learning-based segmentation offers a promising alternative. However, robust segmentation of tubular vascular structures remains challenging, particularly in the presence of anatomical variations and pathological alterations.

Methods: We retrospectively analyzed CE-MRI data from 145 subjects from the ReSect study cohort, including 24 healthy controls and 121 patients with carotid artery dissection. Expert annotations of the common carotid artery (CCA), carotid bulb, internal carotid artery (ICA), and vertebral artery (VA) served as ground truth. Data were split at the patient level into training, validation, and held-out test sets, stratified by pathology. A 3D nnU-Net was trained using its default configuration. Segmentation performance was evaluated on the test set using the Dice similarity coefficient and Jaccard index. Performance was additionally analyzed separately for healthy and dissection subgroups.

Results: The nnU-Net achieved robust segmentation performance across all vessel classes on the held-out test set, with average Dice coefficients and Jaccard index exceeding 0.90 and 0.85 respectively for all targets. Performance varied between anatomical structures, with the highest accuracy observed for the ICA. Subgroup analysis revealed no clear differences in segmentation accuracy between healthy controls and dissection patients. While segmentation of large-caliber vessels was consistently robust, reduced accuracy and increased variability were observed for smaller-caliber vessels.

Conclusion: Deep learning-based methods enable reliable automated segmentation of extracranial arteries in CE-MRI, particularly for large-caliber vessels. These findings highlight the potential of automated vessel segmentation in both healthy and pathological anatomy and represent an important step toward downstream quantitative analysis and image-guided diagnosis and therapy.

Johannes Bereiter-Payr

Introduction/Purpose:

High-resolution peripheral quantitative computed tomography (HR-pQCT) enables in vivo examination of bone microstructure, supporting the investigation of factors influencing bone health and enabling fracture risk prediction. However, clinical adoption is hindered by the time-consuming, semi-manual segmentation required before automated image analysis, and other factors.

We present a robust approach for training and applying Bayesian convolutional neural networks (CNNs), specifically U-Net architectures, to achieve semantic segmentation of volumetric 3D bone images. Using this method, CNNs generate highly accurate segmentation masks for cortical and trabecular bone compartments. Notably, the models also perform well on images from scan sites not included in the training or validation sets (e.g., distal tibiae), demonstrating strong generalizability.

Methods:

3D U-Net CNNs were trained on volumetric HR-pQCT images of human radii, standardized in size and orientation (with left extremities mirrored). To expand the image volume, voxels in the padding region were filled with a mirrored version of the original image. To preserve characteristic noise while eliminating redundant bone structures, the padding was filtered in the frequency domain. An on-the-fly image augmentation pipeline was implemented during training to reduce overfitting. Multiple U-Net architectures, varying in trainable parameters and hyperparameters, were evaluated. The two best-performing networks were selected based on Dice and intersection over union (IoU) metrics, using a test set comprising images of both distal radii and distal tibiae. Test set predictions were further assessed by three experts in a blinded evaluation, which also included conventional segmentation masks and a reference model trained on tibiae.

Results:

All models produced segmentation masks with high accuracy, as confirmed by both quantitative metrics and expert evaluation. Mean Dice scores exceeded 0.9 across all models and prediction modes. In most cases, the best-performing models generated smoother contours and followed the trabecular/cortical interface more closely than manual segmentation masks.

Conclusion:

Bayesian CNNs effectively transfer learned textures to images that differ significantly from the training data, enabling semantic segmentation of HR-pQCT images across multiple scan sites using training data from a single site.

Disclosure:

The training technique has been submitted for patent protection at the European Patent Office (EPA) by the Medical University of Innsbruck, Austria (patent application number: EP 25 224534.5). The authors declare no other competing interests.

Impact of SLS-associated missense mutations on FALDH stability and enzymatic activity

Erica Alfonsi

AUTHORS: Erica Alfonsi1, Theresia Dunzendorfer-Matt1, Markus A. Keller2, Katrin Watschinger1

Affiliation: 1Institute of Molecular Biochemistry, Biocenter, 2Institute of Human Genetics, Medical University of Innsbruck, 6020 Innsbruck, Austria.

Presenting Author: Erica Alfonsi

Sjögren-Larsson syndrome (SLS) is an autosomal recessive neurocutaneous disorder, characterized by a classical triad of congenital ichthyosis, intellectual disability and spastic paraparesis. Mutations in the ALDH3A2 gene, which encodes the membrane-bound enzyme fatty aldehyde dehydrogenase (FALDH; EC 1.2.1.48) lead to SLS. As FALDH reroutes energy-rich aldehyde compounds resulting from lipid degradation into salvage pathways for lipid biosynthesis in addition to detoxifying them, a deficiency causes accumulation of long-chain aliphatic aldehydes and the respective fatty alcohols. This alters cell-membrane integrity and primarily affects the eyes, skin and the central nervous system, which are the tissues most affected in this disorder. Among the approximately 90 ALDH3A2 variants responsible for the disease identified in Sjögren-Larsson syndrome, missense mutations that result in single amino acid substitutions constitute a significant proportion, accounting for approximately 41% of pathogenic alleles.

FALDH activity depends on NAD+ as a redox cofactor for aldehyde oxidation. The enzyme accepts saturated and unsaturated aliphatic aldehydes with chain lengths of 6 – 24 carbons as substrates; lengths of 16 and 20 carbon atoms are preferred. FALDH is a homodimeric protein of 54 kDa comprising three domains: a catalytic domain, an NAD+-binding domain and a C-terminal oligomerization domain. Initial observations from our group have shown that low-molecular-weight compounds might have the ability to stabilize the FALDH protein by acting as chemical chaperones.

In this project, we investigated the influence of five SLS-associated missense mutations (R228C, R228H, C237Y, Y279N, P315S) on the stability and the enzymatic activity of FALDH. The five amino acid residues were selected based on the FALDH crystal structure for their potential impact on folding and dimerization and were successfully mutated and inserted in a Strep-tagged huFALDH expression construct lacking the C-terminal membrane anchor using site-directed mutagenesis. All five mutated proteins were successfully expressed in Escherichia coli and purified via Strep-affinity chromatography after optimizing the expression and purification protocols. Two of the mutated proteins (C237Y and P315S) exhibited pronounced instability and almost absent activities (less than 1%) as demonstrated by HPLC-based enzymatic assays. The other three proteins (R228C, R228H and Y279N were more stable and retained partial FALDH activity (68%, 12% and 8% of WT activity, respectively).

Future work will focus on the stability of these three mutated FALDH proteins and the ability of the previously identified compounds to improve the dimerization and stability of them. Such a strategy could ultimately pave the way to an improved therapeutic option for SLS patients.

Empowering the identification and validation of drug candidates targeting oncoproteins and E3 ligase functions

Alexandra Fritz

Alexandra Fritz1,2,3, Jakob Fleischmann1,2, Sophie Strich1,2, Valentina Kugler1,2, Selina Schweighofer1,2, Thomas Nuener2, Andreas Feichtner3, Philipp Tschaikner3, Eduard Stefan1,2,3

1Department of Molecular Biology and Center for Molecular Biosciences Innsbruck (CMBI), University of Innsbruck, Innsbruck, Austria

2Tyrolean Cancer Research Institute (TKFI), Innsbruck, Austria

3KinCon biolabs GmbH, Innsbruck, Austria

Protein kinases act as spatiotemporal molecular switches that regulate essential cellular processes, with their dysregulation driving oncogenic transformation and therapy resistance. Despite their central role in cancer biology, targeting mutationally activated kinases and notoriously undruggable oncoproteins remains challenging due to context-dependent interactions and unique scaffolding functions. To address this, we employed the Kinase Conformation (KinCon) reporter system, enabling real-time tracking of kinase conformations and direct visualization of target engagement using allosteric and competitive small molecules in living cells and high-content formats. Here, we demonstrate the unique sensitivities of the KinCon reporter system, particularly in tracking BRAF-kinase activity conformations upon melanoma drug binding. The effects of several FDA-approved BRAF inhibitors were validated and compared to next-generation compounds such as Plixorafenib (Röck et al., Sci.Adv. 2019, Mayrhofer et al., PNAS 2020, Kugler et al., eLife 2024). In this context, also MEK1 mutations induce open, active conformations that are reversible upon inhibitor binding (Fleischmann et al., PNAS Nexus 2023), while dual BRAF/MEK1 inhibition synergistically enforcing inactive MEK1 states, providing molecular information on interrelated kinase activity states in cell culture model systems (Fleischmann et al., PNAS Nexus 2023; Biomolecules 2021). Expanding beyond kinases, we recently integrated hard-to-target proteins such as the tumor suppressor p53 and the E3 ligase MDM2. This advancement enables the analysis of small molecule interactions—including PROTACs and molecular glues—and facilitates systemic validation of drug efficacies and specificities. Our findings underscore the critical role of conformational dynamics in cancer-driving enzymes and the persistent challenge of targeting proteins like mutant p53 and MDM2. The protein conformation reporter system provides a powerful approach for real-time analysis of conformational states and drug engagement of both established and hard-to-target cancer proteins within living cells.

Diagnostic and progression biomarkers in early-stage neurodegenerative parkinsonism.

Clancy Cerejo

Clancy Cerejo1, Greta Hemicker1, Frank Jagusch1, Philipp Gallaschik1, Florian Krismer1, Klaus Seppi1, Beatrice Heim1*

1 Department of Neurology, Medical University of Innsbruck, Innsbruck, Austria.

*Correspondence Author

Background: Neurodegenerative parkinsonism comprises disorders with overlapping clinical features but distinct pathologies, complicating early differential diagnosis and progression monitoring, especially when patients do not yet meet criteria for Parkinson's disease (PD), multiple system atrophy (MSA), progressive supranuclear palsy (PSP) or dementia with Lewy bodies (DLB), resulting in a phase of clinical unclassifiability. Diagnostic biomarkers are therefore needed to support early differentiation.

Objective: To identify and validate diagnostic, prognostic, and progression biomarkers in early neurodegenerative parkinsonism through in-depth, multimodal phenotyping.

This prospective cohort study includes patients with suspected neurodegenerative parkinsonism with symptom onset <3 years; secondary causes are excluded. Participants are assessed annually over 24 months. Baseline includes structured history and brain MRI. At baseline and follow-up, neurological examination and standardized assessments are performed (Movement Disorder Society–Unified Parkinson's Disease Rating Scale [MDS-UPDRS], Montreal Cognitive Assessment [MoCA], Frontal Assessment Battery [FAB], Schwab and England Activities of Daily Living Scale [SEADL]). Non-motor assessment includes autonomic and global non-motor symptom measures (Scale for Outcomes in Parkinson's Disease–Autonomic Symptoms [SCOPA-AUT], Non-Motor Symptoms Questionnaire [NMSQ]), olfaction testing, orthostatic blood pressure, depression screening, bladder assessment, and rapid eye movement sleep behaviour disorder screening. Blood is collected at each visit; optional cerebrospinal fluid and skin sampling allow biomarker analyses (e.g., neurofilament light chain, glial fibrillary acidic protein, a-synuclein).

Preliminary observations: To date, 38 patients have been recruited (phenotype suggestive of PD n=29, MSA n=5, PSP n=3, and DLB n=1). Motor disability was greater in MSA and PSP than PD (MDS-UPDRS III: 46.5±16.8 and 34.5±5.0 vs 18.9±8.9). PSP showed lower cognitive performance (MoCA 23.5±0.7; FAB 14.5±0.7) compared with PD (MoCA 26.8±2.3; FAB 17.1±1.0). Autonomic and global non-motor burden was higher in MSA and PSP than PD (SCOPA-AUT 19.8±13.3 and 11.5±5.0 vs 8.4±5.4; NMSQ 9.8±4.3 and 10.5±3.5 vs 4.4±3.2).

Conclusion: Preliminary data suggest greater motor impairment and higher autonomic/non-motor symptom burden in early atypical parkinsonism compared with PD. Ongoing recruitment and longitudinal follow-up will support validation of fluid- and imaging-based biomarkers, refine early diagnostic accuracy and better define disease trajectories in this early phase.

Eva Rauch

The late endosomal and lysosomal adaptor and MAPK and mTOR activator (LAMTOR) scaffolding complex, resides at the lysosomes where it mediates catabolic and anabolic signalling. The pentamer consists of LAMTOR1 whose lipid-modified N-terminal region anchors the complex together with the remaining subunits LAMTOR2-5 in the lysosomal membrane. Previous studies have identified the presence of at least four different LAMTOR assemblies on the lysosomes associated with catabolic or anabolic signalling mediated by its association with Rag-GTPases, SLC38A9, the v-ATPase and AXIN with LKB1. Furthermore, LAMTOR is a negative regulator of the BLOC1 related complex (BORC), an octameric protein complex involved in lysosomal biogenesis and cellular positioning.

The goal of the project is to elucidate the structural organization of native LAMTOR assemblies under varying stimuli, providing insight into how a single scaffolding complex orchestrates these diverse biological functions. We are applying state-of-the-art crosslinking mass-spectrometry (XL-MS) methods with the aim to capture endogenous protein-protein interactions.

We have developed a robust affinity purification protocol for SH-tagged bait proteins via Strep-Tactin columns. Notably, the approach is fully compatible with downstream cross-linking with the enrichable PhoX reagent and subsequent LC-MS analysis. Our workflow enabled the detection of over 300 cross-links in a single LC-MS run. Our AP-XL-MS experiments from SH-BORC and BORCS7-SH expressing cells served as a basis to proof the existence of at least two distinct mixed complexes incorporating both subunits from BORC as well as BLOC1, two complexes that had been assumed to be separate until then.

Furthermore, our detected cross-links combined with in-silico prediction using AlphaLink suggests that LAMTOR2 interacts with BORCS6 by means of beta-sheet extension. We will investigate the binding interface further by characterizing the binding of synthetic BORCS6 derived peptides in-vitro. This could serve as a basis both for a biochemical tool to uncouple lysosomal localization from the cellular energy status as well as a potential peptide inhibitor. In contrast to the known mTORC1 inhibitors called Rapalogs our peptide should specifically target the amino acid responsive branch of this pathway.

We hypothesize that the function of BORC, moving the lysosomes to the periphery, could serve the purpose of activating pathways by means of tyrosine phosphorylation at the lysosomal surface by tyrosine kinases localized at the plasma membrane. To investigate this, we plan to measure the differential lysosomal phosphor-proteome from affinity purified peripheral and perinuclear lysosomes employing TMT labelling and IMAC enrichment.

Tariq Oluwakunmi Agbabiaka

Since SARS-CoV-2 emerged in 2019, it has undergone extensive evolution. Newer variants continue to emerge. Vaccination has been vital to preventing major outbreaks. Viral evolution, however, necessitates updates to the vaccine antigen to match circulating strains and a corresponding booster vaccination for the population. Since antibody-mediated cross-protection against similar or related viruses is well documented, we hypothesise that variant diversification, vaccine antigen updates, and repeated population exposure, either through vaccination, infection, or breakthrough infections, could generate cross-reactive antibodies to other human coronaviruses (hCoVs). We tested plasma samples from our highly controlled HEVACC clinical trial (which compared neutralising antibody response after two or three homologous and heterologous COVID-19 vaccinations) and other multiple-exposure samples for binding antibodies against seasonal (hCoV-HKU1, hCoV-OC43, hCoV-229E, and hCoV-NL63) and highly pathogenic coronaviruses (SARS-CoV, SARS-CoV-2, and MERS-CoV). Repeated SARS-CoV-2 exposure increased binding antibody titres against MERS-CoV and SARS-CoV. Since the rise in binding antibodies was strongest for SARS-CoV, we further analysed neutralising antibodies against SARS-CoV using a pseudovirus neutralisation assay. Increasing exposure frequency boosted SARS-CoV neutralisation. While we observed increasing binding antibody titres against SARS-CoV and MERS-CoV with repeated exposure, titer changes for seasonal coronaviruses may be attributable to the co-circulation of seasonal coronaviruses with SARS-CoV-2 and different levels of non-pharmaceutical measures during the pandemic.

Sex Differences in Pediatric Flexor Tendon Injuries: A 14-Year Retrospective Outcome Analysis

Turkhan Mehdiyev

Background:
Flexor tendons are essential for hand function and play a crucial role in the motor development of children. Early diagnosis and appropriate treatment of pediatric flexor tendon injuries are necessary to prevent long-term functional impairment. While outcomes after flexor tendon repair in adults are well described, data in pediatric populations remain limited. Moreover, potential sex-related differences in injury patterns, outcomes, and complication rates are insufficiently explored. Pediatric flexor tendon injuries differ substantially from those in adults, particularly regarding postoperative rehabilitation strategies, due to children's higher healing capacity and age-dependent compliance. This retrospective study evaluates clinical outcomes and complication rates after pediatric flexor tendon repair, with special emphasis on sex distribution and potential sex-related differences.

Methods:
A retrospective analysis was conducted of all pediatric patients (<18 years) who underwent primary flexor tendon repair for hand injuries between January 2010 and April 2024 at the University Hospital for Plastic, Reconstructive, and Aesthetic Surgery, Innsbruck. Patients with or without associated nerve, vessel, or bone injuries were included. Medical records, operative reports, radiological findings, and photographic documentation were reviewed. Baseline characteristics were analyzed using descriptive statistics. Comparisons between patients with and without tendon rupture or complications were performed using Fisher's exact test for categorical variables and the Mann–Whitney U test for continuous variables. Logistic regression analysis was conducted to evaluate associations between complications or ruptures and factors including sex, age, injury mechanism, suture material, suture technique, number of injured flexor tendons, associated injuries, and postoperative rehabilitation protocols.

Results:
A total of 54 pediatric patients were identified, of whom 39 met inclusion criteria after exclusion due to insufficient follow-up. The cohort consisted of 31 male patients (79.5%) and 8 female patients (20.5%), demonstrating a clear male predominance. Tendon ruptures occurred in four patients (10.3%): three males aged 16–18 years and one female aged 1.5 years. All rupture cases resulted from blunt trauma, and three required revascularization. Additional complications were observed in five patients, including vascular compromise following replantation and tendon adhesions requiring secondary surgery. Logistic regression revealed no statistically significant association between sex, age, surgical or rehabilitation parameters and rupture or complication rates. However, blunt trauma was significantly associated with higher complication rates in Fisher's exact test.

Conclusion:
This study demonstrates a pronounced male predominance in pediatric flexor tendon injuries, particularly in adolescents, while sex itself was not identified as an independent risk factor for tendon rupture or postoperative complications. Age and injury mechanism appear to be more relevant determinants of outcome than sex. These findings highlight the importance of individualized, age-adapted treatment and rehabilitation strategies in pediatric flexor tendon injuries.

Effects of NF-κB Inhibition on Chronic Airway Epithelial Inflammation and Cell Migration

Angelina Ananich

Background: Asthma is a chronic inflammatory airway disease characterized by mucus hypersecretion and structural remodeling, all of which contribute to airway obstruction. The NF-κB signaling pathway plays a central role in regulating inflammatory responses and epithelial dynamics. BAY11-7082, an NF- κB inhibitor, has been shown to modulate cytokine production, mucin expression, and epithelial cell migration.

The objective of this study was to investigate the effects of NF-κB inhibition on the expression of inflammatory mediators, mucin production, and epithelial cell migration using human airway epithelial cell lines (Calu-3 and A549).

Methods: Human airway epithelial cell lines A549 and Calu-3 were treated with BAY11-7082(as an NF-κB inhibitor), LPS (as an NF-kB activator), or both. Gene expression was assessed by qRT-PCR, mucus secretion by PAS staining, and cell migration by cell life imaging

eurofins | Genomics

ACCELERATE YOUR RESEARCH WITH EXPRESS GENES

(UP TO 4KB). YOU ORDER. WE RUN.

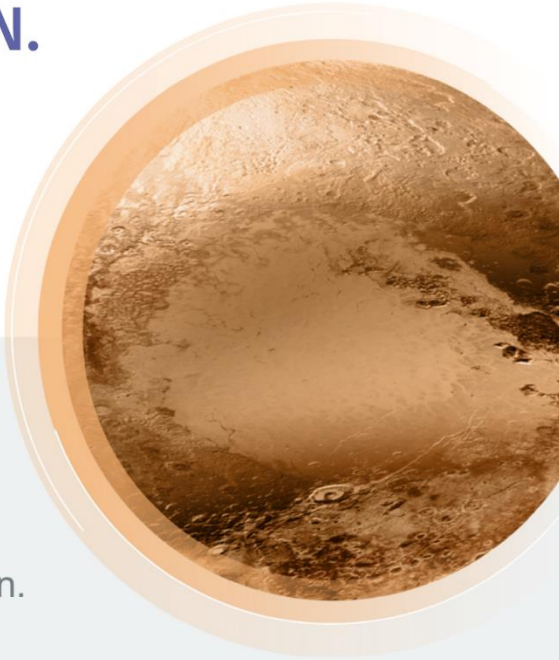

Express Genes Delivered in as Little as Four Business Days*

When time matters, don't let DNA synthesis slow you down. Express Genes from Eurofins Genomics gives your gene orders priority production – so you receive high-quality, sequence-verified genes faster than standard services.

- Priority processing
- Free codon optimization (GENEius)
- Full quality documentation
- Secure & confidential handling
- Optional express subcloning

Get started today »

2026_0202

*Order before 2 p.m. CET and receive your gene in as little as four business days.

Eurofins Genomics
Anzinger Str. 7a | 85560 Ebersberg, Germany | support-eu@genomics.eurofinseu.com
eurofinsgenomics.com| +49 (8092) 337 98 00

The role of RNA modifications in the superwobbling tRNAVal of M. capricolum

Isabell Gonnella

Isabell Gonnella1, Raphael Plangger2, Ronald Micura², Christoph Kreutz2 and Matthias Erlacher1

1Institute of Genomics and RNomics, Medical University of Innsbruck, Biocenter

2Institute of Organic Chemistry and Center for Molecular Biosciences Innsbruck (CMBI), University of Innsbruck, Innrain 80/82

Transfer RNAs (tRNAs) are crucial adapter molecules essential for decoding the genetic code during the process of protein synthesis. While they share a characteristic L-shaped structure, their sequences and modifications vary widely. These modifications are located at different positions within the tRNA, thereby influencing the structural stability and decoding.

To study the molecular basis of "superwobbling," we generated unmodified and site-specifically modified variants of the M. capricolum tRNAValUAC via splinted ligation and tested their ability to decode all four valine codons. While all variants translated GUU, GUA, and GUG well, none could efficiently decode GUC. Genome analysis revealed that GUC codons are extremely rare in M. capricolum, with only two coding sequences containing four GUC codons, which the superwobbling tRNA translates efficiently. These findings suggest that the M. capricolum tRNAValUAC is not a "true" superwobbler capable of decoding all four codons equally, but rather a "sufficiently superwobbling" tRNA that has adapted to the organism's codon usage. We are currently extending this study to other organisms, in order to identify "true" and "sufficient" superwobbling tRNAs. This will allow a deeper insight into the phenomenom of superwobbling and a better understanding of decoding.

Abstract ARGiS – Azole-Resistant fungi: Gradients in Soils

Alina Nowak-Rainer

Fungal pathogens threaten human life directly and indirectly as they are responsible for about 2.5 million human deaths annually and for up to 30% pre- and post-harvest yield losses. Furthermore, resistance development against antifungal agents challenges medicine and agriculture even more. One of the most concerning resistance is the one against the group of azoles. They are commonly used in both medicine and agriculture and this dual use harbors the problem of cross-resistances within azole antifungals. Azoles inhibit the sterol 14a-demethylase in the ergosterol biosynthesis and hence influence cell wall stability. Resistances were found to be due to single amino acid substitutions in the encoding gene cyp51, besides other more general mechanisms like overexpression of the target protein or drug efflux pumps and transporters. The development of azole resistance has been linked to the exposure of fungi to azoles used in agriculture, contributing to cross-resistances against medically used azoles. Yet, other environmental factors and the role of azole burden in soils remain unclear. Furthermore, the diversity of azole resistant fungi in soils has not been studied yet. This work assesses the risk factors and functional traits for azole resistance development in plant, human and putative human fungi inhabiting soils. We study the frequency and diversity of azole resistant fungi along a land-use gradient by culture-based and molecular approaches correlating it to abiotic factors and the azole burden in soil. In the first culture-based approach about 300 azole resistant morphotypes from over 1000 azole resistant isolates have been collected. Azole resistant isolates have been retrieved from all studied soils no matter the land-use and represent a variety of fungal taxa and some yet undescribed species. Collected isolates will be sequenced for species determination and further characterized physiologically including resistance testing. Furthermore, the resistance gene cyp51 will be sequenced to build a library of gene variants. By correlating azole burden, abiotic soil parameters, fungal biodiversity and diversity of the cyp51 a database for a soil functional biodiversity index for resistance will be established.

Michaela Mayr

How cells feel and respond to mechanical stresses is one of the key questions of mechanobiology. Proteins called mechanosensors turn mechanical cues into biochemical signals that then trigger adaptation processes. Most known mechanosensors reside at the plasma membrane, the nucleus or are associated with the cytoskeleton. However, while recent work suggests that the endoplasmic reticulum is affected by mechanical stress, no mechanosensors have been identified at the ER. Here, we show that the proteotoxic stress sensor IRE1 reacts to mechanical stress of the cell. Our data suggest that IRE1 senses tension in the ER membrane and is thus activated without the involvement of the unfolded protein response. Mechanically activated IRE activates JNK to increase translation independently of XBP1 splicing. Collectively, our results uncover a non-canonical role of IRE1 as a mechanosensor and regulator of translation in mechanically challenging environments.

Keeping it cool - INtracerebral findings in early MRI after sports related concussions in American Footballl players - a randomized pilot study

Victoria Schön

Following a traumatic head injury, neuroinflammation, temporarily elevated brain and body temperatures can trigger degenerative processes in the brain. Concussions and repetitive head injuries are particularly harmful, as they can lead to axonal injuries and potentially result in Chronic Traumatic Encephalopathy (CTE).

Sports-related concussions (SRC) are common among male and female athletes, particularly those who experience exercise-induced hyperthermia, which significantly raises the risk of long-term brain damage and poorer cognitive outcomes. Elevated brain temperature is known to exacerbate the negative effects of various types of head trauma. Therefore, brain cooling has emerged as a critical intervention in managing these injuries. By reducing the brain's demand for oxygen and glucose, cooling can mitigate the risk of tissue damage and cell destruction. This approach has been shown to decrease the accumulation of edema within the brain and lower intracranial pressure in severe traumatic brain injuries (TBI).

Physical activity, which increases the demand for glucose, can further aggravate the destructive effects of a compromised blood-brain barrier. Consequently, brain cooling after repeated head collisions may serve as an effective treatment. Returning the brain to normothermic temperature can potentially prevent or limit long-term cognitive deficits. Using cooling devices for athletes prone to repetitive head injuries can alleviate initial symptoms such as dizziness, nausea, and difficulties with concentration and memory.

One such cooling device is the "PolarCap ®" from the Swedish company PolarCool. Studies have demonstrated that the PolarCap® can reduce symptoms and facilitate an earlier return to training or play. Typically, the effects of concussions are only clarified by imaging when neurological deficits are present, and more detailed structural imaging examinations are not standard practice.

However, MRI imaging studies could provide valuable insights into the neuroinflammatory effects following sports-induced TBI. MRI, and specifically SWI, are invaluable tools in the assessment of concussions. While standard MRI provides structural details, SWI offers enhanced sensitivity to microbleeds and diffuse axonal injuries, making it a powerful technique for detecting subtle brain damage associated with concussions. Additionally, biomarkers for the neuroinflammatory process, detectable in the blood post-injury, could be measured and compared to gain a better understanding of the pathology.

Blood biomarkers have emerged as a promising tool in the diagnosis, management, and prognosis of concussions. Concussions, a form of mild TBI, can be challenging to diagnose accurately using traditional methods like clinical evaluation and imaging. Blood biomarkers offer a more objective and quantifiable approach to assess brain injuries.

By purposefully including female athletes, it addresses a population that remains underrepresented in sports trauma research. The study further enables data collection on potential biological differences in the pathophysiology of sport-related concussions between male and female athletes. The anticipated findings may help close existing evidence gaps regarding optimal treatment strategies for female athletes.

Field Study on Iloprost for Treatment of Severe Frostbite at High Altitude

Lea Dümpelmann

Rationale

Frostbite is a significant risk for climbers and trekkers at high altitude, often resulting in long- term disability. Iloprost, a prostacyclin analogue, has shown promise in reducing amputation rates when administered intravenously within 72 hours of frostbite injury 1–8. Treatment delays are frequent due to the remoteness of climbing / trekking sites and limited access to medical facilities capable of administering iloprost. Each hour of treatment delay correlates with decreased digit salvage rates 9. Helicopter evacuations, commonly required to access such facilities, are often impossible or delayed due to harsh weather conditions, potentially compromising patient outcomes. We hypothesize that treatment for frostbites grade 3 & 4 with iloprost is feasible and safe in pre-hospital, high-altitude settings and can contribute to ensuring treatment initiation within the recommended time frame. We anticipate a comparable incidence and severity of side effects to iloprost treatments facilitated in clinical settings. Our primary objective is to systematically evaluate the feasibility and safety of iloprost treatment under high-altitude field conditions. This assessment will encompass the analysis of logistical challenges and the practicality of iloprost use in remote and extreme environments.

Outline

This prospective field study aims to assess the feasibility and safety of iloprost administration for severe frostbite at high-altitude at Everest Basecamp, Nepal (5364m). The research will be conducted during the peak climbing seasons of 2026 and 2027, targeting adult patients (aged 18 and older) presenting with frostbite grades 3 or 4 according to the Cauchy visual grading scale10.

Method

After obtaining written informed consent, patients will receive intravenous iloprost according to current clinical guidelines, ideally within 72 hours after thawing. Throughout the study practical challenges of administering advanced medical therapy in remote, resource-limited environments will be documented. Adverse effects associated with iloprost monitored for and treated as required. Data will be collected on participant demographics, injury characteristics, time to rewarming, time to treatment, drug administration details, and side effects, as well as short-term clinical outcomes such as tissue preservation and functional status upon discharge / further referral for treatment continuation in Kathmandu. If fewer than ten eligible cases are recruited in the first two years, the study will extend for an additional season to achieve its objectives. Whenever possible, follow-up assessments will be conducted to evaluate longer-term recovery and need for amputation. Outcomes will be compared with historical data from similar high-altitude environments to estimate the potential benefit of on-site iloprost treatment.

Discussion

By systematically evaluating the feasibility and safety of field-based iloprost administration for frostbite, this study seeks to generate actionable evidence for improving emergency care protocols in remote and extreme environments. The findings have the potential to reduce morbidity and healthcare costs associated with frostbite, inform future wilderness medicine guidelines, and improve outcomes for climbers and high-altitude workers worldwide.

Horia C. Hermenean

L-type voltage-gated Cav1.3 Ca^{2+} channels mediate Ca^{2+} influx into most excitable cells and regulate diverse physiological functions, such as excitation-transcription coupling, sinoatrial node pacemaking, hearing, neurotransmitter and hormone release and neuronal excitability. De novo heterozygous (HET) missense variants in the pore-forming a1-subunit of Cav1.3 (encoded by CACNA1D) are associated with a broad neurodevelopmental disorder with or without endocrine features. One activity-enhancing variant, A749G, was identified in a female patient with autism spectrum disorder (ASD) and intellectual disability and introduced into a mouse line (Cav1.3A749G), providing a versatile preclinical model.

Here, we aimed at establishing a multimodal strategy to provide complementary tools to explore the pathophysiology of CACNA1D channelopathies. Using in silico modelling, behavioural analyses and electrophysiological recordings in heterologous expression systems, acute brain slices and isolated mouse chromaffin cells (MCCs), we investigated the functional consequences of this activity-enhancing variant across multiple in silico, in vitro and ex vivo systems. Since most CACNA1D variant-expressing patients are heterozygous (HET), tsA-201 cells were transiently-transfected with human exon 8b-containing WT, mutant (homozygous, HOM) or 1:1 WT:mutant a1-subunit stoichiometry (HET) cDNAs, together with β3, a2δ-1, and EGFP (transfection marker).

Previous computational simulations predicted destabilised channel open/closed states. An evolution-based sequence co-variation algorithm yielded an epistatic score of −6.12, indicating pathogenicity. Indeed, a detailed biophysical analysis in tsA-201 cells (15 mM Ca2+ charge carrier) revealed complex gating changes, including hyperpolarising shifts in the voltage-dependent activation compared to WT (voltage of half-maximal activation, V0.5 act.; HOM: ~−14 mV, $p<0.0001$; HET: ~−10.5 mV, $p=0.0018$; ANOVA, Kruskal–Wallis test) and steady-state inactivation (SSI) (voltage of half-maximal SSI, V0.5 inact.; HOM: ~−14.9 ± 1.5 mV, $p<0.0001$; HET: ~−11.2 ± 1.6 mV, $p<0.0001$; one-way ANOVA, Tukey's test). Current density was increased (by: HOM: ~20.6 pA/pF, $p<0.0001$; HET: ~13.9 pA/pF, $p<0.0001$; ANOVA, Kruskal–Wallis test), accompanied by faster inactivation kinetics (during the first 50–500 ms of a 5s depolarising pulse; two-way ANOVA) and slower deactivation kinetics upon repolarisation. In MCCs from male HET mice, L-type currents were pharmacologically isolated and similar shifts in voltage-dependence of activation ($V_{0.5}$ act. ~−6 mV), SSI ($V_{0.5}$ inact. ~−9 mV), and altered inactivation kinetics (100 and 600 ms), were observed. MCCs from female mutants also exhibited negative shifts in activation, more pronounced in HOMS (~−9 mV) than HETs (~−4.5 mV). HET male mice were hyperactive during the first 10min of a 1h open-field test, covering more distance (~6.4 ± 2.3 m, $p=0.011$, unpaired t-test) and spending less time immobile (median difference −74.00 s, $p=0.0002$, Mann–Whitney test). This could reflect the previously-reported increased excitability of dorsomediostriatal (DMS)-projecting substantia nigra (SN) dopaminergic neurons. A similar hyperlocomotive phenotype was observed in HET females, which also spent less time immobile (median difference −36.45 s, $p=0.0229$). Together with preliminary female midbrain-slice data, these findings suggest a potential sexual dimorphism in nigrostriatal hyperexcitability of Cav1.3A749G mice.

Overall, this study demonstrates a comprehensive multimodal framework for elucidating how single missense mutations drive disease-associated molecular, cellular and systemic alterations, with broad applicability to other ion channels and relevance for precision medicine.

Reconstructing lipid class specific fatty acyl compositions with Fatty Acylizer

Janik Kokot

Lipids are active regulators of membrane properties and cellular signaling, whose biological roles depend on both their head group and side chain composition. To maintain membrane homeostasis, their fatty acyl side chains are continuously adapted and remodeled. Perturbations in connected metabolic pathways therefore have the potential to systematically shift lipid compositions at both the overall class level composition and the side chain composition level within a lipid class. As a result, lipids have emerged as sensitive biomarkers, yet interpreting and explaining lipidomic data remains challenging. Especially the lack of full fatty acyl side chain resolution in many datasets limits the obtained insight into metabolic regulation. Lipid metabolism is highly interconnected, with alternative biosynthetic pathways that share enzymes, precursors, and intermediates. Consequently, individual lipids must be interpreted within an integrated metabolic network rather than in isolation. Current metabolic models fall short in this regard and oversimplify the complexity of lipid metabolism, as sufficiently resolved lipidomic data sets are scarce. Especially complex lipid classes such as triacylglycerols and cardiolipins frequently have to be reported without side chain information since numerous isomers and isobars convolute their fragment spectra in mass spectrometry experiments. Automated annotation software can only identify one compound per spectra, leading to a systematic under-representation of the actual lipid diversity in more complex spectra.

To address this limitation, we developed **Fatty Acylizer**, a computational approach that reconstructs unresolved fatty acyl profiles using a combinatorial side chain substitution model. We previously validated this method for cardiolipins and now benchmark its performance across additional lipid classes using independent external datasets. To further explore its role as a potential diagnostic tool, we evaluate its sensitivity in detecting known fatty acid biomarkers within lipid profiles. By enhancing the depth and reliability of fatty acyl information in lipidomic data, **Fatty Acylizer** enables more robust interpretation of lipid composition. This improved resolution supports the development of predictive metabolic models and provides a foundation for uncovering the mechanistic origins of lipid diversity and specificity.

Reverse remodeling of the left ventricle after minimally invasive mitral valve reconstruction

Hamed Wafa

Background: Degenerative MVD, especially MVP, is considered the main cause of MR and plays a significant role in Western civilisation. DMR is associated with LV dilatation. Minimally invasive mitral valve repair, now considered the gold standard, is the treatment of choice and shows the best short- and long-term results in terms of survival and functional benefits. The aim of this study is to identify the reverse remodelling process and the functional benefits for the LV.

Methods: Between 2001 and 2019, 363 patients were retrospectively analysed and included in the study. The echocardiographic data were collected at the three time points pre-, postoperative and follow-up as well as relevant comorbidities and mortality data. The collected data of the longitudinal study were analysed for statistical significance with regard to gender, survival and mortality as well as regarding their development over time.

Results: Of the 363 patients with a median age of 64.10 years, 47 (13.1%) had died. Among the comorbidities, arterial hypertension and atrial fibrillation were the most common. Comparing preoperative vs. postoperative, EF was statistically significantly ($p < 0.001$) but postoperatively decreased at 51.06% (IQR: 43.08-59.18) vs. preoperatively 58.64% (IQR: 50.12-64.82) and LVEDD was also statistically significantly ($p < 0.001$), but postoperatively decreased at 54.7 mm (IQR: 48.7-59.2) vs. preoperatively 58.6 (SD=8.25). The severe MI was also statistically significant ($p < 0.001$) with only 0.6% postoperatively compared to 96.1% preoperatively. Also, statistically significant ($p < 0.001$) was sPAP at 35 mmHg (IQR: 35-45) compared to 45 mmHg preoperatively (IQR: 36.8-55). Comparing preoperative vs. follow-up, EF follow-up was still statistically significantly ($p < 0.001$) decreased (Md=55 %, IQR: 45-60 %). LVEDD was statistically significantly ($p < 0.001$) lower (Md: 50.2 mm IQR: 45-56) than preoperatively (MW: 58.35 mm, SD: 8.61). Similarly, LVESD was statistically significantly smaller at follow-up (Md=32.4 mm IQR: 30-39.4) than preoperatively (Md=37.1 mm, IQR: 33.27-43.3). The severity of MI at follow-up was 3.3% and statistically significantly lower than preoperatively (97.7%). Mild MI at follow-up was 27 % ($p < 0.001$) and moderate was 12.7 % ($p < 0.001$), statistically significantly higher than preoperative mild (1.5 %) and moderate MI (0.7 %).

Conclusion: The results show an improvement of LV geometry, i.e. reverse remodelling and functional improvement of insufficiency as well as sPAP after minimally invasive mitral valve repair. No improvement in EF, RVDLA and RVDSA was observed

Adherence to the SAGER guidelines in psycho-oncology trials: a systematic review of sex and gender reporting practices

Jennifer Birke

Background

Sex and gender substantially shape psychosocial outcomes, supportive care needs, and responses to psycho-oncological interventions among people living with cancer. Inadequate integration of sex and gender into clinical research compromises scientific validity and perpetuates inequities in cancer care. We systematically assessed the quality of sex and gender reporting in randomized controlled trials (RCTs) of psycho-oncology interventions using the Sex and Gender Equity in Research (SAGER) guidelines.

Methods

We conducted a systematic review of RCTs published between 2020 and 2025 and indexed in PubMed. Eligible studies included adult cancer populations receiving psycho-oncological interventions and reporting patient-reported outcomes. Adherence to the SAGER guidelines was coded dichotomously at item level and summarized using total scores, accounting for differences in item applicability between studies including one versus multiple sexes or genders. Item-level frequencies, analyses by tumor entity, sensitivity analyses, and exploratory regression models were used to characterize reporting patterns and their correlates.

Findings

A total of 404 trials were included. More than half of studies (55.2%) used sex and gender terminology inaccurately. Among studies including multiple sexes or genders, the mean SAGER adherence score was 1.23 (SD 0.88) out of 13, with 98.3% fulfilling three items or fewer. Studies including only one sex or gender showed mean adherence score of 0.90 (SD 0·81) out of 3. Reporting deficits were consistent across tumor entities and study characteristics. Regression analyses indicated no association between reporting quality and publication year, sample size, or journal impact factor.

Interpretation

Sex and gender are not systematically integrated into psycho-oncology intervention research. This reflects structural deficiencies rather than isolated study-level limitations and constitute a major barrier to equitable supportive cancer care. Strengthening mandatory reporting standards, editorial enforcement, and targeted training is essential to advance sex- and gender-sensitive psycho-oncology research and to reduce inequities in psychosocial cancer care.

Interaction between Inflammation and Anticoagulation in Cardiopulmonary Bypass

Lukas Vergeiner

Cardiopulmonary bypass (CPB) induces a systemic inflammatory response via activation of the complement system, leukocytes, and cytokine release, which subsequently stimulates endothelial cells and upregulates tissue factor expression, directly linking inflammation to coagulation activation. Patients undergoing major cardiac surgery require intraoperative anticoagulation prior to CPB initiation. Unfractionated heparin (UFH) remains the standard anticoagulant, with reversal by protamine. However, the interplay between inflammation and coagulation regulation is incompletely understood. Systemic inflammation and the phenomenon of heparin rebound may influence postoperative outcomes, including bleeding, thrombosis, organ dysfunction, delirium, and mortality. Therefore, optimizing anticoagulation monitoring in the context of inflammation is essential to improve patient safety.

The Anticoagulation and Inflammation Monitoring after Heart and Vascular Interventions (PAC-AIM) trial is a prospective observational study enrolling 400 adults undergoing elective major cardiac surgery. The primary aim of this PhD thesis, as part of the trial, is to investigate the impact of systemic inflammation on anticoagulation monitoring and patient outcomes after cardiac surgery.

Eligible participants are adults (≥18 years) undergoing elective major cardiac surgery who provide written informed consent. Exclusion criteria include pregnancy, participation in another interventional trial, known coagulation disorders or immunosuppression, planned deep hypothermic circulatory arrest, acute or subacute myocardial infarction within 90 days, or anemia as defined by World Health Organization criteria.

Study objectives include evaluating correlations between inflammatory biomarkers and anticoagulation parameters; assessing the impact of inflammation on test accuracy and sensitivity; analyzing associations between inflammation intensity and postoperative blood loss, heparin rebound, and protamine requirements; and examining links between inflammation, altered anticoagulation needs, and clinical outcomes such as bleeding, thrombosis, extracorporeal membrane oxygenation support, and delirium. Sex-specific inflammatory response patterns and their influence on outcomes will also be explored.

I will hand in the results part later, as soon as I have done a first analysis.

Sebastian von der Emde

Introduction:

In patients with heart failure and reduced ejection fraction (HFrEF), soluble neprilysin has been shown to independently predict the risk of subsequent future clinical cardiovascular events. Furthermore, angiotensin-receptor-neprilysin-inhibitors have become an integral component of contemporary pharmacological standard therapy in patients with HFrEF. However, the clinical relevance of neprilysin in patients with myocardial infarction remains poorly defined. This study was aimed at analysing the impact of plasma levels of soluble neprilysin (SN) on clinical characteristics and infarct size in patients with ST-Elevation Myocardial Infarction (STEMI).

Methods:

This study included STEMI patients which were treated with primary percutaneous coronary intervention (pPCI) at the University Hospital Innsbruck between 2012-2023. Infarct size (IS) and left ventricular ejection fraction (LVEF) where measured by cardiac magnetic resonance (CMR) imaging within a week after the event, using a standardized protocol. Neprilysin levels were measured 48 hours after the index event using a validated immunoassay.

Results:

A total of 657 patients (20% female) with a median age of 58 (IQR: 52-67) years were analyzed. Median plasma levels of SN at 48 hours where measured at 138 (IQR: 32-541) pg/mL. Upon dichotomization according to median SN concentrations, no difference in patient characteristics could be demonstrated, except for significantly lower levels in smoking patients (p=0,002). IS and LVEF after the event did also not show any statistically significant differences according to median SN concentrations. (p=0,559; p=0,399).

Conclusion:

In a population of reperfused STEMI-patients, plasma levels of SN did not show any significant association with baseline patient charactericts, with the exception of smoking status. Above median concentrations of SN did not result in larger IS or worse LVEF.

Ex Vivo Experiments to Assess the Effects of Fibrin(ogen) in Hepatic Insufficiency

Volker Schaefer

Background:

Patients with advanced chronic liver disease exhibit a fragile, rebalanced hemostatic state, resulting in an increased risk of both bleeding and thrombosis. To reduce the need for allogeneic blood transfusions, fibrinogen concentrates are increasingly used in clinical practice. However, the effects of fibrinogen supplementation on coagulation in patients with end-stage liver disease (ESLD) remain incompletely understood. This study aims to investigate the impact of ex vivo fibrinogen supplementation on coagulation dynamics and fibrin network architecture in patients with CHILD-B and CHILD-C liver cirrhosis compared with healthy controls.

Methods:

In this ex vivo experimental study, peripheral venous blood samples were obtained from 19 patients with CHILD-B cirrhosis, 19 patients with CHILD-C cirrhosis, and 18 healthy individuals. Samples were analyzed under native conditions and after supplementation with increasing concentrations of fibrinogen (+50, +100, and +200 mg/dL). Standard laboratory parameters were assessed alongside viscoelastic testing using ClotPro®, thrombin generation assays (ST Genesia®), and three-dimensional confocal live-cell microscopy to visualize and quantitatively analyze fibrin network formation.

Results:

This poster presents the first preliminary results of the study, with a particular focus on sex-specific differences in coagulation profiles and fibrin network characteristics in patients with liver cirrhosis.

Impact of risk factors for hemochromatosis in HFE p.H63D homozygous individuals

Wolfgang Straka

Background and Aims: Hemochromatosis is a common genetic condition characterized by organ iron overload and, in most cases, caused by mutations in the HFE gene. Disease severity is mainly influenced by additional risk factors, such as smoking, alcohol abuse or fatty liver disease. This study investigated the impact of such risk factors in individuals homozygous for HFE p.H63D.

Methods: 8839 individuals with verified Tyrolian residency were genotyped for both the p.H63D and p.C282Y variant. Clinical data as well as laboratory parameters, including risk factors and comorbidities were retrospectively assessed from the electronic health record. The comparison with a propensity score-matched control population was set up to show potential effects of the HFE mutations and risk factors on the survival rate of both cohorts. Additionally, gender-specific comparisons were performed to show differences in male and female individuals.

Results: Comparison of the cohorts, especially by laboratory parameters, revealed that significantly more individuals homozygous for p.C282Y in HFE present with biochemical iron overload, than individuals homozygous for p.H63D. In contrast, alcohol consumption and other risk factors appear to be significantly more common in p.H63D homozygotes. Both HFE mutation groups showed significantly reduced survival compared with the control population.

Conclusion: In summary, homozygous p.H63D variants in HFE are associated with elevated iron parameters in the presence of coexisting comorbidities. However, in HFE p.H63D homozygous individuals iron overload occurs less frequently and with a lower penetrance compared to p.C282Y homozygous individuals.

Developing and Evaluating a Scalable Data Linkage Framework for Longitudinal Stroke Outcome Research and Quality Monitoring in Austria

Petr Simurda

Background:
Long-term outcomes after stroke are key indicators of quality in stroke care, yet systematic outcome monitoring beyond the acute phase remains limited in routine practice. While clinical stroke registries provide high-quality data on acute management and early outcomes, they often lack comprehensive longitudinal follow-up. In Austria, the Austrian Stroke Unit Registry (ASUR) has prospectively collected standardised clinical data from all stroke units nationwide since 2003. In parallel, the Austrian DRG System (Leistungsorientierte Krankenanstaltenfinanzierung, LKF) enables longitudinal tracking of hospitalisations, complications, and mortality through a person-specific pseudonymisation framework. As of January 2025, the linkage between ASUR and LKF data at the patient level has become technically feasible.

Objectives:
The objective of this clinical PhD project is to evaluate the technical, legal and organisational feasibility of establishing patient-level linkage between ASUR and LKF data. The primary aim of this linkage is to enable long-term outcome assessment after stroke, and to strengthen quality assurance at the stroke unit level. A secondary objective is to explore the potential of the linked data infrastructure for future registry-based platform studies.

Methods:
The project employs a multi-step methodological approach. Firstly, the technical feasibility of patient-level linkage between the ASUR and the LKF is assessed, with a particular focus on linkage accuracy, reproducibility, and data security within a pseudonymised framework. Secondly, the ethical, legal, and regulatory requirements for longitudinal use of linked clinical data are systematically analysed in collaboration with relevant stakeholders. Thirdly, key clinical and administrative variables are harmonised and mapped into a research-ready dataset suitable for long-term outcome analyses and quality assurance. Finally, organisational and data governance challenges related to nationwide implementation are examined. Based on these components, a methodological framework for secure registry-based platform research in stroke care is developed.

Expected Results:
The project is expected to enable reconstruction of individual post-stroke patient trajectories, allowing systematic evaluation of long-term outcomes such as rehospitalisation, stroke recurrence, complications, and mortality. This approach will enhance centre-level quality assurance and support data-driven evaluation of evidence-based interventions in routine stroke care. Furthermore, the established infrastructure should provide a reliable foundation for future registry-based platform studies in clinical neuroscience.

Conclusion:
Secure and reliable patient-level linkage of clinical stroke registry data with nationwide administrative health data offers a novel approach to longitudinal outcome

assessment in neurology. This PhD project provides the methodological foundation for sustainable quality monitoring and innovative real-world study designs in Austrian stroke care.

Experimental possibilities beyond confocal standards

ZEISS LSM Airyscan

Sensitive High-Speed Super-Resolution Imaging and Molecular Characterization

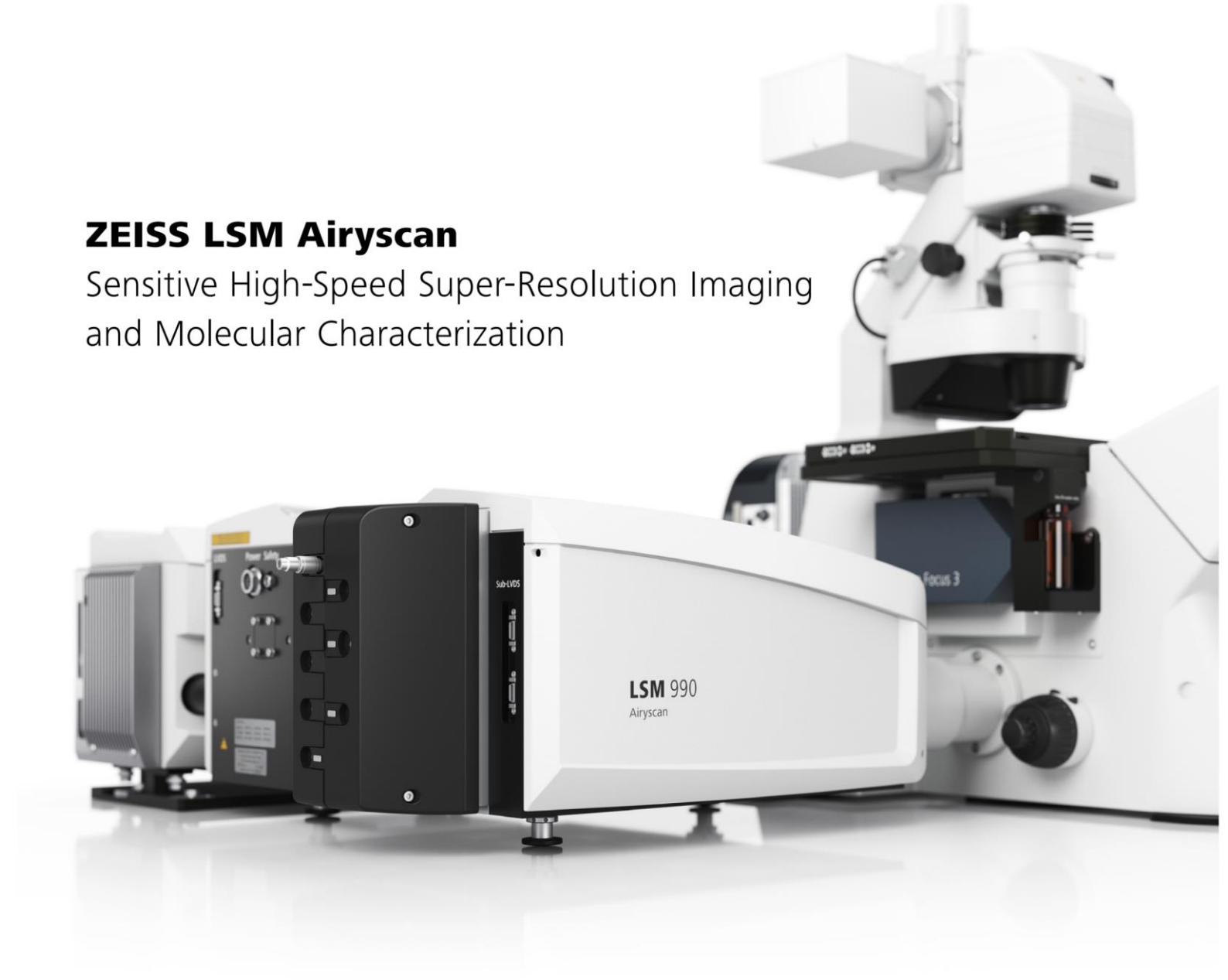

ZEISS

Seeing beyond

Distance-to-tumor analysis of quantitative susceptibility maps in glioblastoma and association with survival Alberto Galimberti

Alberto Galimberti1,2, Stephanie Mangesius1, Julian Mangesius3, Johannes Kerschbaumer4, Christian Freyschlag4, Ute Ganswindt3, Elke R. Gizewski1,2, Christoph Birkl1,2
1 Department of Radiology, Medical University of Innsbruck, Innsbruck, Austria
2 Neuroimaging Research Core Facility, Medical University of Innsbruck, Innsbruck, Austria
3Department of Radiation Oncology, Medical University of Innsbruck, Innsbruck, Austria
4Department of Neurosurgery, Medical University of Innsbruck, Innsbruck, Austria

INTRODUCTION

Glioblastoma (GBM) infiltrates beyond radiologically visible margins, resulting in poor survival. Quantitative susceptibility mapping (QSM), an advanced MRI technique that differentiates local paramagnetic and diamagnetic tissue properties, has emerged as a promising tool for monitoring tumor progression, although its clinical relevance in GBM remains unclear. A diffusion-informed shortest-path framework has recently been proposed to characterize tumor propagation along preferred pathways. Here, we combined QSM-derived maps with diffusion-informed distance-to-tumor mapping to examine how tissue magnetic properties vary with tumor proximity and whether longitudinal changes in these patterns relate to patient survival.

METHODS

Seventeen GBM patients underwent surgery followed by radiotherapy. Magnetic Resonance Imaging (MRI) was acquired before and after radiotherapy, including structural sequences, six-echoes gradient echo and diffusion-weighted imaging sequences. Tumor regions (enhancing tumor, core, edema) were automatically segmented using a top Brain Tumor Segmentation Challenge algorithm and verified by a radiologist. Paramagnetic and diamagnetic susceptibility components were estimated using χ-sepnet, a deep learning-based source separation method. Distance-to-tumor maps were generated using a Hamiltonian Fast Marching algorithm incorporating an anisotropic Riemannian metric based on diffusion MRI, with seeds defined by enhancing tumor masks. Generalized additive models (GAMs) were used to model the relationship between susceptibility values and distance to the tumor. The first derivative of each smoothed curve up to the first local extremum was used to quantify short-range rates of change, and differences in these rates between time points were calculated. Associations with overall survival were evaluated using Cox proportional hazards models, adjusting for clinical (i.e. MGMT methylation status and tumor volume) and demographic (i.e age) variables.

RESULTS

Distance-based GAM analyses revealed significant variations in QSM-derived metrics in the peritumoral region adjacent to the enhancing tumor. At the group-level, both paramagnetic and diamagnetic susceptibility exhibited substantial intersubject variability. Differences in the paramagnetic rate of change showed a trend toward an association with overall survival, with higher rates corresponding to worse outcomes. MGMT methylation status was a significant predictor, with methylated tumors showing improved survival.

DISCUSSION

Results demonstrated marked alterations in tissue composition near the tumor, involving both iron and myelin components. The observed increase in paramagnetic susceptibility changes between pre- and post-radiotherapy scans may reflect elevated iron metabolism toward the tumor. Although the association with overall survival was only marginally significant, it suggests that iron could serve as a marker of tumor aggressiveness. Study limitations include the small sample size and the lack of explicit modeling of tumor proliferation in the distance mapping approach.

CONCLUSIONS

Distance-resolved QSM offers a valuable approach for assessing tissue composition in proximity of the enhancing tumor. Future studies with larger cohorts, additional imaging contrasts.

Towards understanding the role of gut–brain axis in a-synucleinopathies

Magdalena Matić

Magdalena Matic, Antonio Heras-Garvin, Nadia Stefanova
Division of Neurobiology, Department of Neurology, Medical University of Innsbruck, Austria

Synucleinopathies are neurodegenerative disorders characterized by pathological accumulation of a-synuclein (aSyn) (Spillantini et al., 1998). While traditionally studied as central nervous system diseases, increasing evidence indicates early involvement of the gastrointestinal (GI) tract. GI disturbances frequently precede motor symptoms, highlighting the gut as a potential site of early pathology (Abbott et al., 2001). Experimental data support bidirectional communication along the gut–brain axis (Arotcarena et al., 2020; Van der Berge et al., 2019). However, the biological consequences of intestinal aSyn expression and its interaction with local tissue environment remain poorly defined.

The proteolipid protein (PLP)-a-synuclein transgenic mouse expresses human aSyn under the PLP promoter (Kahle et al., 2002) and develops selective neurodegeneration (Stefanova and Wenning, 2016), making it a suitable model to study systemic aspects of synucleinopathy. This project aims to characterize gut–brain axis involvement in the PLP model by defining intestinal aSyn distribution and identifying molecular responses within the GI tract.

We analysed twelve-month-old PLP-a-syn transgenic mice and age-matched wild-type controls. Brains and GI tissues were collected, and the GI tract was segmented into duodenum, jejunum, ileum, and colon. From each intestinal region, samples were allocated for histological and molecular analyses. Histological specimens were processed using an adapted improved Swiss-roll technique (Le Naour et al., 2022), enabling consistent visualization of the full intestinal architecture. Following initial immunofluorescence screening, transcriptomic profiling was performed using RNA sequencing.

Immunofluorescence analysis revealed human aSyn expression within the myenteric and submucosal plexuses of the small intestine and colon in PLP-a-syn mice. Transcriptomic analysis demonstrated robust and regionally distinct alterations in immune-related pathways across intestinal segments. These changes were most pronounced in the ileum, where gene networks associated with innate and adaptive immune activation, barrier regulation, and neuroimmune signaling were strongly modulated. Each gut segment exhibited a unique transcriptional fingerprint, suggesting localized responses rather than a uniform intestinal reaction to aSyn. These findings indicate that enteric aSyn expression is associated with selective remodeling of inflammatory pathways, potentially contributing to the pathology in synucleinopathies.

Ongoing work focuses on validating key pathways and defining cellular contributors to these molecular changes. By mapping early intestinal responses to aSyn pathology, this study advances understanding of peripheral mechanisms in synucleinopathies and supports the concept that gut alterations may represent accessible early biomarkers and therapeutic targets.

Acknowledgement: The study is supported by the intramural funding program of the Medical University Innsbruck PhD Research Training Groups, Project 2022-1-1.

Neutrophil Diversity in Prostate Cancer

Felix Melchior

Introduction: Prostate cancer (PCa) is the most prevalent malignancy in men with limited efficacy of immunotherapeutic approaches. The tumor microenvironment (TME) appears "immunologically cold", characterized by sparse T-cell infiltration, low tumor mutation burden, and elevated immunosuppressive cell populations. Tumor-associated neutrophils (TANs) represent a significant yet understudied immune cell compartment in PCa. Elevated neutrophil levels are associated with worse oncological outcome in different tumor entities. Recent advances in single-cell RNA sequencing (scRNA-seq) have identified distinct neutrophil subpopulations with divergent pro-tumoral and anti-tumoral characteristics, yet, their diversity, heterogeneity, and role in immunotherapy resistance in PCa remain largely unexplored. Findings from lung and colorectal cancer cohorts indicate that neutrophils exhibit substantial heterogeneity and plasticity, organizing into distinct subpopulations with specific transcriptomic signatures. The plasticity of these subpopulations appears to be driven by tumor-derived signals, metabolic factors within the TME, and potentially therapeutic pressure. In PCa, distinct neutrophil states may arise from common precursors in response to tumor-specific signals such as CXCL1/IL-8 chemotactic axes, TGF-B, and hypoxic signaling. The balance between pro-tumoral TANs and potential anti-tumoral normal-associated neutrophils (NANs) could represent a critical determinant of the TME composition and immunotherapy response.

Aim of the Project

This project aims to in-depth characterize neutrophil heterogeneity and plasticity within the PCa TME. We hypothesize that distinct TAN subsets contribute to an immunosuppressive TME through differential expression of pro-tumoral phenotypes, thereby limiting the efficacy of immunotherapeutic approaches. Furthermore, we aim to identify transcriptomic signatures and surface markers that define functionally distinct neutrophil states and determine their association with tumor-promoting versus anti-tumor properties. The possible findings have translational potential for identifying neutrophil-based biomarkers and developing targeted therapeutic interventions to reprogram neutrophils, ultimately improving immunotherapy efficacy and personalized therapy in PCa patients.

Material & Methods

Fresh tissue samples and peripheral blood are obtained from patients undergoing radical prostatectomy for organ-confined PCa (n=10, Gleason Score ≥ 7b). Single-cell suspensions are prepared from tumor tissue, adjacent normal prostate tissue, and peripheral blood through enzymatic digestion and mechanical dissociation. ScRNA-seq will be performed utilizing the BD Rhapsody® platform, raw sequencing data will be processed using BD Rhapsody analysis pipelines and bioinformatics. Clustering algorithms are applied to identify distinct cell clusters based on transcriptional profiles. Multiparametric flow cytometry (mpFC) will be performed to validate scRNA-seq findings and assess surface marker expression patterns. Secondary, co-culture experiments will be conducted with PCa cell lines and neutrophils from healthy individuals to further validate the findings from the scRNAseq analyses.

In an independent analysis we conduct a retrospective analysis in 300 patients with metastatic PCa receiving taxan-based chemotherapy. neutrophil blood counts

before and throughout therapy are assessed along with clinical data to investigate the correlation of neutrophil blood count and oncological outcome.

Outlook: Currently, patient recruitment is ongoing with four patients already included in the scRNAseq analysis. Recruitment phase is expected to be comleted by the end of spring 2026.

The retrospective data analysis is ongoing and planned to be completed by March 2026.

Between arrival and integration: Health, resources, and barriers to healthcare for women* with migration experience in Austria

Judith Stefanie Söller

Authors:

Söller J (1), Birke J(1), Ludwig S(1)

(1) Institute for Diversity in Medicine, Medical University of Innsbruck, Innsbruck, Austria

Background:

People with migration experience report significant barriers to accessing healthcare services in European host countries. Despite a high proportion of people with migration experience in Austria, only limited systematic data is available. The aim of this scoping review is to summarize the available literature on the healthcare of people with migration experience in Austria, with a particular focus on women*, as well as on the access to and the use of healthcareservices.

Method:

A scoping review was conducted according to the Arksey and O'Malley framework and the recommendations of the JBI. The systematic literature search was conducted in PubMed, Web of Science, and CINAHL and included studies from 2015 onwards analyzing the access to healthcare for individuals with migration experience in Austria focusingon women*. The content was mainly on health inequalities, access to and the use of care, as well as health-related social determinants. The data were recorded in a charting table and summarized thematically using qualitative content analysis.

Results:

A total of 92 articles were included. The results show a clear discrepancy between formal entitlement to healthcare and actual access conditions, which are particularly mediated by language barriers (n=25; 28.1%) and insufficient information, leading to reduced health literacy (n=29; 32.6%). There is a lack of culturally sensitive, target group-oriented health services. People with migration experience show an increased burden of mental health problems (n=29; 32.6%) such as depression and anxiety disorders. Female migrants are particularly vulnerable due to gender role expectations, gendered violence, and reproductive health needs. There are also gaps in the use of preventive healthcare measures, such as vaccinations and e.g., cancer screening.

Conclusions:

The results show that people with a migration experience should not be viewed as a homogeneous group, but that health risks and access to healthcare vary according to sex/gender, origin, place of residence and socioeconomic status. Culture- and sex/gender-sensitive reforms in healthcare are needed, including cultural mediation, target group-specific prevention strategies, and systematic, migration-sensitive research and guideline development to reduce inequalities in healthcare in Austria.

*all individuals who identify as women.

Multimodal MRI as a surrogate Marker for prodromal Parkinson's disease – monocentric baseline results of the MUMFORD study

Simon Leiter

Authors: S. Leiter 1, F. Jagusch 1, R. Steiger 1, A. Grams 1, A. Stefani 1, C. Scherfler 1, K. Seppi 1, B. Högl 1, A. Droby 2, A. Thaler 2, F. Krismer 1 and P. Mahlknecht 1, on behalf of the MUMFORD study investigators
Institution: 1 Department of Neurology, Medical University of Innsbruck, Innsbruck, Austria
2 Movement Disorders Unit, Neurological Institute, Tel Aviv Sourasky Medical Center, Tel Aviv, Israel

Background: The cardinal motor symptoms of Parkinson's disease (PD) are preceded by a heterogenous prodromal phase. Polysomnography-proven isolated REM-sleep behaviour disorder (iRBD) is the only single clinical marker associated with a conversion risk for synucleinopathies exceeding 75%. Other signs, as olfactory dysfunction, depression, and obstipation, lack specificity on their own and are currently combined in algorithms, such as the Movement Disorder Society (MDS) criteria for prodromal PD, to improve detection of prodromal individuals from the general population. While different investigational magnetic resonance imaging (MRI) markers of PD including loss of dorsal nigral hyperintensity on iron-sensitive sequences have also been found in RBD, it is currently unknown whether these signs can be observed in other subjects at-risk for developing PD.
Methods: The MUltimodal MRI as a surrogate Marker FOr pRodromal PD (MUMFORD) study is a prospective observational cohort study performed in two centres, Tel Aviv Sourasky Medical Centre (TASMC) and Innsbruck Medical University (MUI). We aim to identify MRI markers that best distinguish between at-risk cohorts and controls and to validate their potential to predict phenoconversion to clinically defined PD. Clinical and imaging characteristics of four different at-risk cohorts including non-manifesting GBA1 and LRRK2 carriers, iRBD patients, and individuals with a MDS prodromal PD score of > 30% or >10% and olfactory dysfunction (possible prodromal PD [PPD] cohort), are compared to a PD and a healthy control (HC) group. Multimodal MRI and clinical phenotyping, including MDS-UPDRS examination, smell testing, and in-depth questionnaires regarding non-motor symptoms, is done at baseline and after two years to enable detection of progression and potential phenoconversion to PD. While follow-up visits are still ongoing, we here summarize the baseline clinical characteristics of our cohort.

Results: Between October 2021 and February 2025, 155 participants (20 LRRK2 and 21 GBA1 carriers, 20 iRBD patients, 29 participants with possible PPD, 34 HC, and 31 PD patients) were included in the MUMFORD study. The mean age in the whole cohort was 60.2 years and 50% of the participants were female. The distribution of demographic data differed between the groups with the LRRK2 carriers having the youngest mean age (55.1 years) and the iRBD group being predominantly male (90%). The median MDS prodromal score was 0.19% for HCs vs. 64.72% in the PPD group. MDS-Unified Parkinson's Disease Rating Scale (MDS-UPDRS) part III scores were highest for the PD cohort (median 22 points) followed by the PPD group (7 points). More non-motor symptoms were reported in the PPD and the iRBD cohort compared to HCs (mean score in the Scales for Outcomes in PD Autonomic of 13.6 for the PPD and 13.3 iRBD cohort vs. 7.5 points for the HCs; mean Becks Depression Index of 9.5 and 6.7 vs.

3.9 points, respectively), while the Montreal Cognitive Assessment (MoCA) scores did not show relevant between-group differences (mean 26.5 points for whole cohort).

Conclusion: Different at-risk cohorts for PD were successfully recruited within the MUMFORD-study, and first clinical characteristics and differences within the cohort were demonstrated, while the baseline MRI data are currently analysed.

Sex-specific association of serum ferritin with persistent infarct core iron after ST-elevation myocardial infarction

Philipp Fischer

Background: Persistent infarct core iron (PICO) after hemorrhagic ST-elevation myocardial infarction (STEMI) is associated with chronic myocardial inflammation, adverse remodeling and worse clinical outcome. However, the pathophysiology and determinants of PICO according to sex-specific occurrence are incompletely understood.

Aim: To investigate the association between biomarkers of systemic iron homeostasis measured in the acute and chronic post-infarction phases and PICO following STEMI.

Methods: STEMI patients treated with primary percutaneous coronary intervention and enrolled in the prospective Magnetic Resonance Imaging in Acute ST-Elevation Myocardial Infarction study (MARINA-STEMI, NCT04113356) were included. Serum markers of iron metabolism (serum ferritin, iron, transferrin and transferrin saturation (TSAT)) were serially measured at hospital admission for index STEMI and at 4-months follow-up (4FU). Presence of PICO was measured on T2* magnetic resonance imaging (MRI) mapping at 4FU.

Results: In total, 442 patients (median age 59 [IQR: 53-67] years, 20% female) were analyzed. PICO was observed in 91 (21%) patients, 14 (3%) of whom were women and 77 (18%) men. Concentrations of serum ferritin were significantly higher in men compared to women both at baseline (men: 242 [146-393] µg/L vs. women 158 [102-242] µg/L, p<0.01) and at 4 months Follow-up (4FU) (men: 183 [108-292] µg/L vs. women: 99 [52-189] µg/L, p<0.01). While serum iron, transferrin and TSAT levels did not show a significant association with PICO, serum ferritin concentrations at hospital admission (271 [194-465] µg/L vs. 205 [127-365] µg/L, p<0.01) and at 4FU (221 [128-305] µg/L vs. 167 [81-256] µg/L, p<0.01) were significantly higher in patients with PICO than in those without PICO. The associations of serum ferritin concentrations with PICO remained significant after adjustment for clinical parameters including serum ferritin, age, sex, body mass index (BMI), hypertension, current smoker, hyperlipidemia and diabetes mellitus both at admission (Odds ratio (OR) 2.36 [95% confidence Interval (CI), 1.40-3.95]; p<0.01) and at 4FU (OR: 2.23 [95% CI: 1.34-3.71]; p<0.01).

Conclusions: Serum concentrations were higher in men compared to women. In patients with STEMI, both acute and follow up serum ferritin concentrations were significantly and independently associated with PICO. These findings suggest a pathophysiological link between systemic iron stores and irreversible myocardial iron deposition following STEMI.

Biomarker Profiles and Functional Recovery after Acute ST-Elevation Myocardial Infarction

Anita Sandor

Circadian Dependence of Intramyocardial Haemorrhage in reperfused ST-Elevation Myocardial Infarction

Background: The circadian clock regulates cardiovascular physiology and may modulate

susceptibility to ischaemia-reperfusion injury in acute myocardial infarction. Whether

intramyocardial haemorrhage (IMH), the most severe form of microvascular injury, after

reperfused ST-elevation myocardial infarction (STEMI), exhibits time-of-day dependence

remains unknown.

Aim: To investigate time-of-day associations of symptom onset with IMH occurrence, assessed by cardiac magnetic resonance (CMR), in patients undergoing primary percutaneous coronary intervention (PCI) for acute STEMI.

Methods: Patients with first acute STEMI treated with primary PCI at the University Heart Center of Innsbruck were analysed. Based on symptom onset, patients were categorized as daytime (08:00-21:59) or nighttime (22:00-07:59). CMR was performed 4 days [Interquartile range (IQR): 3-5] after PCI. The primary endpoint was the occurrence of IMH on T2* mapping.

Results: A total of 777 patients (140 women, 18%) with a median age of 59 years (IQR: 53-67) were included. IMH was present in 276 (36%) patients. IMH occurred more frequently in the nighttime than in the daytime group (43% vs 33%, $p<0.01$). Median total ischaemic time was 185 min (IQR: 119-310) and was longer at night than during daytime [227 min (IQR: 153-389) vs 167 min (IQR: 109-275), $p<0.01$].

Conclusion: Symptom onset at night was associated with a higher occurrence of IMH after reperfused STEMI and with longer total ischaemic time compared with daytime presentation

Clinicogenetic Characterization of Sporadic Late Onset Ataxias

Lina Schwaighofer

Introduction

Since the identification of RFC1 and FGF14 as two novel genes in association with sporadic late onset ataxias (SAOA) in recent years, many ataxias previously classified as idiopathic late onset ataxias (ILOCA) or as probable multiple system atrophy of cerebellar type (MSA-C) after Gilmans consensus criteria were able to be reclassified. Still, 70% of SAOA remain with unclear aetiology to this day.

While a homozygotic mutation in RFC1 leads to the autosomal recessive CANVAS phenotype, a repeat expansion in FGF14 causes the autosomal dominant spinocerebellar ataxia type 27b (SCA27b). Both diseases are characterized through late onset cerebellar ataxia (onset after 40 years of age) and cerebellar syndrome including dysarthria, dysphagia and nystagmus. As these are the leading motor symptoms in MSA-C as well, differentiation between the three diseases has proved to be quite difficult. In previous studies, autonomic failure and REM sleep behavioural disorders (RSBD) are shown to be characteristic and early manifestations of MSA-C. Since autonomic failure can also appear in SCA27b and CANVAS, further investigation of leading autonomic symptoms and their onset in disease stage is imperative.

This study will therefore focus on phenotyping SCA27b, CANVAS, MSA-C as well as ILOCA to elucidate differences in presentation to facilitate diagnosis and pathway to genetic testing to improve accurate early diagnostic rates and therefore optimize individual patient care.

Materials and Methods

In a monocentric, mixed retro- and prospective study we will investigate about 100 patients with ILOCA, probable MSA-C and genetically confirmed SCA27b and CANVAS. Demographic data will be extracted from the clinic internal system (KIS) and a subset of patients will be seen at a baseline visit as well as at a one-year follow up to investigate disease progression. At baseline and at the follow up, a series of questionnaires regarding autonomic function, screening for RSBD and quality of life will be collected. Each patient will also receive a Schellong-test to test for orthostatic dysregulation and at least one MRI as part of a routine diagnostic work up. If clinically indicated, patients will also receive head-up tilt table test, a DAT Spect scan, a nerve conduction study and polysomnography. Group differences for the main outcome (phenotypical differences between MSA-C and monogenetic SAOA patients) will be compared using logistic regression including a Bonferroni corrective to account for alpha-mistakes, as well as Chi-Quadrat-test or odds ratio as appropriate.

Results

Up until now no patients have been included in this study, therefore no results are available. We expect to highlight differences in presentation of autonomic failure of MSA-C in comparison to monogenetic SAOA as well as in velocity of disease progression. We also suspect the presence of RSBD in ILOCA patients to be an early sign for possible conversion into MSA-C phenotype later on. We hope to lay the foundation for clinical guidelines of diagnostic pathways and aid in reducing the diagnostic gap in SAOA.

Samuel Pröll

Extracting waveforms from electrocardiography (ECG) printouts remains a difficult task even today. A recent challenge organized by Physionet highlights the need for practical solutions which could give access to billions of ECGs globally stored in image formats. A key limitation of the Physionet challenge is its focus on a single fixed layout (3x4 matrix), which does not reflect the variety encountered across devices and health care systems.

To account for variations in ECG layouts and styles, we develop an ECG paper synthesis tool that is capable of gener-ating different layouts (3x4, 6x2, 12x1, optional rhythm strips) with random positioning and styling of visual ele-ments. High-fidelity segmentation masks for each ECG trace are generated. We use this tool to create random images and masks on-the-fly while training a 2D U-Net to segment each pixel into background, 12 leads and rhythm. Post-processing is applied on the segmentation output to extract the 12-lead ECG time-series.

Trained on augmented synthetic images, the pipeline is evaluated on internal, real-world ECG images in two ways. First, for a set of 5011 images, extracted signals are visually overlaid with the original image and the signal quality is judged independently by three team members. Through majority voting, we find the quality to be "good but some er-rors" or "excellent" in 92.9% of cases, while only 2.4% are "bad" extractions (remaining 4.7% are "invalid" or incon-clusive images). Second, a subset of 960 high-quality digital PDFs with available ground-truth signals are quantitative-ly evaluated. We obtain a median signal to noise ratio (SNR) of 41.2dB (IQR: 34.4dB).

The presented workflow allows development of ECG digitization algorithms using fully synthetic data. The derived pipeline achieves qualitatively good ECGs signals for a majority of images. The high SNR highlights strong model performance, paving the way for large-scale biosignal data access from paper-based ECGs.

Vanessa Heim

Background:

Intimal hyperplasia represents the primary cause of venous graft failure. Early injury to endothelial cells (ECs) initiates leukocyte recruitment, which promotes inflammatory responses that drive the migration and proliferation of vascular smooth muscle cells (VSMCs) within the venous wall. These pathophysiological mechanisms closely resemble those observed in atherosclerosis. Recent clinical evidence has identified colchicine as an effective agent for secondary prevention of atherosclerosis progression. This study aims to evaluate the impact of colchicine on intimal hyperplasia, focusing on its anti-inflammatory and anti-proliferative effects as a potential strategy to prevent venous graft failure.

Methods:

Cell culture studies were performed using human endothelial cells and human vascular smooth muscle cells. Dose–response analyses were carried out to assess the effects of colchicine on cell proliferation and apoptosis in both cell types. Endothelial cells were exposed to an inflammatory stimulus, after which Vascular Cell Adhesion Molecule-1 (VCAM-1) expression was quantified by qPCR. Monocyte adhesion was evaluated using a co-culture system with fluorescently labeled monocytes. VSMC migration and proliferative capacity were examined using scratch and transwell migration assays. For in vivo analysis, a venous bypass model was established in C57Bl/6J mice by grafting a donor inferior vena cava (IVC) into the carotid artery. The patency of the grafts was assessed with laser Doppler imaging. Mice in the treatment group received colchicine via drinking water for four weeks, after which venous graft intimal hyperplasia was measured by histological analysis.

Results:

Colchicine suppressed the proliferation of both vascular smooth muscle cells (VSMCs) and endothelial cells (ECs) in a dose-dependent manner. Importantly, even at higher concentrations, colchicine did not induce marked apoptosis. Furthermore, colchicine markedly reduced leukocyte adhesion to ECs following inflammatory stimulation by inhibiting VCAM-1 upregulation. In vitro analyses demonstrated a significant reduction of VSMC proliferation and migration, as evidenced by scratch assays. Transwell migration assays verified a reduction in VSMC motility in vitro after colchicine treatment. In vivo, colchicine treatment led to a significant decrease in venous graft intimal hyperplasia and was associated with a reduced αSMA-positive area compared with untreated controls. Laser Doppler imaging further demonstrated significantly increased graft perfusion in the colchicine-treated group compared with controls.

Conclusion:

Colchicine effectively suppresses critical mechanisms underlying intimal hyperplasia by limiting endothelial activation, leukocyte adhesion, and vascular smooth muscle cell proliferation and migration. These results support colchicine as a promising therapeutic strategy to enhance venous graft patency and reduce graft failure following bypass surgery.

Modern imaging techniques in the neuroradiological diagnosis of neuro oncological diseases.

Florian Vogetseder

PI: Ass. Prof. Priv.-Doz. Dr. med. univ. Stephanie Mangesius, PhD

Introduction

Glioblastoma is the most frequent primary malignant brain tumour and is associated with a poor prognosis, with an untreated survival time of only a few months. After surgical resection followed by combined radiotherapy and chemotherapy, survival can be extended to more than one year.

Radionecrosis (RN) and pseudoprogression (PSP) are treatment-related changes. PSP is defined as an early, self-limited radiographic change that mimics tumour progression but shows no inflammatory process histopathologically. In contrast, RN typically occurs at a later stage, requires therapeutic intervention, and is characterised by inflammatory reactions, necrosis, and vascular rarefaction.

Using conventional MRI, differentiation between RN, PSP, and true tumour progression is not possible in the early phase. Since the therapeutic consequences differ substantially, an accurate diagnosis is essential.

Several studies have shown promising results in differentiating treatment-related changes from tumour progression using quantitative MRI and Contrast Clearance Analysis. However, studies with larger cohorts are still needed. The current project builds upon these findings. The first objective is the retrospective analysis of regions showing treatment-related changes or tumour progression. All MRI examinations with visible changes, as well as the examination immediately preceding the first detectable alteration, are analysed longitudinally to assess changes in quantitative imaging sequences. The aim is to evaluate whether quantitative imaging sequences reveal detectable changes prior to the appearance of visible alterations on conventional MRI.

Methods

This thesis uses data from the prospective, multidisciplinary trial "Contrast Clearance Analysis and Mapping Sequences for Monitoring Treatment Response in Primary Brain Tumours after Radiotherapy" (CAMEO), which was initiated by the PI.

In the current project, only patients from the CAMEO-trial with histopathologic diagnosis after suspected tumor progression are included.

The study employs a specialised MRI protocol that incorporates both clinically established MR methods and more experimental quantitative imaging sequences. The acquired images are analysed using the post-processing software Olea Sphere®. The anonymised results are then imported into a unified dataset. Demographic, quality-of-life, treatment, clinical progression, and histopathological data are entered into a specifically designed REDCap® database.

Statistical analyses of both the imaging dataset and the clinical database are performed using Python® or R®.

Findings

The image-analysis pipeline and the database have been successfully implemented. Initial tests confirmed the feasibility and functionality of the analysis.

Conclusion

In the current project, we analyse regions where tumour progression or treatment related changes occurred to determine whether such alterations can already be detected in quantitative imaging sequences. Clinical and imaging data are available, and both the analysis pipeline and the database have been successfully implemented.

Celina Wilgermein

Background:

Schizophrenia is a pathoetiologically heterogeneous disorder that involves complex, interrelated mechanisms, including neuroinflammation at least in a subset of patients. Females generally exhibit a stronger innate and adaptive immune response than males, which is amongst others due to hormonal influences. The protective effects of estrogen are also considered to be the reason why women develop the disease later than men. Although schizophrenia affects both sexes equally, women are often underrepresented in studies.

Within the sub-project of the European Long-acting Antipsychotics in Schizophrenia Trial (EULAST), we tried to identify a potential neuroimmune profile by investigating associations between inflammatory parameters, symptomatology, and treatment response. To take gender aspects into account, we compared inflammation parameters between male and female patients and tested whether gender acts as a constant cofactor in the association of inflammatory markers and psychopathological outcome.

Methods: Serum levels of pro-and anti-inflammatory cytokines, brain-derived-neurotrophic factor (BDNF) and neurotransmitter precursor amino acids and derivatives were measured in samples from a total of 360 schizophrenia patients from different study centers. Symptomatology was assessed using the Positive and Negative Syndrome Scale (PANSS). The impact of inflammatory parameters on psychopathological outcome was analyzed using mixed effect models, linear and logistic regression analyses.

Results: Since female patients accounted for only 34% of our study, female data was underrepresented in our study sample. Diffeneces in neurotransmitter precursor amino acids and derivatives were only marginally verifiable within our study sample. Gender was the second most influential cofactor in the association of inflammation markers and psychopathological outcome, however not continuously verifiable. Hierarchical cluster analyses based on age, gender, BMI and symptomatology did not identify distinct subgroups.

Stac2 Variants Define Molecular Interfaces and Biophysical Outcomes in Neuronal L-type calcium channels

Isabella Weisleitner

Isabella Weisleitner1, Luca T. Rieder2, Carla Neuwirth1 Nadine J. Ortner2, Stefanie M. Geisler1
1Department of Pharmacology and Toxicology, Institute of Pharmacy, University of Innsbruck, Austria
2Division of Medical Physics and Biophysics, Gottfried Schatz Research Center, Medical University of Graz, Austria

Ca2+ influx through neuronal voltage-gated L-type calcium channels (LTCCs; CaV1.2/CaV1.3) regulates cellular excitability, gene expression, and synaptic plasticity. Stac proteins, which contain Src homology three (SH3) and cysteine-rich domains, suppress Ca2+-dependent inactivation (CDI), thereby prolonging LTCC Ca2+ influx. The Stac2 isoform is highly abundant in brain regions that also express CaV1.2 and CaV1.3, while Stac3 is restricted to skeletal muscle and is essential for CaV1.1-dependent excitation-contraction coupling. Despite detailed knowledge of Stac3-CaV1.1 interactions, it remains largely unknown whether Stac2 employs analogous interfaces to modulate neuronal LTCCs and how sequence variation in Stac2 affects LTCC biophysical parameters. Notably, de novo STAC2 missense variants have been associated with neurodevelopmental disorders, underscoring the need for functional assessment.

We aimed to define Stac2 domains that interact with neuronal LTCCs and to determine how engineered and patient-derived Stac2 variants affect channel function. Prior work has mapped distinct LTCC–Stac interaction interfaces, well established for CaV1.1–Stac3, but only partially characterized for CaV1.2/1.3–Stac2. Building on this, we performed structural and sequence analyses across Stac proteins and LTCC-binding regions to identify conserved motifs predicting Stac2–neuronal LTCC interfaces and guiding variant design. Where structural templates were available, we generated homology models of Stac2 domains in complex with CaV1.2/CaV1.3 peptides; for domains lacking structural data, we relied on literature and sequence analysis. Functional effects of Stac2 variants were assessed by whole-cell voltage clamp recordings in HEK293 cells stably expressing auxiliary α2δ1 and β3 subunits, co-transfected with human CaV1.3 (long splice variant) and either Stac2 wild type (WT), engineered Stac2 variants, or no Stac2 (control), plus eGFP as transfection marker.

Consistent with prior work, Stac2 WT significantly reduced inactivation (12.9 ± 2.0%), indicating robust CDI suppression. As previously published, the ETL/AAA U-motif variant (Niu et al., 2018, eLife) restored inactivation kinetics to control-like values (control: 34.1 ± 2.1%; ETL/AAA: 38.0 ± 2.4%), confirming a critical role of the U-motif in CDI modulation. The engineered R140A variant, located within the C1 domain previously implicated in CDI modulation, preserved CDI suppression (R140A: 15.6 ± 1.7%). However, it accelerated activation, yielding a time to peak between WT and control. In contrast control and ETL/AAA variant activation kinetics were comparable and significantly faster than WT (time to peak: Stac2 WT: 14.8 ± 1.1 ms; R140A: 11.9 ± 0.7 ms; ETL/AAA: 6.5 ± 0.4 ms; control: 6.9 ± 0.4 ms). Current density and the voltage dependence of activation did not differ significantly across conditions, consistent with previous reports.

These data support a model in which Stac2 employs distinct motifs to bind LTCCs and modulate their function, linking defined structural interfaces to discrete biophysical outcomes. Functional assays of additional engineered and patient-derived variants of Stac2, CaV1.2 and CaV1.3, are underway. Together, our work characterizes the molecular determinants and functional consequences of Stac2 modulation of neuronal LTCCs, refining our understanding of Stac2's roles in physiology and pathology.

SZABO SCANDIC

Part of Europa Biosite

My personal scientific support

Buzzing with solutions as diverse as your needs

Trusted lab essentials to accelerate your discoveries

Exploring the endogenous BORC assemblies at the lysosomal membrane using crosslinking mass spectrometry

Martina A. Höllwarth

M.A. Höllwarth1, E. Rauch1, V. Vigorito2, L.L. Fava2, L.A. Huber1, T. Stasyk1

1) Biocenter, Institute of Cell Biology, Medical University of Innsbruck, Innsbruck, Austria

2) Armenise-Harvard Laboratory of Cell Division, Department of Cellular, Computational and Integrative Biology - CIBIO, University of Trento, Trento, Italy

The hetero-octameric BLOC-1-related complex (BORC) regulates lysosomal positioning by recruiting ADP-ribosylation factor-like protein 8 (Arl8) to the lysosomal surface. This initiates a chain of interactions that promotes anterograde lysosomal transport along microtubules. Under amino acid- or EGF-depleted conditions the late endosomal/lysosomal adaptor and MAPK and mTOR activator (LAMTOR/Ragulator) negatively regulates this process. In previous work, we have demonstrated that the BORC subunit BORCS6 serves as the linker between BORC and LAMTOR using chemical crosslinking. Beyond its role in positioning, BORC is also involved in lysosome-autophagosome fusion and lysosomal reformation. However, the molecular architecture and regulatory mechanisms governing these functions remain largely unknown.

Our objective is to elucidate the subunit topology of BORC protein assemblies, define the specific protein-protein interactions involved and investigate their structural dynamics under different physiological conditions. Therefore, we employ crosslinking mass spectrometry (XL-MS) on native BORC complexes isolated by affinity purification from cells expressing endogenously tagged BORC subunits.

We generated hTERT-RPE1 cells with N-terminally ALFA-tagged BORCS7 via CRISPR/Cas9 ribonucleoprotein-mediated knockin. Lysates from these cells are immediately subjected to chemical crosslinking to stabilize BORC assemblies and then affinity-purified using ALFA-nanobody-immobilized beads. Following a bottom-up proteomics approach, crosslinked peptides are analyzed by liquid chromatography-tandem mass spectrometry (LC-MS/MS). To enhance the detection and identification of crosslinked peptides, we optimized the workflow by incorporating an immobilized metal affinity chromatography (IMAC) enrichable crosslinker.

Currently, we are establishing a workflow using an MS cleavable crosslinker that is enrichable via click-chemistry and features a longer spacer, enabling the covalent linkage of more distantly positioned amino acids. Furthermore, we investigated the contact inhibition induced quiescence in RPE1 cells and identified differential BORC-interactors between the contact inhibited and proliferating states. We are performing biological replicates and hit validation, intending to integrate contact inhibition and XL-MS to analyze BORC assemblies in quiescent cells.

Early but Waning Humoral Immunity after 2025/2026 Trivalent Influenza Vaccination in Tyrolean Adults

Nicolas Melcher

Nicolas Melcher, Michael Jäger, Gabriel Diem and Wilfried Posch

Institute of Hygiene and Medical Microbiology, Medical University of Innsbruck, Innsbruck, Austria

Seasonal influenza vaccination remains the primary strategy to reduce influenza-associated morbidity, yet data on the quality and durability of systemic and mucosal immune responses to current vaccines in Austria are limited. This study evaluates the immunogenicity of the 2025/2026 trivalent inactivated influenza vaccine in inducing humoral and cellular immunity against circulating influenza variants in Tyrol, Austria. We specifically assess systemic and mucosal antibody responses, as well as T-cell responses, to influenza A (H1N1, H3N2) and influenza B (Victoria lineage) over a three-month period following vaccination.

We conduct a prospective cohort study in healthy adults aged 20-64 years (mean age 39.6), including both women and men (52% / 48%). Peripheral blood mononuclear cells (PBMCs), plasma, serum, and saliva samples are collected prior to vaccination and at 1 and 3 months post-vaccination. Humoral immunity is characterized by quantitative and semi-quantitative ELISA for IgG and IgA specific for influenza A and B. Functional antibody activity is assessed by virus neutralization assays using vaccine strains (H1N1, H3N2, B/Victoria) and representative circulating clinical variants to determine the breadth and neutralizing capacity of vaccine-induced responses. Cellular immunity is evaluated by stimulating PBMCs with replication-competent influenza virus variants and quantifying antigen-specific T-cell responses using IFN-γ ELISpot assays.

Preliminary analyses demonstrate a significant increase in plasma IgG and IgA levels against influenza A and B one month after vaccination. For influenza B, IgG responses rise markedly, whereas plasma IgA shows a more modest increase. In saliva, influenza A- and B-specific IgG and IgA are largely undetectable at baseline and one month post-vaccination, with measurable mucosal responses mainly restricted to individuals with previous infection. A pronounced ceiling effect is observed in participants with high pre-vaccination IgG or IgA titers, suggesting that pre-existing immunity constrains further antibody boosting. At three months, plasma IgG and IgA levels against influenza A and B are no longer significantly elevated compared with pre-vaccination values, indicating waning systemic humoral immunity within this time frame.

Collectively, these data indicate that the 2025/2026 trivalent influenza vaccine induces a robust but, for influenza B, transient systemic humoral response, while mucosal antibody induction in saliva remains limited. The decline in antibody levels by three months and the observed ceiling effect highlight the influence of pre-existing immunity on the magnitude and durability of vaccine-induced responses. Ongoing analyses of neutralizing activity and T-cell responses will further define the persistence, breadth, and potential protective relevance of vaccine-induced humoral and cellular immunity against simultaneously circulating influenza variants in the Tyrolean adult population.

Humoral and Cellular SARS CoV 2 Vaccine Immunity in Immune Mediated Inflammatory Diseases

Sophie Ann Erckert

Sophie Ann Erckert1, Wolfram Mayr2, Günter Weiss2 and Wilfried Posch1

1 Institute of Hygiene and Medical Microbiology, Medical University of Innsbruck, Innsbruck, Austria

2 University Clinic of Internal Medicine II, Medical University of Innsbruck, Innsbruck, Austria

Immune-mediated inflammatory diseases (IMIDs) can alter vaccine-induced immunity due to underlying immune dysregulation and the use of immunomodulatory therapies. We investigated how these factors influence SARS-CoV-2 vaccine responses by analyzing humoral and cellular immunity in four IMID patient cohorts - rheumatoid arthritis, psoriasis, collagenosis, and vasculitis - compared with age-matched healthy controls. Peripheral blood mononuclear cells and serum samples were collected at baseline (T0), after the primary vaccination series (T1), and after booster vaccination (T3), enabling detailed comparison of response kinetics across groups.

Humoral immunity was assessed by ELISA and virus neutralization assays. Antibodies and neutralizing activity were detectable in all cohorts at T1, but titers differed substantially between groups. Healthy controls mounted the strongest responses, whereas several IMID cohorts, particularly patients with collagenosis and vasculitis, showed reduced early neutralization capacity after two vaccine doses. Three months after booster vaccination (T3), robust neutralization was observed across all cohorts and early differences were largely abrogated, indicating that IMID-associated deficits can be compensated by boosting. Variant-specific analyses revealed a gradient of decreasing neutralization from wild-type to Delta and Omicron, with Omicron variants remaining poorly neutralized in all cohorts despite booster vaccination.

Cellular immunity, assessed by IFN-γ ELISpot and SARS-CoV-2–specific T-cell activation, showed cohort-specific alterations paralleling the neutralization data. ELISpot responses increased after primary vaccination in all groups but were lower in individuals with collagenosis and vasculitis. Booster vaccination markedly enhanced IFN-γ spot formation and partially homogenized variant-specific T-cell immunity. Phenotypic T-cell analysis demonstrated reduced early $CD8^+$ T-cell activation in patients with rheumatoid arthritis, psoriasis, and collagenosis, and selectively diminished Th1-type $CD4^+$ T-cell activation in vasculitis. These differences were most pronounced at T1 and resolved after boosting, consistent with delayed activation kinetics rather than an inability to mount cellular responses.

In summary, IMID patients can generate effective humoral and cellular responses to SARS-CoV-2 vaccination, but early responses are weaker, more heterogeneous, and less cross-protective against immune-evasive variants such as Omicron. Timely booster vaccination is therefore critical to achieve immune responses comparable to healthy individuals and should be prioritized in vaccination schedules and clinical monitoring strategies for IMID populations.

Immune and Metabolic Rewiring Through Fasting Mimicking Diet in Localized Prostate Cancer

Nastasiia Artamonova

Artamonova N.1, Höller A2., Trebo M.3 Pichler U.2, Nagl L3, Guastadisegni M.3, Sopper S.3, Salcher S.3, Ormanns S4, Eder I. E.1, Puhr M.1, Pircher A.3 and Heidegger I.1
1 Medical University Innsbruck, Department of Urology, Innsbruck, Austria
2 Tirol Kliniken, Department of Nutritional Sciences, Innsbruck, Austria
3 Medical University Innsbruck, Department of Internal Medicine V, Hematology and Oncology, Innsbruck, Austria
4 Medical University Innsbruck, Institure of General Pathology, Innsbruck, Austria

Introduction & Objectives

Fasting mimicking diet (FMD) has been shown to improve metabolic parameters and enhance antitumor immune responses in several malignancies, including breast cancer. Nevertheless, its potential role in immunologically 'cold' tumors, such as prostate cancer (PCa) remains unknown.

Materials & Methods

17 patients (median age: 62 years; median BMI: 26.1) with localized PCa underwent a 5-day FMD (600 kcal day 1; 300 kcal days 2–5) prior to radical prostatectomy (RP). Beside routine metabolic serum markers (e.g. glucose, insulin, HbA1c, triglycerides), plasma and urine were collected at baseline and after FMD. Peripheral immune cell subsets were characterized by multicolor flow cytometry (FCM) before and after FMD. Immunohistochemistry (IHC) on both diagnostic biopsies and on RP specimens was performed to validate FCM findings. Spatial transcriptomic analyses are ongoing to investigate in depth local immune–metabolic reprogramming.

Results

Elevated ketone levels in blood and urine, observed in 88% of patients, confirmed the metabolic efficacy of FMD. Importantly, FMD demonstrated an acceptable safety and feasibility profile, with 53% of patients experiencing grade 1 and 18% experiencing grade 2 adverse events according to CTCAE criteria. All laboratory alterations were grade 1 and comprised hypoglycemia (47%), hyperuricemia (65%), and transient elevations of AST (24%) or ALT (12%).

Despite the short duration, FMD significantly improved metabolic parameters, lowering the levels of glucose ($p<0.05$), insulin ($p<0.01$), HbA1c ($p<0.0001$), and triglycerides ($p<0.001$).

Importantly, FMD rapidly shifted the immune profile towards activation, increasing the absolute count of CD 141+ dendritic cells (DCs) ($p<0.05$), especially plasmacytoid DCs ($p<0.01$), supporting enhanced $CD8^+$ T-cell activation, while lowering the levels of $CD8^+$ T $CD38^+$ ($p<0.05$) and $CD38^+HLA\text{-}DR^+$ ($p<0.05$) cells. IHC and spatial transcriptomics are currently ongoing to validate these systemic immune alterations on tissue.

Conclusions

Short-term FMD induces favorable metabolic and immunological effects in patients with localized PCa. Ongoing tissue-based analyses will provide deeper insight into the immune–metabolic reprogramming induced by FMD and may support the integration of nutritional immunomodulation into personalized PCa therapy.

HIF2a in Endothelial-to-mesenchymal Transition: A new strategy to tackle cardiac fibrosis

Jonas Eder

Eder J1, Seeberger D1, Schmidt S1, Stranger L1, Plattner C2, Pölzl L1, Hirsch J1, Nägele F1,3, Engler C1, Ioannou-Nikolaidou M4, Heim V1, Lohmann R1, Trajanoski Z2, Bonaros N1, Grimm M1, Cooke JP3, Holfeld J1, Gollmann-Tepeköylü C1, Graber M1,3
1 Department of Cardiac Surgery, Medical University of Innsbruck, Innsbruck, Austria
2 Institute of Bioinformatics, Medical University of Innsbruck, Innsbruck, Austria
3 Center for Cardiovascular Regeneration, Houston Methodist Research Institute, Houston, TX, United States
4 Department of Clinical and Functional Anatomy, Medical University of Innsbruck, Innsbruck, Austria

Objective
Cardiac fibrosis is a hallmark of heart failure and a major driver of disease progression, contributing to myocardial stiffening, impaired contractility, and adverse cardiac remodeling. A key cellular mechanism underlying fibrotic remodeling is endothelial-to-mesenchymal transition (EndoMT). In EndoMT, endothelial cells lose their lineage-specific characteristics and acquire a fibroblastic phenotype, thereby promoting excessive extracellular matrix deposition. Hypoxia-inducible factor 2 alpha (HIF-2a, EPAS1) is a regulator of phenotype plasticity and has been implicated in cellular fate transitions. This study aims to investigate the contribution of HIF-2a to EndoMT in heart failure and tests the hypothesis that its inhibition attenuates cardiac fibrosis and preserves cardiac function.
Methods
EndoMT was induced in human coronary endothelial cells using TGF-β and angiotensin II. Metabolic alterations were analysed by Seahorse flux analysis. Endothelial function was assessed by tube formation assay and EndoMT was confirmed by immunofluorescence. In vivo, non-ischemic heart failure was induced in mice via continuous angiotensin II infusion and L-NAME administration for four weeks. Mice were treated with HIF-2a inhibitor C76 intraperitoneally. Cardiac function was assessed by echocardiography. Histologically, hearts were examined for fibrosis and endothelial cell integrity.
Results
EndoMT induction in human coronary endothelial cells was associated with a metabolic reprogramming toward glycolysis and increased HIF-2a expression. Pharmacological inhibition of HIF-2a via C76 effectively suppressed EndoMT, preserving endothelial gene expression and endothelial cell function. In a murine model of non-ischemic heart failure, HIF-2a inhibition resulted in preserved left ventricular function as assessed by transthoracic echocardiography. Histological analyses revealed a reduction in myocardial fibrosis, characterized by decreased collagen deposition and reduced myofibroblast accumulation. Furthermore, microvascular density was maintained in HIF-2a–inhibited mice, suggesting a protective effect on endothelial integrity.
Conclusion
In conclusion, we were able to show that HIF-2a plays a major role in the development of cardiac fibrosis in a non-ischemic heart failure model and is a key regulator of EndoMT in vitro. Its inhibition prevents the transition of endothelial cells toward a

mesenchymal phenotype, thereby reducing cardiac fibrosis and preserving left ventricular function. In summary, these findings support our hypothesis that HIF-2a inhibition could represent a novel therapeutic strategy to target cardiac fibrosis and the progression of heart failure.

Sex differences in quality of life among a cohort at risk of developing Parkinson's disease: a cross-sectional analysis from the Healthy Brain Ageing (HeBA) project.

Noelia Peña Arauzo

Noelia Peña Arauzo1, Claire Pauly2,3, Sonja Jónsdóttir2, Christoph Theyer1, Atbin Djamshidian1, Iris Egner1, Laura Zamarian1, Corinne Horlings1, Simon Leiter1, Werner Poewe1, Brit Mollenhauer4, Claudia Trenkwalder4, Sebastian Schade4, Rejko Krüger2,5, Daniel Pilco6, Fernanda Farfan6, Alicia Garrido6, Venkata Satagopam7, Soumyabrata Ghosh7, Kavita Rege7, Alastair Noyce8, Philipp Mahlknecht1; on behalf of the HeBA consortium.
1 Department of Neurology, Medical University of Innsbruck
2 Luxembourg Institute of Health, Luxembourg
3 Parkinson's Research Clinic, Centre Hospitalier de Luxembourg, Luxembourg
4 Paracelsus-Elena-Klinik Kassel, Germany
5 Department of Neurology, Centre Hospitalier de Luxembourg, Luxembourg
6 Parkinson's Disease and Movement Disorders Unit, Hospital Clinic de Barcelona, Spain
7 Luxembourg Centre for Systems Biomedicine, University of Luxembourg, Luxembourg
8 Centre for Preventive Neurology, Wolfson Institute of Population Health, Queen Mary University of London, London, UK

Parkinson's disease (PD) negatively affects quality of life (QoL), specifically in psychological and physical domains (Zhao, 2020; Prashun, 2017). However, little is known about sex differences in QoL in individuals at risk of developing PD.

In a cohort from the Healthy Brain Ageing (HeBA) project, we examined which Parkinson's disease (PD) risk factors influence QoL. For this particular analysis, all participants who completed the online data and remote smell testing from Innsbruck and Luxembourg centers were considered.

The total sample comprised of 3,245 participants (mean age 61.5 ± 7.5 years; 57.2% female). Mean Non-Motor Symptoms Questionnaire (NMSQ) score was 4.9 ± 3.7, Movement Disorders Society - Unified Parkinson's Disease Rating Scale (MDS-UPDRS) part Ib, 3.9 ± 2.4, and part II, 0.9 ± 1.8. The mean QoL index was 0.91 (higher in men; P = 0.02), and the Visual Analogue Score was 81.5 (higher in women; P = 0.03). In the QoL subdomains, women showed more pain/discomfort (P=0.05), more impairment in usual activities (P=0.02) and more anxiety/depression (P<0.001) than men. Reduced QoL was associated with older age, fewer education years, and higher Charlson Comorbidity Index (CCI). In an analysis adjusted for sex, age, CCI, and education years, NMSQ (adjusted R^2 = 0.29; B = -0.02) and MDS–UPDRS part Ib (adjusted R^2 = 0.30; B = -0.19) and part II (adjusted R^2 = 0.24; B = -0.03) scores were associated with lower QoL Index. When analysed separately in men and women, the same associations were observed. Lower QoL was also linked to higher probability percentage score to develop PD according to MDS criteria (adjusted R^2 = 0.18; B = -0.005; adjusted for CCI and education years).

In summary, individuals at risk of developing PD exhibit a lower QoL, with notable sex differences. Prospective follow-up will provide insight into whether QoL is indeed compromised in the early stages of the disease and, if so, in which areas sex differences are evident.

Thanida Laopanupong

Seizure Threshold 2 (SZT2) is highly expressed in the parietal and frontal cortex, and biallelic SZT2 variants are linked to Developmental and Epileptic Encephalopathy 18 (DEE18). SZT2 is a core subunit of the KICSTOR complex, which negatively regulates lysosomal mTORC1 signaling during amino acids, glucose and cholesterol deprivation. Here, we investigate how SZT2-deficient cells adapt to catabolic conditions and address the role of ER–lysosome crosstalk in maintaining cellular homeostasis under these conditions.

SZT2 knockout (KO) HEK293 Flp-In™ T-Rex™ cells were analyzed under nutrient-fed and aminoacid–starved conditions. mTORC1 activity was assessed by P70S6K and 4EBP1 phosphorylation, protein translation by puromycin labeling, and stress responses by eIF2a phosphorylation. Cell size, Golgi and mitochondria volume, Lysosome and ER-exit site (ERES) numbers were quantified. Finally, global protein degradation was determined via Boncat.

SZT2KO cells exhibited persistent mTORC1 signaling under catabolic conditions and increased cell size. Despite sustained phosphorylation of P70S6K and 4EBP1, global translation rates were not increased in either of the conditions tested. Instead, SZT2KO cells activated the integrated stress response, indicated by elevated Ser51 phosphorylation of eIF2a, required to elicit translational control and allow cell survival. Moreover, we determined that the increase in protein per cell was likely triggered by reduced protein degradation.

Although SZT2KO cells dynamically adjusted cell size in response to AA availability, they displayed enlarged and fragmented Golgi structures, increased ERES numbers with impaired recovery after AA re-stimulation, increased number of lysosomes and reduced mitochondria volume.

Together, these findings indicate broader changes in cellular homeostasis triggered by ablation of SZT2. Future work will focus on elucidating the mechanisms underlying the observed changes and assessing their dependence on mTORC1.

A novel isoform of Skp2 generated by alternative translational initiation

Betül SARI

The cell cycle consists of four distinct phases that are named as G1 (Gap1), S (Synthesis), G2 (Gap2) and M (Mitosis). Most cell cycle phase transitions are under a strict regulation of Cdk (cyclin-dependent kinase) – cyclin kinase activities. CDK inhibitors (CKIs) can regulate the kinase activities of Cdk/cyclin complexes. The protein levels of some CKIs, such as p27, are regulated by the ubiquitin-proteasome system in the cell. One of the most important E3 ubiquitin ligase that targets CKI proteins is SCF-Skp2. Skp2 (S-phase kinase-associated protein 2) is able to associate with other SCF (Skp, Cullin, F-box containing complex) components and as the SCF-Skp2 E3 ubiquitin ligase complex; it mediates polyubiquitylation of several CKIs and triggers their proteasomal degradation.

Skp2 is an oncoprotein, which is often deregulated in cancer. In the human cell lines, the Skp2 protein can be detected as two bands in the Western Blots, with the size of app. 47kDa and 43kDa. The smaller, faster migrating band has been considered as a degradation product. We have observed that the second isoform is translated from an alternative translation codon, Methionine-36. We observed that the shorter isoform is more stable than the full-length isoform during the G1-phase, due to the lack of the "destruction box" sequence. The destruction box of Skp2 has been shown to target Skp2 for ubiquitination by its canonical E3 ubiquitin ligase, APC-Cdh1. Using CRISPR-Cas9 edited cell lines, we observed that cyclin D1 accumulated in cells lacking Skp2 expression, but also in cells expressing only the N-terminal truncated Skp2 isoform initiated at Methionine-36. Both Skp2 isoforms were able to downregulate the Skp2 substrates p27, p21 or p57. Due to this observation, we initially speculated that the Skp2 full length protein might be a subunit of an E3 ubiquitin ligase for cyclin D1, while the shorter Skp2 protein initiated at Methionine-36 was not able to trigger cyclin D1 degradation. However, in immunoprecipitation experiments, both isoforms of Skp2 could interact with Cyclin D1. These experiments confirm that both Skp2 isoforms can initiate the degradation of p27, however, the consequences of cyclin D1 binding to Skp2 and the molecular cause for the cyclin D1 accumulation in cells lacking full length Skp2 remain to be determined.

Anti-inflammatory effects of N-chlorotaurine on granulocytes and alveolar macrophages

Alexandra Ioannou

Authors: Alexandra Ioannou, Andrea Windisch, Markus Nagl

N-chlorotaurine (NCT), a product of activated human granulocytes and monocytes, can be synthesized chemically and applied as an endogenous antiseptic for treatment of infections. It has also anti-inflammatory effects and is thought to be involved in the resolution of inflammatory response. NCT can be inhaled, too, and recently demonstrated strong curative effects in the mouse model of fungal pneumonia. The aim of the present study was to investigate the influence of NCT on the production of cytokines of granulocytes and alveolar macrophages to improve the understanding of its effects in pneumonia.

Murine granulocytes were separated from the bone marrow and alveolar macrophages obtained from bronchoalveolar lavage. The isolation was perfomed using a Neutrophil Isolation Kit by magnetic depletion of non-target cells, which were labeled with biotin-conjugated antibodies and anti-biotin MicroBeads and retained in a magnetic column. The cells were subsequently stimulated with lipopolysaccharide (100 ng/ml) derived from Escherichia coli (E. coli) or with Aspergillus fumigatus spores, Staphylococcus aureus or E. coli. Produced levels of interleukin 6 (IL-6) and tumor necrosis factor alpha (TNF-a) were measured by ELISA. Different incubation times and concentrations of reagents were tested. NCT 0.05% (2.75 mM) completely reduced the levels of IL-6 and TNF-a to that of unstimulated controls, while their levels were reduced by 0.01% (0.55 mM) and hardly by 0.005% (0.275 mM) NCT.

NCT demonstrated a concentration-dependent downregulation of cytokines of LPS- and pathogen-stimulated granulocytes and alveolar macrophages, too. These findings indicate that NCT effectively modulates innate immune cell responses under inflammatory conditions. At clinically applied concentrations, this immunomodulatory activity may contribute to the termination of the inflammatory response and thereby support its therapeutic potential in the treatment of pneumonia.

Maria Ioannou-Nikolaidou

Objective

Reverse cardiac remodelling is characterised by the recovery of ventricular function and a reduction in ventricular wall thickness. We recently identified the mechanism of KIAA0408, an undescribed gene involved in reverse cardiac remodelling after right ventricular (RV) myocardial infarction. This study aimed to investigate whether the regenerative potential of the RV can also be observed in humans and to characterise and explore the function of this gene.

Methods

The regenerative capacity of the RV was analysed in the prospective conducted MRI STEMI registry ("MARINA-STEMI" NCT04113356). To investigate the gene's impact on cell function, cardiac fibroblasts were isolated and functional assays were performed on fibroblasts lacking KIAA0408. In an attempt to rescue the phenotype the migration assay was repeated in fibroblasts overexpressing the novel gene. Secretome analysis was conducted to reveal the effects of the KIAA0408 and immunofluorescence staining revealed the location of the gene within the cell. To investigate the effect of the newly discovered gene on reverse cardiac remodelling RV myocardial infarction was induced via ligation of the right coronary artery in wild type and knock out mice. Scar formation was analyzed in histological sections and ventricular function via transthoracic echocardiography.

Results

Within MRI scans a significantly improvement of the RV function was observed during the first four months after RV myocardial infarction (RV Strain -14% to -19%).

Knockout fibroblasts exhibited significantly higher proliferation and migration rates ($p < 0.001$). Conversely, the migration rate was significantly reduced in fibroblasts with an overexpression of the novel gene ($p = 0.05$). Secretome analysis showed altered expression profiles, particularly of ECM components. Immunofluorescence staining revealed that KIAA0408 is located in focal adhesions. Therefore, fibroblasts lacking the novel gene required a longer time to adhere than wild type cells.

Mice lacking KIAA0408 showed impaired RV function ($p=0.001$) and increased scar formation ($p=0.048$) compared to wild type mice after myocardial infarction.

Conclusion

For the first time we demonstrated a regenerative capacity of the RV after myocardial infarction in a prospective MRI STEMI registry. KIAA0408 is a key regulator of fibrotic pathways. Deletion of the gene disrupts reverse remodelling, exacerbates fibrosis and leads to RV dysfunction following afterload stress. Conversely, overexpression of the novel gene leads to reduced fibroblast migration, highlighting its role as a key regulator of fibrosis. These findings highlight KIAA0408 as a promising therapeutic target for cardiac fibrosis and right heart failure.

Cognitive and Subjective Influences on Arithmetic Learning in Adults

Katharina Thaler

Katharina Thaler1, Elisabeth Goettfried1, Paula Maldonado Moscoso2, Demis Basso3, Manuela Piazza2, Michael Knoflach1, Margarete Delazer1, Laura Zamarian1

1 Department of Neurology, Medical University Innsbruck, 6020 Innsbruck, Austria

2 Center for Mind/Brain Sciences, University of Trento, 38068 Rovereto, Italy

3 Cognitive and Educational Sciences Lab (CESLab), Faculty of Education, Free University of Bolzano-Bozen, 39042 Bressanone-Brixen, Italy

Introduction: Proficiency with numbers is an indispensable skill for navigating the multifaceted demands of a rapidly evolving world. Impairments in numerical abilities can compromise individuals' day-to-day life, for example in health management or financial decision-making. This study investigates the acquisition of new arithmetic skills in healthy adults and examines possible cognitive and subjective influencing factors.

Methods: In total, 144 Participants (aged 18-68 years; 52% female) underwent a comprehensive neuropsychological assessment. This included tests of executive functions, memory, vocabulary, as well as simple and complex calculations, arithmetic principles and approximation. In addition, participants completed questionnaires on math anxiety, motivation, attitudes towards mathematics and perceived competence. Participants then trained on twelve new arithmetic problems via two distinct approaches over five days. In the procedural approach, an algorithm had to be applied to solve the problem, whereas the associative approach required memorising operand-result pairs.

Results: Both learning approaches yielded significant performance improvements. The associative condition exhibited greater gains over time, associated with older age, lower educational level and lower cognitive abilities, including memory, executive functions and prior arithmetic proficiency. The improvements in the procedural condition were predominantly associated with lower memory performance and lower prior arithmetic proficiency. Subjective factors showed moderate associations with procedural learning. No significant gender effects were found.

Discussion: Healthy adults are capable of acquiring new arithmetic skills and achieve performance improvements through training. Improvements are dependent on the unique cognitive profile and subjective attitudes. Individuals with greater initial disadvantages can also profit from arithmetic training. The findings emphasise the importance of customised cognitive training approaches in optimising efficacy.

Key Words: Adult learning; Memory-based learning; Strategy-based learning; Cognitive profiles; Math attitudes.

Lukas Prüfer

Background:

Digital impression techniques are widely used in contemporary dentistry, with intraoral scanning (IOS) and cone-beam computed tomography (CBCT) representing two established modalities for three-dimensional data acquisition. While both techniques are routinely applied in clinical workflows, their spatial accuracy under conditions of reduced dentition remains insufficiently understood. A decreasing number of teeth may compromise spatial orientation and reconstruction quality, particularly in volumetric imaging modalities. This study aimed to evaluate the accuracy and reproducibility of IOS- and CBCT-derived surface models in partially edentulous situations using a geometry-based reference approach.

Methods:

An in vitro maxillary model with initially fourteen removable teeth was equipped with five fixed spherical reference markers. The true spatial positions of the marker centers were determined using a coordinate measuring machine (CMM) with nanometer-level accuracy and served as the reference standard. The model was scanned repeatedly using an intraoral scanner and CBCT. After each scanning series, one tooth was removed sequentially to simulate progressive tooth loss. CBCT datasets were segmented into surface models. A custom Python-based algorithm calculated pairwise Euclidean distances between marker centers, enabling a geometry-driven comparison independent of surface-based alignment. Deviations, mean absolute error (MAE), root mean square error (RMSE), bias, and coefficients of variation were analyzed as a function of the number of remaining teeth.

Results:

CBCT-derived surface models exhibited a clear increase in spatial deviation with decreasing numbers of remaining teeth. Mean errors and RMSE values increased progressively, particularly for longer inter-marker distances, indicating cumulative geometric distortion under reduced anatomical reference conditions. In contrast, IOS-derived measurements demonstrated comparatively stable mean deviations across all dentition stages. However, IOS showed increased variability, reflected by greater dispersion and lower coefficients of determination. Overall, IOS displayed lower systematic bias relative to the CMM reference, whereas CBCT accuracy deteriorated markedly as dentition was reduced.

Conclusions:

The spatial accuracy of CBCT-based surface models is strongly influenced by the number of remaining teeth, while intraoral scanning maintains consistent mean accuracy but exhibits increased variability. Reduced dentition represents a critical challenge for CBCT-based digital workflows when used as a standalone modality. The complementary strengths and limitations of IOS and CBCT support the concept of hybrid imaging strategies to improve geometric accuracy in partially edentulous dental applications.

Delineating hepatocytic apical trafficking defects in myoVb associated liver disease

Doris Stepić

Doris Stepić 1, Stephan Geley2, Lukas A. Huber 1, Georg F. Vogel 1,3

1 Institute for Cell Biology, Medical University of Innsbruck, Innsbruck, Austria

2 Institute of Pathophysiology, Medical University of Innsbruck, Innsbruck, Austria

3 Department of Paediatrics I, Medical University of Innsbruck, Innsbruck, Austria

The existence of apical, lateral and basal domains of the plasma membrane in polarized epithelial cells, each with distinct functions and protein composition necessitates targeted protein trafficking. Therefore, disturbed polarized trafficking might result in disease. One example is the intestinal microvillus inclusion disease (MVID) which is characterized by defects in enterocyte polarity and mislocalization of apical proteins. MVID is caused by mutations in the MYO5B, STX3, and STXBP2 genes, which encode the proteins myosinVb (myo5b), syntaxin3 (stx3), and munc18-2, respectively. Myo5b is a motor protein that carries apically destined vesicles, while stx3 and munc18-2 facilitate the fusion of vesicles with the apical membrane. Interestingly, some patients with MVID develop cholestatic liver disease (CLD) characterized by mislocalization of the apical membrane proteins in hepatocytes. How apical trafficking functions in hepatocytes remains unclear, particularly given that only dominant-negative missense mutations in myo5b result in CLD and that stx3 is not present. To investigate this, we are using polarized hepatocytic HepG2 cells, from which basis we developed transgenic lines expressing key players in apical protein trafficking in hepatocytes. MYO5B knockout transgenic cell lines will allow to identify a possible compensation in the apical trafficking machinery observed in patients. To map these differential interactomes mass spectrometry analysis coupled with affinity purification will be used. To further evaluate and validate potential interactions and to gain a better insight into the subcellular proteomes of our interest, a split-TurboID assay enabling spatially specific biotinylation of proteins will be perfomed. Additionally, we found that stx2 resides apically and may substitute for stx3 in hepatocytes. Generating a STX2 and STX3 knockouts will enable us to test this hypothesis and further understand apical trafficking in hepatocytes.

Outcome after post resuscitation care: a matter of sex?

Sebastian Schauflinger

S. Schauflinger1, F. Perschinka1, T. Mayerhöfer1, N. Prokes1, A. Krösbacher2, M. Joannidis1
1 Division of Intensive Care and Emergency Medicine, Department of Internal Medicine I, Medical University Innsbruck, Innsbruck, Austria.
2 Department of Anesthesiology and Intensive Care Medicine, Medical University of Innsbruck, Austria.

Background:

Cardiac arrest (CA) remains a major global health burden, affecting approximately 82 per 100,000 individuals annually in Europe. Despite international efforts to strengthen the chain of survival and advances in resuscitation and intensive care medicine, overall survival rates remain low at approximately 10%. While current guidelines emphasize early initiation of high-quality cardiopulmonary resuscitation (CPR), timely defibrillation, and standardized post-resuscitation care, growing evidence suggests that sex-specific factors substantially influence CA characteristics and outcomes after out-of-hospital cardiac arrest (OHCA).

Methods:

In the absence of a national resuscitation registry, we conducted a retrospective cohort study to investigate sex-related differences in patient characteristics and outcomes after presumed cardiac OHCA among patients treated at the Medical University of Innsbruck, the largest tertiary care center in Western Austria. Multivariable logistic regression analyses were performed to identify predictors of 30-day mortality, including age, female sex, bystander CPR, initial shockable rhythm, acute percutaneous coronary intervention (PCI), and mild therapeutic hypothermia (MTH).

Results:

A total of 418 comatose patients who received post-resuscitation care between 2018 and 2023 were included; 100 (24%) were women and 318 (76%) were men. Female sex was independently associated with increased 30-day mortality (odds ratio 2.23, 95% confidence interval 1.33–3.79; p = 0.003). Before propensity score matching (PSM) women less frequently presented with an initial shockable rhythm (53 vs. 70%, p=0.002) and received fewer defibrillations (1 vs. 2, p=0.0004). Women also exhibited higher 30-day mortality (61 vs. 38%, p<0.05) and lower rates of favorable neurological outcome at hospital discharge (CPC 1–2: 36 vs. 39%, p=0.026). Among 30-day survivors, women had shorter durations of mechanical ventilation (2 vs. 4 days, p=0.003) and intensive care unit (ICU) stay (5 vs. 8 days, p= 0.003).

To reduce confounding, PSM was performed using initial shockable rhythm, defibrillation, and bystander CPR. One-to-one nearest-neighbor matching without replacement was applied. After PSM, 30-day mortality remained significantly higher in women than in men (63 vs. 42%, p=0.008), whereas rates of favorable neurological outcome were no longer significantly different (35 vs. 43%, p=0.266). Women continued to have shorter durations of mechanical ventilation (2 vs. 5 days, p=0.013) and ICU stay (6 vs. 8 days, p=0.012).

Even after adjustment, women continued to have significantly lower 30-day survival rates than men. Further research is needed to explain the sex gap associated with post-resuscitation care following non-traumatic OHCA.

Conclusion:

Despite adjustment for key confounders, women demonstrated significantly lower 30-day survival after presumed cardiac OHCA. Further research is needed to explain the mechanisms underlying sex-specific differences in post-resuscitation care outcomes following non-traumatic OHCA

VectorBuilder

One Partner Every Solution

Design

Use the **Vector Design Studio** or **VectorBee** to create and order experiment-ready vectors.

Deliver

Easily add downstream **plasmid** preparation, **virus** packaging, and **RNA** transcription.

Discover

Take your research further with **library** design and screening, **stable cell line** engineering, and more.

Develop

Seamlessly transition to the clinic with **CliniVec**™ consultation, advanced **IP technologies**, and **GMP manufacturing**.

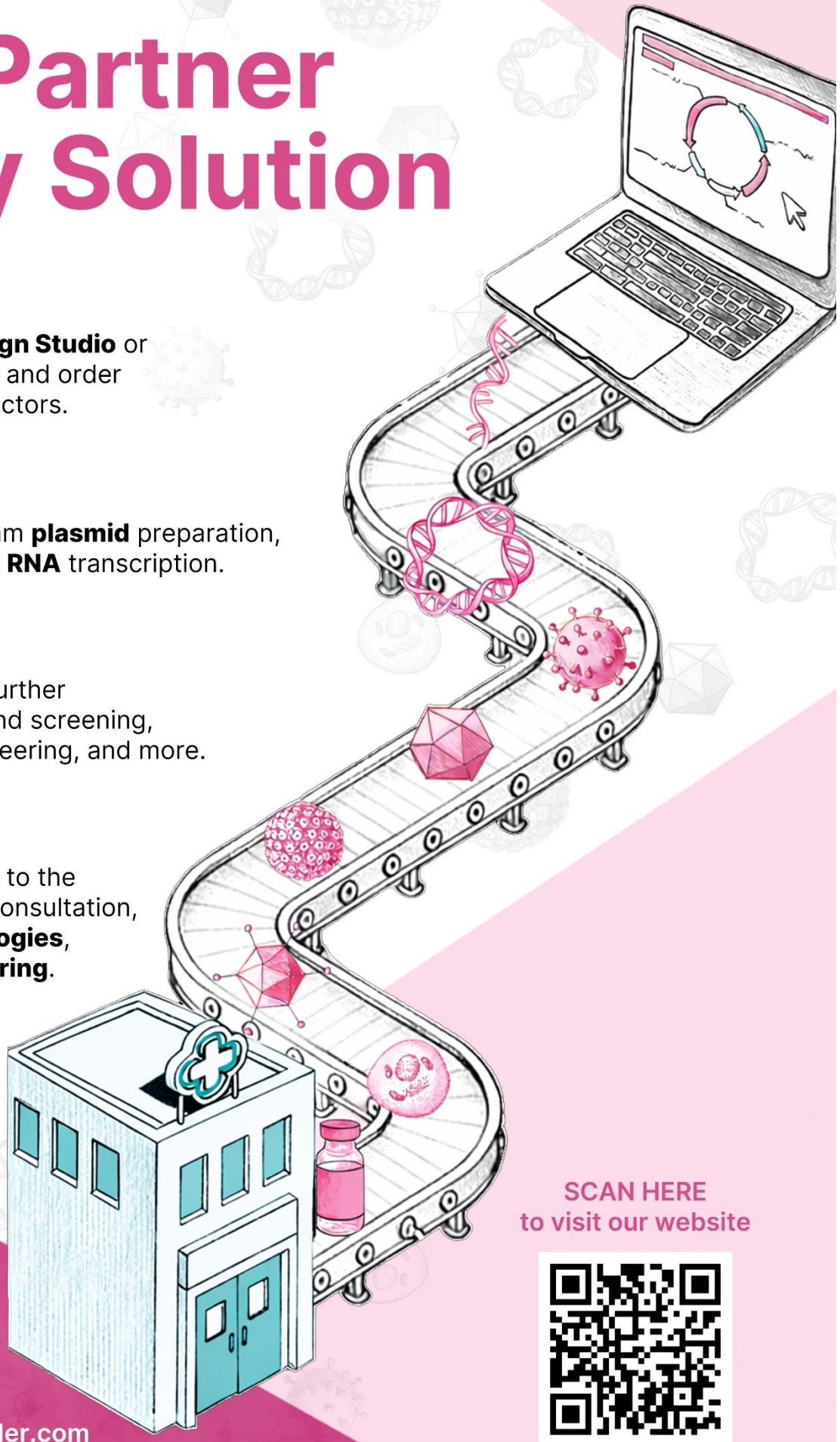

SCAN HERE
to visit our website

VectorBuilder.com
service@vectorbuilder.com

Iron status, bone health, and recovery after orthopedic surgery - IRONBONE study

Martina Saretto

Authors: Martina Saretto1, Alexa Schaufler2, Felix Riechelmann2, Gerald Degenhart3, Sonja Wagner1,4, Elke Pertler1,4, Laura Obholzer1, Benedikt Schäfer1, Herbert Tilg1, Clemens Hengg2, Rohit Arora2, Heinz Zoller1,4

1Department of Internal Medicine I, Medical University Innsbruck, Austria

2Department of Orthopaedic and Trauma Surgery, Medical University Innsbruck, Austria

3University Hospital for Radiology, Core Facility MicroCT, Biocenter, Medical University Innsbruck, Austria

4Christian Doppler Laboratory for Iron and Phosphate Biology, Innsbruck, Austria

Introduction: Iron is an essential micronutrient which plays a central role in oxygen transport, DNA synthesis and energy metabolism. At the same time, iron deficiency (ID) is one of the most common micronutrient deficiencies worldwide. Emerging data indicate that iron status plays a crucial role in musculoskeletal health. In orthopedic surgery, bone-health and regeneration are major determinants of early postoperative recovery. Impaired bone quality and turnover can result in slower recovery and a higher risk of complications.

Aim: The aim of this study is to investigate the association between ID and bone health as well as postoperative recovery in patients undergoing elective orthopedic surgery. Furthermore, the project aims to generate clinically relevant evidence to optimize perioperative iron management and improve bone health and functional outcomes in patients undergoing orthopedic surgery.

Methods: This prospective study includes adult patients undergoing elective orthopedic surgery. Patient data are collected at baseline (surgery ± 1 month) and during a follow-up visit (3 months after surgery). Bone microarchitecture is assessed using high-resolution peripheral quantitative computed tomography (HR-pQCT). Serum samples are collected to analyse parameters including iron status and markers of bone metabolism. Intraoperatively obtained bone fragments are used for molecular and structural analyses, including detailed assessment of bone microarchitecture using micro-CT, histological evaluation and analyses of gene and protein expression related to bone formation and bone resorption. Clinical data, including patient history, medication, surgical parameters, functional recovery assessed by validated questionnaires, length of hospital stay and re-intervention rates are systematically recorded. All data will be compared between patients with ID and patients without ID.

Endpoints: The primary outcome measure is the ratio of trabecular bone volume to total volume (BV/TV) at baseline. Secondary outcome measures include changes in additional HR-pQCT texture and finite element simulation parameters as well as clinical outcome data. Exploratory endpoints focus on alterations in serum parameters and on structural and molecular alterations in intraoperatively obtained bone fragments.

Preliminary Results: By January 2026, 24 patients have been included in the study (75.00% females). Out of 24 included patients, 16 patients (81.25% females) had

laboratory parameters, clinical data and bone samples available at baseline. Additionally, 14 (85.74% females) out of these 16 patients had also an HR-pQCT measurement available at baseline. Out of 16 patients with available laboratory parameters at baseline, one patient was identified having ID.

Discussion: The results of this study are expected to make a significant contribution to the prevention and follow-up care of patients, as well as to improve the understanding of metabolic bone alterations associated with ID. By combining imaging, molecular analyses, and clinical outcomes, this project may help to identify clinically relevant risk factors and support the development of more targeted strategies for perioperative management and patient care. Addressing ID early could therefore reduce surgical risk and improve patient outcomes.

Profiling the tumor microbiome and its role in antitumor immunity: The impact of Malassezia in pancreatic cancer

Katja Rungger

Katja Rungger [1,2], Leonie Madersbacher [1], Pablo Monfort-Lanzas [1,3], Cornelia Speth [4], Ruben Bellotti [5], Manuel Maglione [5], Hubert Hackl [1

1. Institute of Bioinformatics, Biocenter, Medical University of Innsbruck, Innsbruck, Austria
2. MYCOS Antimycotic resistance – Approach from a One Health Perspective
3. Institute of Medical Biochemistry, Biocenter, Medical University of Innsbruck, Innsbruck, Austria
4. Institute of Hygiene and Medical Microbiology, Medical University of Innsbruck, Innsbruck, Austria
5. Department of Visceral, Transplant and Thoracic Surgery, Medical University of Innsbruck, Innsbruck, Austria

The role of intratumoral microbiota in tumor biology and anticancer immunity is increasingly recognized, with potential applications in diagnosis and therapeutic strategies such as immunotherapy. However, their effects are largely species-specific, and many of these relationships need to be elucidated. To address this, we are developing an automated pipeline to identify intratumoral microorganisms, characterize their composition, and discover potential immunoregulatory mechanisms.

Our workflow is implemented in Nextflow to ensure scalable and reproducible analyses. It processes reads not mapping to the host genome, that originate from metatranscriptomic or metagenomic sequencing. Taxonomic classification is performed with Centrifuge or Kraken2, followed by quality control of the alignment results using Recentrifuge. Contaminants in the test samples can be identified from negative control samples or based on DNA/RNA concentration using decontam by the inverse relationship between relative abundance and nucleic acid concentration. Downstream analyses include (1) calculation of alpha and beta diversity parameters, (2) identification of the core microbiome, (3) inference of microbial co-occurrence using SPIEC-EASI, and (4) metabolite prediction with HUMAnN3. From bulk RNA sequencing data various immune related parameters and immune cell fractions can be estimated and correlated with microbial abundance. Impact on survival can be assessed if clinical outcome data is available, and potential molecular mimicry can be assessed with known tumor-associated antigens.

We applied this pipeline to RNA sequencing data from pancreatic adenocarcinoma (PDAC) from The Cancer Genome Atlas. Analyses of microbial diversity revealed that bacterial species richness was greater than that of fungi and viruses. Among the identified fungal species were *Malassezia restricta* and *Malassezia globosa*, whose metabolites have been shown to activate the immunomodulatory aryl hydrocarbon receptor (AhR) signaling pathway. In fact, the inferred AhR signature, in combination with the presence of *Malassezia spp.*, showed a significant impact on patient survival.

In summary, this pipeline provides a framework for the characterization of the intratumoral microbiome and hypothesis generation regarding microbial-immune interactions, including the potential role of *Malassezia spp.* and AhR in pancreatic cancer.

Establishing a spatial proteomics platform to investigate interactions between VSV-GP, cancer-associated fibroblasts and immune cells

Meike Terwort

Oncolytic viruses (OVs) preferentially infect and replicate in cancer cells, ultimately leading to lytic cell death. Additionally, OVs mediate anti-tumour immunity due to the resulting inflammation and the simultaneous release of danger-associated molecular patterns, pathogen-associated molecular patterns and tumour antigens. This makes OVs a promising anticancer immunotherapy. One of the remaining challenges for viral immunotherapy is the tumour stroma, comprised of cancer-associated fibroblasts (CAFs), extracellular matrix, tumour vasculature and tumour-associated macrophages, which facilitate a pro-tumoural niche and can exert immunosuppressive functions. So far, little is known about the interactions of our VSV-based oncolytic virus (VSV-GP) with the stromal compartment. Therefore, it is of interest to investigate the impact of VSV-GP on the stromal compartment with a focus on cancer-associated fibroblasts, as well as investigating resulting effects on the immune system.

For this, we aim to establish a spatial proteomics platform to deeply phenotype immune and stomal cells, study cell-cell interactions, and characterise microenvironments, such as immune cell or stromal niches. This will allow us to investigate changes within the stromal compartment upon VSV-GP treatment, as well as elucidating the effect of such changes on the tumour infiltrating immune cells.

Does KCNE2 Co-Expression Affect Cav1.4 Channel Gating?

Franziska Reier

Franziska Reier, Elisa Roth, Mareike Uthoff, Matthias Ganglberger and Alexandra Koschak

Institute of Pharmacy, Pharmacology & Toxicology unit, University of Innsbruck. Innsbruck, Austria

Voltage-gated Cav1.4 L-type Ca2+ channels are predominantly expressed at photoreceptor terminals, but also in bipolar cells. Cav1.4 channels are essential for mediating a sustained Ca2+ influx, that permits a tonic glutamate release at the photoreceptor ribbon synapses. Characteristics of Cav1.4 channels are fast activation, slow voltage-dependent inactivation and a lack of calmodulin-dependent Ca2+-dependent inactivation. The biophysical properties of Cav1.4 channels are modulated by different auxillary subunits and interaction partners, as well as through intramolecular C-terminal modulation. Mutations in the CACNA1F gene, that encodes Cav1.4, or in genes encoding some of its interaction partners can alter Cav1.4 function. In humans, pathogenic variants result in channelopathies including congenital stationary night blindness type 2 (CSNB2). The voltage-gated potassium channel subfamily E member 2 KCNE2 (also called MinK-related peptide MiRP1) is an auxiliary subunit of voltage-gated cation channels primarily known for modulating voltage-gated K+ channels. Mutations in the KCNE2 gene are associated with ventricular fibrillation and long QT syndrome. However, KCNE2 also modifies the properties of other cation channels, including Cav1.2 in cardiomyocytes and HEK-cells. KCNE2 maintains the cardiac electrical stability by influencing the activation- and inactivation-properties of Cav1.2 through interaction with its N-terminal inhibitory module. For example, overexpression of KCNE2 leads to decreased Ca2+ current. Given the established interaction of KCNE2 with Cav1.2 in cardiomyocytes and HEK-cells, the high sequence homology of Cav1.2 and Cav1.4 and KCNE2 expression in photoreceptors, we hypothesized that KCNE2 could be a possible interaction partner of Cav1.4 and modulate its activation- and inactivation properties. Indeed, whole-cell patch-clamp recordings in HEK-cells revealed a trend to reduced current densities in the presence of KCNE2 in both Cav1.2 and Cav1.4, albeit the effect was stronger in Cav1.2. In addition, KCNE2 expressing cells showed a slight trend towards an accelerated inactivation of Cav1.2 and Cav1.4, compared with the cells not expressing KCNE2. KCNE2 binds to and enhances the inhibitory function of an N-terminal inhibitory module of the Cav1.2 N-terminus, although the precise binding site is unknown. However, our findings suggest that KCNE2 modulates Cav1.2 through an extended N-terminus, which contains approximately 40 additional amino acids absent in Cav1.4, potentially accounting for the channel-specific differences in KCNE2 sensitivity and resulting in a stronger decrement of current densities in Cav1.2 compared to Cav1.4.

FWF: DOC 30-B30, P36262 and P32747 to AK; TWF: F52779 to MG, University Innsbruck, CMBI

Julia Rudek

Single vs. Double Plating in Low Transverse Sacral Fractures – A biomechanical study
Introduction: High transverse sacral fractures (HTSF) are rare fracture types. Low transverse sacral fractures (LTSF) are even less common. Whereas studies have been carried out on HTSF, including biomechanical studies and case reports, no biomechanical studies have been conducted on LTSF. The goal of surgical fracture treatment is to achieve full weight-bearing and stability. Currently, there is no specific implant for this fracture type and there are no data or guidelines for stabilization. The purpose of this study was to compare fracture stabilization with single or double plating with currently available implants.

Methods: 20 fresh frozen human cadaveric sacra were evenly distributed in two groups with comparable BMD and age. A low transverse sacral fracture was created through the S3 foramina. Two commercially available implants of other fracture entities were applied. One group was stabilized with single plating (SP) with four 4.0 mm screws, the other one with double plating (DP) with four

2.7 mm screws in each plate. Using a material testing machine cyclic axial loading resulting in a bending load was applied to the sacrum: The initial load was oscillating between 5 to 10 N, while the upper load magnitude was increased by 5 N every 50 load cycles until construct failure. Different failure criteria for the fracture fragment motion were evaluated.

Results: Double plating with 8 screws reaches higher loads until failure than single plating with 4 screws. A displacement of 5 mm was observed at 212 cycles ± 148,2 (30 N ± 13,9) in SP and 865 cycles ± 290,8 (94 N ± 28,7) in DP.

However, DP showed a significantly higher amplitude than SP at the load steps of 40 N (SP = 0,832 vs. DP = 2,175) and 60 N (SP = 1,292 vs. DP = 3,755), which indicates a higher flexibility of the double plating. The tilting of the fracture gap was 9,5° at 5 mm,

14° at 7,5 mm and 18,4° at 10 mm. The results were consistent and statistically significant for all three criteria, with a p-value of < 0,001.

Discussion: Double plating with 4 screws each resisted higher loads with less displacement before failure. However, adaption of the single plating implant to also encompass 8 screws may be desirable in a newly designed implant for this fracture entity and provide higher stability and durability.

Sex-specific differences in cerebral oxygenation during individualized continuous versus standard bolus administration of adrenaline during cardiopulmonary resuscitation (CPR)

Jonas Dunz

Background

Bolus administration of adrenaline remains a central component of cardiopulmonary resuscitation (CPR) because it improves systemic and cerebral hemodynamics and increases the rate of successful return of spontaneous circulation (ROSC). Nevertheless, neurological outcome after guideline-compliant CPR remains poor.[1] Previous work by our research group has shown that continuous adrenaline administration during experimental CPR significantly improves brain tissue oxygen tension compared to bolus administration during CPR.[2] Recent studies also indicate that female piglets exhibit poorer tolerance to hypoxia than males.[3] Therefore, in the present study, we investigated sex-specific differences in brain tissue oxygenation under bolus versus continuous adrenaline administration during CPR.

Methods

This experimental study was conducted on a pig model using multimodal neuromonitoring. The primary endpoint was the partial pressure of oxygen in brain tissue ($PbtO_2$), which reflects the balance between oxygen supply and consumption at the brain tissue level. After induction of ventricular fibrillation and 5 minutes of untreated cardiac arrest, the animals underwent 30 minutes of standardized resuscitation, including mechanical ventilation, mechanical chest compressions, simulated defibrillation, and adrenaline administration. The animals were randomized to receive either a bolus administration of adrenaline as recommended by current guidelines, or a continuous infusion of adrenaline targeting a mean arterial pressure (MAP) of 40 mmHg. The animals were provided randomly, regardless of sex.

Results and Discussion

15 animals of either sex (nfemale=8, nmale= 7) were included in this analysis. Animals in the bolus group achieved a mean $PbtO_2$ of 17.81% compared to baseline (BL), while the MAP-targeted group achieved a mean $PbtO_2$ of 51.18% compared to BL during 30 minutes of CPR ($p = 0.05$). In terms of sex differences, the analysis showed that regardless the group, female pigs achieved higher $PbtO_2$ values compared to males (18.39% vs. 17.47% in the bolus group and 68.02% vs. 9.08% in the MAP-targeted group). However, the limited sample size precluded statistical significance.

A previous study by Ishii et al. showed improved neurological outcome in young female patients after cardiac arrest.[4] Our data however do not allow conclusions regarding whether the seen differences in $PbtO_2$ are associated with improved neurological outcome; further studies are needed to investigate whether increased $PbtO_2$ values during CPR have an effect on neurological outcome.

Conclusion

In this study, female piglets demonstrated consistently higher $PbtO_2$ values than males across both bolus and MAP-targeted adrenaline administration. This finding may indicate a sex-specific difference in cerebral oxygen metabolism or oxygen availability during CPR.

Cardiovascular Medicine - Biomechanical Rupture Risk in AAA

Kristina Jasmin Grassl

Zielsetzung: Die Zielsetzung der Studie war die patientenspezifische morphodynamische Progression bei abdominellen Aortenaneurysmata (AAA) zu untersuchen, wobei wir uns neben den standardmäßigen biomechanischen Parametern insbesondere auf die Lumenerweiterung, das Thrombus-Remodeling und die Veränderungen des gesamten Aortendurchmessers konzentrierten. Darüber hinaus sollten bildgebende Indikatoren für das Rupturrisiko zu identifiziert werden, die über die derzeitigen, ausschließlich auf dem maximalen Durchmesser basierenden Schwellenwerte hinausgehen.

Methoden: In einer pseudoprospektiven Single- Center-Studie wurden 30 Patienten (15 Paare) eingeschlossen: 15 mit rupturierten abdominellen Aortenaneurysmata (rAAA) und 15 mit asymptomatischen, nicht rupturierten AAA (Kontrollgruppe), jeweils mit zwei Bildgebungszeitpunkten. Das Matching erfolgte anhand des initialen Durchmessers, des Geschlechts und des Bildgebungsintervalls. Zusätzlich zur Finite-Elemente-Analyse (FEA) wurden die Veränderungen des Lumendurchmessers, der Dicke des intraluminalen Thrombus (ILT) und des Gesamtdurchmessers des Aneurysmas zwischen CT1 und CT2 ausgewertet. Die Verhältnisse von Lumen zu Wand und Lumen zu Thrombus wurden berechnet und statistische Vergleiche zwischen den Gruppen durchgeführt.

Ergebnisse: Die initialen Gesamtdurchmesser der Aorta waren vergleichbar (Mittelwert 5,5 cm). In der rAAA-Gruppe zeigten sich signifikant größere Zunahmen des Lumendurchmessers (+13,5 mm vs. +5,6 mm; p = 0,016) und des Gesamtdurchmessers (+1,35 cm vs. +0,64 cm; p = 0,008). Die Thrombusdicke nahm in der Kontrollgruppe stärker zu (+4,2 mm vs. +2,2 mm; p = 0,38, n.s.). Zum Zeitpunkt der ersten Bildgebung war das Verhältnis von Lumen- zu Gesamtdurchmesser in der rAAA-Gruppe höher (7,96 vs. 6,72), während das Verhältnis von Lumen- zu Thrombusdurchmesser vergleichbar war (3,36 vs. 3,43).

Es wurden signifikante Korrelationen zwischen dem Lumendurchmesser und dem Gesamtdurchmesser (r=0,43, p=0,019) sowie eine inverse Korrelation zwischen dem Lumendurchmesser und der Thrombusdicke (r=–0,61, p=0,0004) festgestellt, was auf eine mögliche Schutzfunktion eines dickeren Thrombus bei stabilen AAAs hindeutet.

Schlussfolgerungen: Morphodynamische Parameter – insbesondere ein rascher Anstieg des Lumendurchmessers und des gesamten Aortendurchmessers – scheinen Patienten mit erhöhtem Rupturrisiko zu identifizieren, selbst bei vergleichbaren Ausgangsdurchmessern. Ein höheres Lumen-Wand-Verhältnis und eine inverse Korrelation mit der Thrombusdicke stützen die Annahme, dass ILT eine protektive Rolle spielen könnte. Diese quantitativen, bildgebenden Marker ergänzen biomechanische Daten und könnten die Rupturvorhersage über herkömmliche Durchmesser-Schwellenwerte hinaus verbessern. Weitere Studien mit größeren, multizentrischen Kohorten sind erforderlich, um diese Ergebnisse zu bestätigen.

Christoph Frisch

Chemical warfare agents (CWA) remain a current clinical and security concern, with recurring use reported from early historical records to recent armed conflicts and terrorist incidents. One potentially underappreciated physiological sequela of CWA exposure is a shift in hemoglobin–oxygen ($Hb–O_2$) affinity, an intrinsic erythrocyte property that governs oxygen loading and unloading and is typically characterized by the oxygen dissociation curve (ODC) and the P50. In parallel, methemoglobin (MetHb) will be quantified on a blood gas analyzer. This project tests whether selected CWAs alter $Hb–O_2$ affinity in vitro and whether any effects differ between male and female samples.

We will conduct an experimental in-vitro pilot study using blood from healthy volunteers (N = 40; 20 male and 20 female). Aliquots will be exposed in vitro to predefined CWAs at specified dosages.

$Hb–O_2$ affinity will be determined by spectrometric/photometric measurement of the ODC and calculation of P50 using a high-throughput microplate reader approach. MetHb will be measured concurrently via blood gas analysis to capture oxidative hemoglobin conversion as a plausible mechanistic contributor to observed affinity changes.

Overall, this pilot study is intended to establish feasibility and generate quantitative effect estimates to inform subsequent, larger confirmatory studies on CWA-related perturbations of oxygen transport physiology.

Protocol for Developing a Questionnaire on Transvestic, Fetishistic, Sexual Sadistic or Sexual Masochistic Preferences

Felix Puster

Background. While the 10th revision of the International Classification of Diseases (ICD-10) lists fetishism, transvestic fetishism, and sexual sadomasochism as psychiatric disorders, this classification is no longer made in the ICD-11, which will completely replace the ICD-10 by 2027. However, existing questionnaires (1) conceptualize fetishism, transvestic fetishism, and sexual sadomasochism as disorders, implying clinical pathology rather than sexual pleasure and sexual well-being; (2) lack psychometric validation; (3) fail to distinguish between sexual interests, sexual fantasies, and sexual behaviors; (4) lack measurement invariance across gender, sexual orientation, and language; (5) do not consider the role of age; (6) lack cross-linguistic validation.

Objective. This study aims to develop and validate a non-pathologizing questionnaire assessing fetishism, transvestic fetishism, and sexual sadomasochism that is invariant across genders, sexual orientations, and English- and German-speaking populations, thereby enabling interpretable group comparisons.

Methods. A literature review of existing scales assessing fetishism, transvestic fetishism, and sexual sadomasochism will guide category development and item formulation. Additionally, a set of items pertaining to normophilia will gauge general sexual interest. The categories will be assessed in terms of shown interest, imagined fantasies, and behavioral experiences. A pretest (N = 100) will examine latent structure, reduce items, collect open-text feedback on missing content, and clarify item interpretation using a written think-aloud procedure. A subsequent pilot study (N = 700) will evaluate quantitative descriptive item properties (e.g., variance, skewness, kurtosis). In a large validation sample (N = 4000; including ≥200 sexual minority and ≥200 gender minority participants), psychometric properties and measurement invariance across gender and sexual orientation will be tested.

Expected Results. The resulting questionnaire will likely comprise five subscales (fetishism, transvestic fetishism, sexual sadism, sexual masochism, normophilia) with approximately 37 items addressing the domains of Interest, Fantasy, and Behavior. The instrument should (1) demonstrate invariance across gender, sexual orientation, and language; (2) not correlate with participants' social desirability response style; (3) correlate with measures for sexual sensation seeking and sexual conservatism (convergent validity); (4) barely correlate with measures of anxiety and depression (divergent validity). Based on existing literature, it is anticipated that men will report a greater number of sexual interests and higher levels of behavioral engagement than women. Discrepancies between reported interests and enacted behaviors are also expected.

Relevance. This questionnaire represents an initial step toward the non-pathologizing, psychometrically sound assessment of sexual interests and behaviors formerly labeled as pathological. As ICD-11 implementation renders pathologizing measures obsolete, this questionnaire will offer clinicians and researchers a brief, multilingual tool to assess prevalence and correlates of potentially stigmatized sexual interests and behaviors.

Authors. Puster, F.; Žegura, I.; Neves, S.; Komlenac, N.

Bridging the Gap: Sex-Specific Differences in Huntington's Disease

Greta Hemicker

Authors: Greta Hemicker1, Katarína Schwarzová1, Samuel Labrecque1, Clancy Cerejo1, Federico Carbone1, Marina Peball1, Bernadette Wimmer1, Philipp Mahlknecht1, Florian Krismer1, Atbin Djamshidian1, Klaus Seppi1,2, Beatrice Heim1*

Institution: 1Department of Neurology, Medical University of Innsbruck, Austria, 2Department of Neurology, District hospital Kufstein, Austria

*Corresponding author

Background: Huntington's disease (HD) is a progressive neurodegenerative disorder caused by an expanded cytosine–adenine–guanine (CAG) trinucleotide repeat in the Huntingtin gene on chromosome 4. Examining sex-related differences in disease onset, presentation, and progression may reveal key pathophysiological mechanisms and inform targeted therapeutic approaches.

Objective: The aim of this study is to examine sex-related differences in the clinical presentation and functional outcomes, such as working capacity and use of supportive therapies in a single-center HD cohort.

Methods: We retrospectively analyzed 102 individuals with HD receiving regular care at the Department of Neurology, Medical University of Innsbruck. CAG repeat length data were available for 101 participants. Multinomial logistic regression was used to assess sex-related differences in symptom distribution, access to neurorehabilitation, and employment status.

Results: The study sample consisted of 44 men and 58 women with genetically confirmed HD. CAG repeat data were available for 101 participants, showing no sex differences in repeat length or in the onset of motor and non-motor symptoms (all $p>0.05$). Irritability occurred more frequently in women ($p=0.033$), who also showed a lower employment rate ($p<0.001$). Utilization of neurorehabilitative treatments, including physiotherapy, occupational, speech, and psychotherapy did not differ between male and female patients ($p>0.05$).

Conclusion: Female HD patients exhibited higher rates of irritability and lower participation in the workforce, suggesting clinically relevant sex-related differences. These results underscore the need to consider sex as both a biological and social determinant in clinical management and rehabilitation planning.

Outlook: We plan to conduct a comprehensive international analysis using the Enroll-HD registry to characterize sex-specific patterns in disease-related symptomatology, access to and utilization of neurorehabilitative therapies, and working capacity.

Beyond Injury: Sex- and Diversity-Specific Aspects of Peripheral Nerve Injury and Axonal Regeneration

Caren Agreiter

Peripheral nerve injuries represent a clinically relevant cause of long-term functional impairment. Although the peripheral nervous system exhibits a higher regenerative capacity than the central nervous system, functional recovery after nerve injury remains frequently incomplete. In addition to established determinants such as injury type, lesion level and timing of surgical repair, biological diversity including sex and age has increasingly been discussed as a potential modulator of regenerative processes.

The aim of this contribution is to provide a systematic and critical overview of current clinical and preclinical evidence on sex- and diversity-specific aspects of peripheral nerve injury and axonal regeneration. Rather than presenting original experimental data, this work focuses on contextualizing existing findings, highlighting methodological limitations and identifying relevant knowledge gaps.

Epidemiological data reveal pronounced sex-specific differences in incidence and exposure depending on the type of peripheral nerve pathology. Traumatic peripheral nerve injuries predominantly affect men, largely attributable to higher exposure to occupational and traffic-related risks. In contrast, focal compression neuropathies such as carpal tunnel syndrome occur more frequently in women. For generalized peripheral neuropathies, sex differences are less consistent and strongly influenced by age, comorbidities and social determinants of health, underscoring the importance of integrating a broader diversity-sensitive perspective.

Preclinical studies provide evidence for sex-specific differences in axonal regeneration and functional recovery. In particular, sex hormones—especially estrogens—modulate neuroprotective and regenerative processes at neuronal, glial and immunological levels. Experimental models indicate that female animals may exhibit faster axonal elongation and earlier sensory recovery following peripheral nerve injury. However, some findings suggest that these effects are not solely mediated by systemic hormone levels but may also involve local, sex-specific mechanisms within peripheral nerve tissue, including differential Schwann cell responses. Transcriptomic analyses further support the presence of sex-dependent regulatory programs affecting genes involved in inflammation, cytoskeletal organization and neuronal signaling after nerve injury.

In contrast, clinical evidence addressing sex differences in regenerative outcomes after peripheral nerve injury is limited and heterogeneous. Prospective studies explicitly designed to assess sex as a biological variable are largely lacking and existing clinical data do not allow for definitive conclusions regarding superior regenerative capacity in either women or men. Consequently, there is currently no basis for sex-specific therapeutic recommendations in clinical practice.

In summary, this overview highlights biological sex and diversity as relevant yet insufficiently integrated variables in peripheral nerve regeneration research. Future preclinical, translational and clinical studies should systematically incorporate sex-sensitive study designs to improve mechanistic understanding and to critically evaluate the potential for individualized therapeutic approaches.

Lacosamide Safety During Pregnancy and Breastfeeding: A Single-Centre Experience and Narrative Review

Kamila Saramak

Kamila Saramak 1, Manuela Kaml 1, Marina Peball1, Luisa Delazer1, Gerald Walser1, Anna Hussl1, Iris Unterberger1, Alexandra Astner-Rohracher 1,*

1 Medical University of Innsbruck, Department of Neurology, Innsbruck, Austria

* Correspondence: alexandra.rohracher@i-med.ac.at

Background The management of epilepsy during pregnancy, particularly in refractory cases requires balancing effective seizure control against potential teratogenic effects of antiseizure medications (ASMs). Data on the safety and efficacy of lacosamide (LCM) - a new generation sodium channel blocker - during pregnancy and breastfeeding remain limited.

Methods We searched our institutional database for patients treated with LCM during pregnancy and/or breastfeeding. Data on seizure frequency, pregnancy and labour complications, birth outcomes, congenital malformations, and early neurodevelopmental outcomes with a minimum follow-up of one year were collected. In addition, a systematic literature search using PubMed, Europe PMC, and the Cochrane Library for original human studies published in English was conducted.

Results Twenty-two cases of maternal exposure to LCM throughout pregnancy (1 monotherapy, 21 cases of polytherapy) were identified resulting in 21 livebirths (95.5%) and one spontaneous abortion at 13 weeks of gestational age (4.5%). One infant was delivered preterm at 29 weeks of gestational age due to maternal preeclampsia with subsequent neurodevelopmental delay. Congenital malformations (atrial septal defect) were observed in one offspring exposed to a combination therapy with LCM and levetiracetam (4.8%). Twelve newborns were breastfed during maternal LCM treatment (57.1%) without neurodevelopmental delay observed at twelve months. The systematic literature search identified 16 studies (8 case reports, 3 case series, 4 cohort/observational studies, 1 pharmacovigilance report), overall reporting data on 392 pregnancies with LCM (166 monotherapy, 226 polytherapy). The proportion of livebirths was 87.2% (50/392), one infant died one day after birth. Major congenital malformations were reported in 18/392 offsprings (4.6%), in four infants (1.0%) bradycardia was observed which resolved spontaneously.

Conclusions

The available data do not indicate major safety concerns associated with LCM exposure during pregnancy and breastfeeding, and our findings are consistent with the existing literature. However, conclusions are limited by the small number of exposed cases, particularly those receiving LCM monotherapy. Larger, prospective studies with longer follow-up periods are required.

Tendral Sekar

Background

Invasive fungal infections and fungal crop diseases represent a growing burden for public health and agriculture, while the antifungal drug pipeline remains limited. Azoles represent the most widely used class of antifungal agents and act by inhibiting lanosterol 14a-demethylase (CYP51), an essential cytochrome P450 monooxygenase (CYP) in the ergosterol biosynthesis pathway. However, the long-term clinical utility of azoles is increasingly undermined by the emergence of resistance mechanisms. In parallel, many azoles display clinically relevant off-target inhibition of human hepatic cytochrome P450 enzymes, contributing to toxicity. A major bottleneck in antifungal discovery is the lack of scalable, and mechanistically informative early-stage screening tools that enable prioritisation of compounds with strong fungal CYP51 inhibition and minimal interaction with human CYP enzymes. Most available commercial CYP activity assays are optimised for mammalian CYP isoforms and use probe substrates that are not tailored for fungal CYP51, limiting their applicability for antifungal screening.

Methods

This project evaluates and adapts a commercially available human CYP450 fluorescence activity assay for functional detection of fungal CYP51 activity in a heterologous yeast expression platform. Saccharomyces cerevisiae strains overexpressing clinically relevant fungal CYP51 variants together with their cognate cytochrome P450 reductase (CPR) were cultured and the crude membranes were prepared using mechanical disruption and differential centrifugation. CYP activity was assessed using the Vivid™ CYP450 assay platform using BOMCC and related fluorogenic probe substrates in the presence of an NADPH-regeneration system to support catalytic turnover. Baculosomes™ expressing human CYP3A4 and mouse liver homogenate were used as positive controls. Reaction parameters were systematically evaluated to identify factors influencing assay performance, including buffer composition, ionic strength, and metal co-factor availability, with the aim of improving catalytic turnover in fungal crude membranes.

Results

The adapted human CYP assay generated a reproducible fluorescence signal in fungal CYP51-containing crude membrane preparations, including Aspergillus fumigatus CYP51A, demonstrating the feasibility of detecting fungal CYP activity using a repurposed mammalian CYP assay platform. Assay output was strongly dependent on reaction composition, with buffer conditions and metal co-factors identified as key determinants of signal intensity, reproducibility, and overall assay robustness. These results indicate that fungal CYP51 activity can be monitored using fluorogenic probe conversion, while highlighting specific optimisation requirements to enhance sensitivity and improve assay suitability for high-throughput workflows.

Conclusion

This work demonstrates proof-of-concept that a commercial human CYP450 fluorescence activity assay can be repurposed for functional screening of fungal CYP51 in S. cerevisiae membrane preparations. With continued optimisation, this approach has potential to serve as a rapid and mechanistically informative screening cascade within antifungal discovery pipelines. Importantly, it enables early prioritisation of candidate compounds based on CYP51 inhibition while supporting parallel assessment of off-target interaction risk with human hepatic CYP enzymes, thereby facilitating identification of selective antifungal leads.

Sex-related differences in a psoriasis cohort at risk for the development of psoriatic arthritis: First results from the STOP PsA study

Martina Steinlechner

Background: Approximately 20% of psoriasis (PsO) patients develop psoriatic arthritis (PsA). Both diseases are equally prevalent in females and males, but manifestations differ between sexes. Whereas psoriasis is more severe in men, women report greater impact on life quality irrespective of disease activity. Up to now, underlying pathophysiological mechanisms and determinants of transition from PsO to PsA remain to be elucidated. The study aims to further characterize the transition phase in the development of psoriatic arthritis in psoriasis patients. This abstract presents first results of the baseline study population characteristics.

Objectives: To study sex-related differences of patients with PsO included in the Susceptibility of Transition from Psoriasis to Psoriatic arthritis (STOP PsA) study cohort at baseline.

Methods: In this prospective cohort study PsO patients were recruited at two centers (Medical Universities Vienna and Innsbruck). We stratified PsO into a low- (no inflammatory joint pain) or high-risk group (possible/probable inflammatory joint pain) for the development of PsA. Patients with clinical arthritis, enthesitis, synovitis or preexistent rheumatic disease were excluded. Patients were evaluated by Patient-reported outcome (PsAID12, DLQI, VAS, BASDAI), clinical assessment (BASMI, swollen/tender joint count, MASES, PASI), musculoskeletal ultrasound and cardiovascular risk assessment.

Results: Overall, 291 patients were included in the STOP-PsA cohort. At baseline visit 139 patients (47.8 %) were female and had a mean age of 45.3 years. Slightly more women were assigned to the high-risk group (33.8 % vs. 23.7 %). Significant differences were found between women and men in life-quality assessment (DLQI score 6.6 +- 7.0 vs. 4.3 +- 4.6, p-value 0.01060) subjective overall burden of psoriasis (PsAID12 score 2.6 +- 2.4 vs. 1.8 +- 1.8, p-value 0.01156), whereas extent of psoriasis (PASI score 3.1 +- 3.4 vs. 3.4 +- 5.4) was not different between men and women. Similarly, burden of pain and associated features like morning stiffness and fatigue is higher in women (BASDAI score 2.7 +- 2.2 vs. 1.7 +- 1.6, p-value 0.00029), while number of tender joints (2.8 +- 6.0) and swollen joints (0.2 +- 0.9 vs. 0.1 +- 2.4) is not significantly different. However, more entheses were tender in women (MASES score 0.9 +- 0.3 vs. 0.3 +- 0.8, p-value 0.00084).

Conclusions: Although psoriasis severity is similar in both sexes, women report a higher impact of the disease on quality of life. Furthermore, the same is true for the impact of pain. Thereby, MASES is indicative of enthesitis, but evaluation with ultrasound is needed. Nevertheless, this results further strengthen previous findings of women experiencing more functional disability and pain during psoriatic disease than men independent of disease severity. Beyond these first results, this study will allow further characterization of the transition phase and paves the way for a more individualized management of PsO patients at-risk for PsA with regard to sex-specific differences.

Christopher Schaar

Schizophrenia is a profoundly disabling psychiatric disorder affecting approximately 1% of the population and marked by persistent psychotic and non-psychotic symptoms. Among the most consequential impairments is disrupted cognition and social cognition, which is strongly associated with poor functional outcomes, reduced social participation, and substantial burden extending beyond healthcare systems to families and society. Despite its clinical significance, the developmental course of social cognition in schizophrenia remains poorly characterized. Longitudinal studies capable of capturing lifespan trajectories are scarce, in part because they are time-consuming, resource-intensive, and highly vulnerable to attrition, underscoring the need for more efficient designs and robust statistical approaches.

Accelerated longitudinal designs (ALDs) offer a powerful solution by combining multiple age cohorts with overlapping age ranges to estimate developmental trajectories within a feasible study period. However, their successful application depends on careful design choices to ensure sufficient statistical power to detect clinically meaningful effects. Here, we systematically evaluate the performance of ALDs for studying cognitive and social cognitive trajectories in schizophrenia using simulation-based methods. We simulated linear mixed-effects models with random intercepts and slopes, incorporating empirically informed parameters for within-person correlation, measurement variability, and attrition. Power was evaluated to detect (i) group differences in social cognition across the lifespan, (ii) time-by-cohort interactions and fixed effects, and (iii) age-related change indexing differential aging trajectories between individuals with schizophrenia and controls.

Across a wide range of plausible parameter settings and sensitivity analyses, our results delineate the conditions under which ALDs can reliably detect lifespan differences in social cognition. The resulting design recommendations provide a principled framework for selecting cohort structures, follow-up intervals, and sample sizes that maximize inferential yield within constrained data-collection windows. By optimizing ALDs for cognitive and social cognitive research, this work advances methodological approaches for elucidating the developmental dynamics of schizophrenia and supports more efficient investigation of mechanisms underlying long-term functional disability.

Redox Modulation by Azole Antifungals: Dose-Dependent Effects on Reactive Oxygen Species and Oxidative Stress Signaling in a Hepatic Cell Model

ALDRIEN RYAN NACES REYNALDO

Aldrien Ryan Naces Reynaldo1,2, Lucia Parrakova1, Pablo Monfort-Lanzas1,3, Michaela Lackner2,4, Johanna M Gostner1,2,5
1 Institute of Medical Biochemistry, Biocenter, Medical University Innsbruck, Innsbruck, Austria.
2 MYCOS consortium, Medical University of Innsbruck, Innsbruck, Austria.
3 Institute of Bioinformatics, Biocenter, Medical University of Innsbruck, Innsbruck, Austria.
4 Institute for Hygiene and Medical Microbiology, Medical University of Innsbruck, Innsbruck, Austria.
5 Core Facility Metabolomics II, Biocenter, Medical University of Innsbruck, Innsbruck, Austria.

Background:

Fungal infections represent a growing public health concern, and azoles are among the most widely used antifungal agents. Their activity relies on inhibition of lanosterol 14a-demethylase (CYP51), thereby blocking ergosterol biosynthesis and compromising fungal membrane integrity. Despite clinical efficacy, azole therapy is associated with hepatotoxicity, endocrine disruption, and drug–drug interactions. Oxidative stress has been proposed as a contributing mechanism of azole-induced liver injury, yet evidence remains inconsistent, as some azoles display antioxidant effects in certain experimental settings. A systematic dose- and time-resolved characterization of azole-mediated modulation of reactive oxygen species (ROS) and redox-sensitive signalling pathways is lacking.

Objectives:

We investigated the intrinsic redox behaviour of selected azoles and their interference with redox-regulated immunobiochemical pathways by assessing cytotoxicity, ROS dynamics in distinct cellular environments, and activation of nuclear factor erythroid 2–related factor 2 (Nrf-2)–dependent antioxidant responses. In addition, we explored azole-regulated genes and transcription factors using publicly available transcriptomic and interaction databases.

Methods:

HepG2 cells and HepG2-derived reporter cell lines were exposed to miconazole and ketoconazole. Cytotoxicity was determined using a resazurin assay. Intracellular ROS formation or quenching was quantified with dichlorodihydrofluorescein diacetate under basal and oxidative stress conditions. Activation of Nrf-2/antioxidant response element signaling was measured using a β-lactamase reporter assay. Computational analyses included extraction of azole-associated genes from DSigDB, enrichment analysis with Enrichr, and transcription factor prediction using TRRUST.

Results:

Non-cytotoxic exposure ranges were established for both azoles. Short-term treatment revealed concentration-dependent modulation of ROS signalling. Miconazole

induced oxidative stress responses at higher concentrations, whereas ketoconazole exhibited a biphasic profile, suggesting both ROS-quenching and ROS-promoting effects. Nrf-2 activation showed a similar biphasic pattern. Enrichment analyses indicated broad transcriptional networks and pathways affected by both compounds.

Conclusion:

Miconazole and ketoconazole modulate oxidative stress and cellular defence mechanisms in a concentration- and time-dependent manner, extending beyond Nrf-2 signalling. Understanding azole-induced redox modulation may clarify mechanisms underlying hepatotoxicity, immunomodulation, and resistance development.

Riccardo Lunelli

Electrocardiograms (ECGs) are a widely used, inexpensive and standardized modality to assess cardiac functionality. The amount of publicly available ECGs is very large, with approximately 20 million ECGs in various public datasets. However, given the high cost of expert annotations, most of them have incomplete or unavailable labels. Nevertheless, this data landscape remains highly valuable for the development of foundation models, that can learn abstract representations without the need for labels. Despite this opportunity, a critical challenge persists in the lack of consistent evaluation: prior work often relies on narrow task selections and inconsistent datasets, making meaningful comparisons of foundation models difficult.

With this work we address this problem by proposing BenchECG, a standardized benchmark comprising a comprehensive suite of publicly available ECG datasets and versatile tasks. These tasks span (1) different signal characteristics (different number of leads and varying signal length), (2) dataset characteristics (clinically different cohorts and geographical diversity) and (3) task characteristics (classification, segmentation, regression, detection and survival analysis tasks). We also propose xECG, a novel recurrent architecture trained in a self-supervised manner on approximately 8 million ECGs.

Our xECG model outperformed previous state-of-the art publicly available foundational models, performing strongly on all datasets and tasks. xECG was the only model achieving strong performance on the sleep apnea task with an AUC of 0.93. Overall, our model had an average ranking of 1.5 and a BenchECG score of 0.87 where the second best model, ST-MEM had an average ranking of 2.6 and a BenchECG score of 0.82.

BenchECG enables systematic and rigorous comparison of ECG foundation models, aiming to accelerate progress in ECG representation learning. xECG achieved superior performance over earlier approaches, defining a new state-of-the-art baseline for future ECG foundation models. Moreover, the ease of use of this model will be beneficial in developing new solutions for more specific clinical tasks

Targeting mitochondrial defects in a 3D-bioprinted LCHADD/VLCADD model

Antonia Degen

Background: 3D bioprinting technologies are revolutionizing tissue engineering, especially in studying metabolic processes using patient-derived cells. Long-chain-3-hydroxy-acyl-CoA-dehydrogenase-deficiency (LCHADD) and Very-long-chain-acyl-CoA-dehydrogenase-deficiency (VLCADD) are rare disorders of the oxidation of long-chain fatty acids (LC-FA). Therapy mainly involves a diet restricted in LC-FA, supplement substitution, and fasting avoidance. Innovative strategies are needed to reduce mortality and improve quality of life. Methods: The study examines mitochondrial rearrangement in β-oxidation-defective fibroblasts by exposing them to various rescuers in 2D. Mitochondrial morphology was analyzed using live cell fluorescence microscopy and quantified by counting the number of branches and dots. To mimic tissue physiology, a 3D-bioprinted, vascularized tissue model with healthy and patient-derived fibroblasts was developed. Findings: Analysis of mitochondrial morphology in patient fibroblasts revealed significant alterations of mitochondrial morphology, reduced oxidative phosphorylation, but increased glycolysis and significantly increased intracellular ROS levels caused by NOX2. NOX2 inhibitors and other rescuers led to mitochondrial network refusion. 3D-bioprinted tissue surrogates showed impaired vessel formation in the presence of patient fibroblasts. Interpretation: Our findings will improve the understanding and therapy of LCHADD/VLCADD, as there are no direct therapies for elevated ROS levels and mitochondrial dysfunction. 3D-bioprinted patient tissue models will be used for testing novel treatment modalities and tissue response during physiologic stress.

Impact of iron availability and azole treatment on the mycobiome and resistance development

Nidhi Srinivasan

Background / Introduction:

Fungal infections are a major complication in immunocompromised patients, including those with myelodysplastic syndromes (MDS). Azole antifungal medications are widely used for prophylaxis and treatment; however, they have been linked to rising antifungal resistance. Iron availability also affects fungal growth and host-pathogen interactions. In MDS, iron overload and chelation therapy may influence the mycobiome and susceptibility to antifungals. However, the combined effects of iron modulation and azole exposure remain poorly understood. This project will investigate how iron availability and azole therapy shape the mycobiome and resistance development in patients with MDS.

Objectives / Aims:

We aim to perform a cohort study of MDS patients to

1. characterize the gut mycobiome under iron chelation and/or azole therapy, and

2. compare it with untreated patients to identify fungal taxa and resistance patterns associated with iron modulation or antifungal exposure.

Methods:
Stool samples collected from a previous MDS patient cohort were processed for internal transcribed spacer (ITS) sequencing to characterize the gut mycobiome composition. Sequencing data were analyzed to assess fungal diversity, relative abundance, and potential resistance-associated taxa. Clinical treatment data, including azole exposure, iron chelator use and cardiovascular drug use were integrated with the analysis to explore the associations between therapeutic interventions and mycobiome alterations.

Results:
Although preliminary findings suggested potential shifts in the mycobiome associated with azole exposure in MDS patients, no definitive patterns were identified. This cohort had a non-significant group of patients who underwent azole treatment, which made it implausible for sequencing analysis. There were no significant differences between the mycobiome compositions in patients based on any other grouping. Differential abundance testing for each cluster did not reach significance, with no robust results.

Conclusion:
In this initial cohort, gut mycobiome composition was largely homogeneous, with no robust differences attributable to iron or azole therapy. The findings emphasize the need for larger, prospectively sampled cohorts to validate subtle treatment-related effects and to improve detection of therapy-associated fungal signatures.

Ongoing activities:
Stool, oral swab, and oral rinse samples from a second cohort of MDS patients are currently being collected for comparative mycobiome analysis. These additional samples will enhance the resolution of treatment-related effects and help identify consistent mycobial signatures linked to antifungal and iron-modulating therapies.

The *Xanthoria parietina* lichen mycobiont produces ferrichrome in the thallus and in axenic culture

Isidor Happacher

Lichens are symbiotic associations between a fungal mycobiont and a photosynthetic photobiont. They thrive in nutrient-poor environments; yet the mechanisms underlying their adaptation to iron limitation remained largely unknown. Here, we characterize the iron acquisition system of Xanthoria parietina, a globally distributed lichen-forming fungus associated with the microalgal photobiont Trebouxia decolorans. We demonstrate that the mycobiont produces the siderophore ferrichrome and possesses the full genetic repertoire not only for siderophore biosynthesis, but also reductive iron assimilation, iron detoxification, and regulation. The ferrichrome-synthesizing non-ribosomal peptides synthetase exhibits a lichen-specific compact architecture but retains functionality when heterologously expressed in a non-lichenized ascomycete. Transcriptomic analysis reveals substrate-dependent regulation of the siderophore system, with upregulation on concrete compared to bark. Importantly, ferrichrome promotes photobiont growth independent of extracellular iron reduction, indicating direct utilization. These findings provide the first functional evidence of siderophore-mediated iron acquisition in a lichen symbiosis and highlight ferrichrome as a key mediator of mutualistic nutrient exchange.

Sex Reporting in Avalanche Survival Research: A Rapid Evidence Map

Frederik Eisendle

Background: Avalanche survival research spans epidemiologic registry analyses, field rescue studies and controlled field-studies and investigations. While sex differences may influence both exposure patterns and physiological responses during burial, it is unclear how consistently sex is reported and analytically considered across this literature.

Objective: To quantify the frequency and quality of sex-related reporting in avalanche survival research and to outline practical recommendations for improved reporting and analysis.

Methods: We will conduct a rapid evidence map of human studies on avalanche burial, rescue, survival outcomes, and related interventions. Studies will be identified through targeted literature searching and reference screening. For each included study, we will extract whether sex is reported, whether female proportion is explicitly stated, and whether outcomes are presented in a sex-disaggregated manner or include sex in statistical models. Findings will be summarized descriptively across study types.

Conclusions: A structured overview of sex reporting practices can identify low-burden, high-impact improvements for avalanche survival science. Routine reporting of sex distribution and, where feasible, sex-disaggregated outcome reporting may strengthen external validity and support more generalizable translation of rescue and intervention research.

Trained Immunity Enhances Valvular Calcification: The Role of Age and Sex in Calcific Aortic Valve Disease

Lynn Muller

Calcific aortic stenosis (AS) is a leading cause of valvular heart disease, with risk factors including age, sex, hypercholesterolemia, diabetes, and hypertension. Calcific aortic valve disease (CAVD) is characterized by progressive thickening and calcification of the aortic valve leaflets, leading to impaired blood flow. Traditionally considered a passive degenerative process, CAVD is now recognized as an active and complex inflammatory disease. Currently, no pharmacological treatment exists, and surgical valve replacement remains the only therapeutic option.

A growing body of evidence suggests that chronic inflammation is a key driver of CAVD. Increased mechanical stress leads to endothelial injury and activation of valve interstitial cells (VICs), promoting fibrosis and calcification. This activation triggers a pro-inflammatory cascade involving macrophages, IL-6, IL-1β, and TNF-α, as well as the NF-κB pathway, ultimately inducing osteogenic factors such as BMP-2, Notch1, and Runx2.Recent research highlights the involvement of trained immunity in atherosclerosis, a closely related vascular pathology. Trained immunity refers to the epigenetic and metabolic reprogramming of innate immune cells, particularly monocytes and macrophages, following exposure to inflammatory stimuli such as oxLDL. This results in an exaggerated immune response upon subsequent challenges, contributing to chronic inflammation and tissue remodelling. Given the similarities between atherosclerosis and CAVD, trained immunity may play a critical role in the pathogenesis of aortic valve calcification. Hypercholesterolemia and persistent inflammatory stimulation could induce trained immunity in VICs and macrophages, exacerbating the fibrotic and calcific processes.

Trained monocytes exhibited a hyperinflammatory phenotype characterized by elevated IL-6 production in vitro and promoted a pronounced calcific response in valvular interstitial cells (VICs) under co-culture conditions. Echocardiographic analysis of aged mice demonstrated age-associated valve degeneration, with male mice exhibiting more severe pathological changes than their female counterparts. These sex-specific differences were corroborated by ex vivo experiments.

Innate immune training induces a heightened pro-inflammatory state in monocytes, contributing to enhanced calcification in valvular cells in vitro. Monocytes derived from aged male mice display an enhanced pro-calcific capacity, consistent with the sex-specific progression of valvular degeneration observed in vivo. These findings provide a compelling basis for further investigation of immune training in calcific aortic valve disease (CAVD) and its potential as a therapeutic target.

The Effect of pH on Auditory Hair Cell Excitation

Lukas Hallbrucker

Synaptic transmission between inner hair cells (IHCs) and spiral ganglion neurons (SGNs) is fundamental for sound encoding in the mammalian inner ear. Before the onset of hearing, the developing cochlea is characterized by recurrent waves of spontaneous activity that encompass IHCs, SGNs, and supporting cells—a process thought to be essential for auditory synaptic maturation, refinement of afferent pathways, and the establishment of a precise frequency–place map required to faithfully encode the full hearing range. While the mechanisms underlying this spontaneous activity have been extensively studied in recent years, it remains unclear how IHC firing itself is regulated during these events.

In this context, neurotransmitter loading and release are intrinsically linked to proton dynamics, as synaptic vesicles (SVs) are acidified prior to neurotransmitter uptake and release protons (H^+) into the synaptic cleft upon vesicle fusion. Once in the cleft, these protons may alter the function of excitability-related ion channels in the immediate vicinity, thereby fine-tuning presynaptic activity patterns. Given the prolonged and multivesicular nature of spontaneous burst firing, local and transient pH changes may thus act as powerful direct regulators of IHC synaptic output. This hypothesis is supported by electrophysiological recordings from IHCs demonstrating that extracellular pH strongly influences several Kv and Cav1.3 channels.

To gain deeper insights into the physiological role of pH regulation within the intact sensory epithelium, we aim to establish a live-cell pH-imaging approach using organotypically cultured cochlear explants. This multimodal platform combines pH-sensitive fluorescent dyes with calcium imaging to correlate pH fluctuations with spontaneous synaptic activity. Initial experiments demonstrate the feasibility of pH dye loading and structural visualization, although temporal resolution and signal specificity still require improvement.

In addition, we employ immunohistochemistry and MINFLUX super-resolution microscopy to map the spatial distribution of key proteins involved in pH homeostasis at IHC synapses—such as glutamate transporters and calcium pumps—with single-digit nanometer precision. Together, these approaches will provide a framework for linking protein localization, pH regulation, and spontaneous activity in the developing auditory system.

Ulrich Sturm

The World Health Organisation identifies emerging antimicrobial-resistant fungal diseases as a public health crisis and one of the major therapeutic challenges of the 21st century. Similarly, five EU health and environment agencies warn about the growing burden of antifungal-resistant pathogens and call for novel antimycotic agents operating under innovative mechanisms-of-action that do not provoke resistance.

Photosensitisers, certain molecules with π electron-rich scaffolds, harness the ability to generate ROS in vivo by irradiation with light, in a long-standing medical treatment option known as photodynamic therapy. A new strategy to implement photosensitisers of natural origin such as anthraquinones is promising against fungal diseases but lacks cellular selectivity. Conversely, antifungal azoles target a specific enzyme in the fungal metabolism and are today a widely used treatment option for most mycoses in humans, animals, and crops. However, pathogens are known to lose susceptibility due to mutations in the active site of the protein.

In order to combine the favourable properties of both therapeutic methods, we aim to chemically combine (conjugate) the azole enzyme binding group and naturally derived photosensitisers into light-activatable antifungal agents. First synthetic conjugates could be obtained and bio-evaluations are on the way for proof-of-concept tackling antimicrobial resistance in a One Health approach.

David Wippel

Objective

This study assessed two different 3D-printed endovascular simulation models and a digital simulator for training of endovascular interventions.

Methods

Thirty-two vascular surgeons and radiologists at a university vascular center completed interventions using two transparent 3D-printed models—a flexible model, printed via the additive manufacturing process of Stereolithography (SLA), and a stiff model, manufactured using Fused Deposition Modelling (FDM) technology —as well as a digital simulator. A standardized questionnaire assessed the models' perceived face and construct validity using a Likert scale, and their concurrent validity through single-choice questions. Additionally, the impact of model material (flexible vs. stiff) on perceived fidelity and utility, and gauging interest in a routine endovascular simulation-based training program were evaluated.

Results

All participants completed the three interventions successfully. There was an even distribution of sex (16 male and female) and experience (ranging from <5 years to >20 years of experience and <20 to >100 performed interventions) among the participants. The flexible 3D-printed model demonstrated significantly higher face and construct validity scores compared to the stiff 3D-printed model and the digital simulator ($p<.001$). No significant differences were observed between the digital and stiff models ($p=1.0$ for face validity, $p = .38$ for construct validity). Regarding concurrent validity, there was a significant preference for the 3D-printed models (72% vs. 16%; $p<.001$). Among the 3D-printed models, the flexible one was strongly favored (82% vs. 9%; $p<.001$) likely due to higher scores regarding the fidelity of the experienced resistance and tactile response ($p<.001$). Most participants (81%) expressed a desire for regular simulation training.

Conclusion

Transparent 3D-printed models present a valuable, and potentially superior, alternative to established digital simulators. They achieve higher scores in face and construct validity as well as surpass the digital simulator in concurrent validity. Flexibility emerges as a key factor, significantly enhancing the fidelity and overall training experience of 3D-printed models.

XPseq Analytics

Accelerating science with
rapid RNA-seq analysis

Your RNAseq data. Ready in days, not weeks.

We know waiting for results is the most frustrating part of doing a PhD. We help you to accelerate your PhD projects with our rapid RNAseq gene expression services.
From the moment your samples arrive at our lab, we typically deliver your high-quality data in just 5-6 workdays.

Still doing RT-qPCR? We have you covered.

Our service is a drop in replacement for RT-qPCR based gene expression profiling. Run your experiments as usual, isolate the RNA and just hand it off to us. We will take care of the analysis and will deliver publication ready results.

Fast-track your research. 3 simple steps.

Just fill out a short form, mix your samples with a stabilization buffer, and ship them off at room temperature. We handle the rest.

1. Online Form

2. Stabilize Samples

3. Ship at RT

**Free sample pickup
for labs in Innsbruck**

Get Your Data Next Week
99 € net/sample

www.xpseq.com

SCAN ME

Patient-Reported Outcomes in Pediatric Oncology – Diversity Aspects

Alexander Tilg

Introduction: Patient-reported outcome measures (PROMs) are increasingly recognized in clinical research and routine care and have even been associated with improved survival among adult cancer patients. In pediatric oncology, the implementation of PROMs has similarly been linked to improved symptom control. Therefore, the aim of this analysis was to assess diversity-related aspects of PROMs in pediatric oncology and provide information potentially relevant for optimizing patient- and diversity-specific supportive care.

Methods: In this prospective single center cohort study, 110 pediatric cancer patients aged 0–18 years receiving chemotherapy were enrolled at the Medical University of Innsbruck between May 1, 2020 and December 31, 2024. Daily symptom reports were collected via the ePROtect app with six concise questions, either self reported by patients or observer reported by caregivers. Nausea, pain, sleep disturbance, and fatigue were each scored on a 0–100 scale, with lower values indicating greater symptom burden. Patients were followed from diagnosis through the end of intensive therapy. Outcomes were analyzed for differences according to biological sex, age group, and reporter type (patient vs. observer).

Results: A total of 110 patients were included, resulting in around 11,000 days of symptom assessment within over 21.000 patient-days of surveillance. In the domains of pain, nausea, and sleep, patients aged 5 to 7 years showed a significantly lower symptom burden compared with both younger and older patients. In contrast, fatigue did not differ between age groups. Additionally, regarding sex and reporter type, no relevant differences were observed among the assessed PROM domains.

Conclusion: The analysis demonstrated significant age-related differences in PROMs, supporting the need for individualized supportive care and helping to identify subgroups that may require additional attention. Furthermore, the absence of differences by biological sex and reporter type contributes to a better understanding of diversity aspects in pediatric oncology.

rAAV-mediated gene supplementation approach addressing a CACNA1F CSNB2 truncation variant in mice

Abdallah Abdalhady

Abstract: The L-type calcium channel truncation mutation CaV1.4-R1827X (RX) disrupts the distal C-terminal regulatory domain, altering channel function and expected to compromise sustained calcium entry at rod ribbon synapses. This variant causes incomplete congenital stationary night blindness type 2 (CSNB2) in humans. Prior work in a heterologous expression system showed that co-expression of the missing C-terminal peptide rescued truncated channels to wild-type function. Here, we establish preclinical proof-of-concept for gene supplementation therapy by delivering a complementary peptide to rod photoreceptors. We generated a rhodopsin promoter-driven tdTomato-peptide construct and investigated photoreceptor targeting and subcellular localization immunohistochemically following subretinal delivery in C57BL/6J and RX mice. The construct drove robust rod-restricted expression confined to the photoreceptor containing layers. Importantly, tdTomato-peptide displayed enrichment beneath the ribbon in the outer plexiform layer in RX retinas, whereas wildtype retinas lacked this enrichment, suggesting specific localization to synaptic sites where the therapeutic peptide is needed.

We also compared delivery routes in wild-type mice: subretinal injection achieved high transduction confined to the injection bleb, while intravitreal injection produced retina-wide distribution but lower transduction efficiency.

These findings demonstrate rod-specific expression and appropriate subcellular localization of the therapeutic peptide at ribbon synapses in mutant photoreceptors, supporting the feasibility of gene supplementation therapy for this truncation mutation. Ongoing work focuses on optimizing the transduction efficiency to enable functional and behavioral rescue studies.

Alessia Rossi

Understanding the immunosuppressive tumor microenvironment (TME) is essential to improve immune checkpoint inhibitor (ICI) therapies and to better predict patient response. Tumor infiltrating lymphocytes (TILs) are key determinants of clinical outcome, and their relevance depends not only on cellular composition and activation state, but also on their spatial organization within the tumor. Based on these features, tumors can be broadly classified into inflamed, immune-excluded, or immune-desert spatial phenotypes, which can be inferred using gene expression-based classifiers. However, the prognostic value of these phenotypes in colorectal cancer (CRC) remains unclear, and their robust identification in spatial transcriptomic datasets poses significant analytical challenges.

In this study, we analyzed formalin-fixed paraffin-embedded (FFPE) tumor samples from CRC patients (n = 15) profiled using the 10x Genomics Xenium platform. Our primary objective was to characterize spatial immunophenotypes in CRC and to explore the biological mechanisms associated with their emergence. In parallel, we addressed key technical limitations inherent to high-resolution spatial transcriptomics data that can compromise downstream analyses.

We implemented a data-driven strategy to redefine spatial phenotypes tailored to our dataset, adapting published concepts to the available molecular information. This approach enabled a clear separation of spatial immune states and revealed spatial patterns consistent with known immunological features, particularly in relation to $CD8^+$ T-cell organization.

In addition, we developed a workflow to mitigate background signal contamination arising from Xenium's three-dimensional image acquisition and subsequent projection into two-dimensional space. By removing transcripts originating from non-source cell types and performing cell-type-specific differential expression analyses, we improved statistical power and biological interpretability. This framework allowed the identification of phenotype-associated transcriptional programs within distinct cellular compartments. Findings provide a foundation for dissecting immune-tumor interactions in CRC and for refining spatial biomarkers relevant to immunotherapy response.

Pallavi Saxena

Chemical Footprints: Prevalence of Azole Antifungals in Tyrolean Blood Donors

Background

Azole antifungals are essential for the treatment of invasive fungal infections and are widely used as fungicides in agriculture. The extensive and overlapping application of azoles across clinical and agricultural domains has raised concern about environmental contamination and the emergence of antifungal resistance in both environmental and human-associated fungi. Despite growing awareness of azole resistance as a public health threat, population-level data on human azole exposure remain limited, particularly in European regions with intensive agricultural activity. Tyrol represents a relevant study area due to its heterogeneous land use, seasonal pesticide application, and mixed rural–urban population. Blood donors serve as a valuable proxy for the generally healthy adult population, enabling assessment of background environmental exposure outside therapeutic contexts. This study aims to address a critical knowledge gap by systematically evaluating the prevalence and concentration of azole antifungals and other persistent agrochemicals in Tyrolean blood donors.

Objectives

1. To determine the proportion of Tyrolean blood donors with detectable azole antifungals in blood samples

2. To quantify absolute blood concentrations of azole antifungals and evaluate variation by age, sex, season, and geographic location

3. To assess associations between azole levels and dietary habits, including consumption of organic foods and specific food products

4. To explore the presence of additional persistent pesticides and biocides in blood samples

Methods

Between November 2025 and July 2026, 4-mL EDTA blood samples are collected from 1,000–2,000 consenting blood donors across 16 donation events in Tyrol. Sites were selected based on 2023 blood donation turnout data to ensure representation of regions with differing agricultural intensity and exposure profiles, spanning non-pesticide, moderate, and high pesticide seasons. Residual blood samples are transported to the blood bank, centrifuged to obtain serum, aliquoted into 1–2 mL tubes, and stored at −80 °C until analysis. Participants complete a standardized dietary and exposure questionnaire using REDCap on tablets, with QR-code–based anonymized linkage to biological samples. Azole antifungals are quantified using validated liquid chromatography–mass spectrometry (LC-MS) protocols. Statistical analyses include prevalence estimates with 95% confidence intervals, multiple linear regression for concentration data, and binary logistic regression to identify predictors of detectable exposure.

Current Status and Preliminary Results

Autumn and winter sample collection has been completed successfully. Participation prevalence was approximately 50% during initial smaller donation events and increased to 60–70% during larger events, indicating high acceptability of the study

design among blood donors. Sample handling, transport, and questionnaire completion were feasible across all sites, supporting continued data collection during spring and summer.

Expected Results

This project will generate the first population-level biomonitoring data on azole antifungal exposure in an Austrian region. We expect to define the prevalence and concentration range of azole antifungals in blood donors and to identify demographic, seasonal, geographic, and dietary determinants of exposure. Detection of co-occurring persistent pesticides and biocides will further contextualize the environmental chemical burden.

Conclusion

By integrating biomonitoring with environmental and lifestyle data, this study provides essential baseline evidence on azole exposure in the general population. The findings will inform risk assessment, surveillance strategies, and policies aimed at reducing environmental contamination and preserving the long-term effectiveness of azole antifungals.

Keywords: Azole antifungals, biomonitoring, environmental exposure, antifungal resistance, population health

Elena Mayer

Chimeric antigen receptor (CAR) T cell therapy has achieved remarkable clinical success in several hematological malignancies, yet its efficacy in acute myeloid leukemia (AML) remains limited. A major obstacle is the intrinsic resistance of AML blasts, particularly in TP53-deficient disease, where resistance to CAR T cell-mediated cytotoxicity has been linked to upregulation of the mevalonate pathway. Systemic pharmacological inhibition of such resistance mechanisms is frequently associated with substantial toxicity, highlighting the need for localized and target-restricted therapeutic strategies.

This project proposes a novel approach that leverages trans-synaptic vesicles (TSVs) released at the immunological synapse between CAR T cells and their target cells. TSVs have recently emerged as important mediators of intercellular communication and are enriched in small non-coding RNAs (sncRNAs). We hypothesize that TSVs can be repurposed as contact-dependent delivery vehicles to transfer functional sncRNAs from CAR T cells directly into tumor cells, enabling localized modulation of tumor-intrinsic resistance pathways while avoiding systemic toxicity.

The first aim of this project is to establish bead-supported lipid bilayers (BSLBs) displaying defined surface antigens as inert, artificial targets for CAR T cells. This system will be used both to model antigen-specific immune synapse formation and to capture released TSVs in a controlled and scalable manner. In parallel, we will validate TSV-transferred RNA barcodes as a robust and quantitative readout of RNA transfer from CAR T cells.

Building on this platform, we will perform pooled CRISPR screens in CAR T cells to identify key regulators of TSV biogenesis and RNA transfer. In this approach, TSV-delivered sgRNAs act as molecular barcodes, directly linking CAR T cell genetic perturbations to RNA transfer efficiency and functional target engagement. In a third step, top candidate genese will be functionally tested and the screening framework extended to live leukemic targets.

Ultimately, this work aims to define the molecular basis of TSV-mediated RNA delivery and establish CAR T-mediated local RNA transfer as a new therapeutic modality to overcome resistance in AML and inform next-generation CAR T cell design.

Carina Spitzauer-Perger

Der akute ischämische Schlaganfall ist weltweit eine der häufigsten Ursachen für Mortalität und langfristige Behinderung. Mehr als 80 % aller Schlaganfälle sind ischämischer Genese, wobei der funktionelle Outcome maßgeblich vom Zeitpunkt der Diagnostik und Intervention abhängt („time is brain"). Neben etablierten medizinischen Faktoren gewinnen geschlechts- und diversitätssensible Aspekte zunehmend an Bedeutung, da sie Risiko, klinische Präsentation, Versorgung und Prognose beeinflussen.

Biologische Geschlechtsunterschiede zeigen sich unter anderem in Inzidenz, Alter bei Erstereignis, Risikoprofil und Mortalität. Darüber hinaus spielen Aspekte des sozialen Geschlechts eine Rolle, etwa in der Wahrnehmung von Symptomen, im Gesundheitsverhalten sowie im Zugang zu medizinischer Versorgung. Weitere relevante Diversitätsdimensionen sind der sozioökonomische Status, kulturelle und ethnische Zugehörigkeit, Bildungsstand, Alter, bestehende Beeinträchtigungen sowie Schwangerschaft. Diese Faktoren sind mit Unterschieden in Schlaganfallhäufigkeit, Risikofaktorenlast, Behandlungsintensität und klinischem Outcome assoziiert und können bestehende Ungleichheiten in der Versorgung verstärken.

Mein Poster gibt einen Überblick über aktuelle Erkenntnisse zu geschlechts- und diversitätssensiblen Aspekten des akuten ischämischen Schlaganfalls und diskutiert deren klinische Relevanz. Ergänzend wird ein Ausblick auf meine sich in Arbeit befindende retrospektive Kohortenstudie „Acute Ischemic Stroke – Impact of Pre-Intervention Imaging Modality on Functional and Imaging Outcomes" gegeben. In dieser Studie werden Patient:innen untersucht, die vor einer mechanischen Thrombektomie entweder eine CT- oder MRT-basierte Bildgebung erhielten. Ziel ist es, neben dem Vergleich der Bildgebungsmodalitäten auch potenzielle Geschlechts- und Diversitätsunterschiede im Zusammenhang mit dem akuten ischämischen Schlaganfall zu analysieren.

Matthias Demetz

Objective:

Subvisual 5-ALA–induced fluorescence in gliomas remains poorly understood, yet it may offer critical insights into tumor biology and infiltration patterns. By integrating spectroscopic fluorescence analysis with spatial transcriptomics and immunohistochemical profiling, this project aims to elucidate the molecular characteristics underlying subvisual 5-ALA fluorescence in gliomas. Ultimately, this work seeks to inform surgical decision-making, enhance extent of resection, and improve patient outcomes.

Methods:

Fresh-frozen glioma samples were prospectively collected during first-time surgical resection and were classified intraoperatively as 5-ALA-positive or -negative based on visible fluorescence using a Zeiss surgical microscope. Spectroscopic fluorescence analysis was performed on both fresh and thawed tissue samples using a prototype device provided by Stryker, in collaboration with the Department of Neuropathology. Spectral data acquisition included the assessment of emission peaks and fluorescence intensity, with particular emphasis on identifying subvisual fluorescence signatures. Fluorescent hotspots were precisely localized, and corresponding tissue was processed for downstream immunohistochemical and spatial transcriptomic analyses. Immunohistochemical staining will be conducted to investigate protein pathways associated with 5-ALA metabolism and fluorescence. Spatial transcriptomic analyses are planned in matched regions to characterize gene expression profiles within areas exhibiting visual and subvisual fluorescence.

Results:

In total, 70 tissue samples from 52 patients were analyzed, including 58% male and 42% female patients. No 5-ALA-induced fluorescence was detected in any thawed samples using conventional surgical microscopy. Using spectroscopic analysis, 5-ALA fluorescence was identified in 5 of 15 samples from WHO grade 2 gliomas (33.3%), 4 of 18 samples from grade 3 gliomas (22.2%), and 32 of 37 samples from grade 4 gliomas (86.5%). Notably, no fluorescence was detected in oligodendrogliomas, whereas astrocytomas and glioblastomas demonstrated measurable fluorescence signals. Analysis of gender-related differences revealed comparable fluorescence detection rates between male and female patients, with no statistically significant association between gender and 5-ALA fluorescence ($p>0.05$).

Next steps:

Immunohistochemical staining will be performed to visualize the expression of 5-ALA-associated proteins in precisely defined tissue regions. In parallel, spatial transcriptomic analyses will be conducted to map gene expression patterns within 5-ALA-positive and -negative areas. By integrating molecular, histopathological, and spectroscopic data, this project aims to characterize subvisual fluorescence and elucidate its potential biological and therapeutic relevance. The resulting findings are intended for publication in peer-reviewed journals and presentation at international scientific meetings, and will form a central component of the author's PhD thesis.

Gabapentin alters β-cell Na+ channels, and pancreatic islet Ca2+ dynamics

Ryoichi Taguchi

Authors: Ryoichi S. Taguchi[1], Laura E. Häfele[1], Noelia Jacobo-Piqueras[1], Stefanie M. Geisler[1], Petronel Tuluc[1]

[1]Institute of Pharmacy, Department of Pharmacology and Toxicology, University of Innsbruck

Gabapentinoids are widely prescribed for chronic pain and exert their primary effects by binding the α2δ-1 auxiliary subunit of voltage-gated calcium channels, thereby reducing channel trafficking and neuronal excitability. In pancreatic β-cells, calcium influx through these channels is essential for insulin secretion, and genetic deletion of α2δ-1 impairs β-cell Ca^{2+} entry and causes diabetes. Paradoxically, clinical reports associate gabapentinoid treatment with an increased incidence of hypoglycaemia, suggesting additional, islet-specific mechanisms.

Here, we investigated how gabapentin (GBP) modulates calcium signaling and electrical activity in intact pancreatic islets and single β-cells. Calcium imaging revealed that GBP-treated islets exhibited increased glucose-induced Ca^{2+} activity, including spontaneous Ca^{2+} transients at subthreshold glucose (5 mM) and a transition from oscillatory activity to a sustained Ca^{2+} plateau at 10 mM glucose. Despite this heightened excitability, depolarization with 50 mM KCl elicited significantly reduced Ca^{2+} transient amplitudes, indicating preserved but altered calcium handling. Electrophysiological recordings showed that GBP induced action potential firing at subthreshold glucose and promoted continuous action potential trains at stimulatory glucose concentrations.

Unexpectedly, whole-cell recordings revealed no significant changes in β-cell Ca^{2+} currents, L-type channel contribution, K^+ currents, or maximal KATP conductance following GBP treatment. In contrast, voltage-gated Na^+ currents were significantly reduced and exhibited slower inactivation kinetics. As β-cell action potentials rely predominantly on Ca^{2+} rather than Na^+ channels, this reduction is unlikely to directly explain the increased β-cell excitability. However, α- and δ-cells depend more strongly on Na^+ channels for glucagon and somatostatin release.

Taken together, these data indicate that gabapentin modifies pancreatic islet excitability through mechanisms that are not explained by direct alterations in β-cell Ca^{2+} influx or major ionic conductances. The dissociation between increased β-cell electrical activity and largely unchanged β-cell Ca^{2+}, K^+, and KATP currents points toward an indirect, islet-level mode of action. Based on the observed reduction in Na^+ currents and the known reliance of α- and δ-cells on Na^+ channels for hormone secretion, we will next examine whether gabapentin preferentially alters non-β endocrine cell function and paracrine signaling within the islet. Future experiments will focus on defining cell type–specific effects of gabapentinoids on hormone release and intercellular communication, and on determining how these changes influence β-cell responsiveness across physiological glucose ranges.

Erika Kvalem

Emerging evidence supports a bidirectional gut–pancreas axis in which microbial dysbiosis, barrier dysfunction, and altered metabolite fluxes contribute to pancreatogenic diabetes (T3cDM). Whether gut microbial changes reflect systemic metabolic disturbances or primarily arise from exocrine pancreatic insufficiency (EPI) remains unclear. We profiled the gut microbiome of 48 outpatients with T3cDM, type 1 diabetes (T1DM), and healthy controls. Genus-level 16S rRNA data were analysed using cross-validated LASSO logistic regression and patient-specific community metabolic models. T3cDM showed reduced α-diversity and distinct β-diversity compared with T1DM and controls. Key compositional shifts included enrichment of Enterobacteriaceae (notably Escherichia–Shigella) and Streptococcaceae in T3cDM. LASSO models discriminated T3cDM from T1DM (AUC 0.867; accuracy 0.818), highlighting Blautia, Escherichia–Shigella, Streptococcus, Clostridium, and Faecalibacterium as predictors. Metabolic modelling indicated elevated Escherichia–Shigella growth in T3cDM and disease-specific metabolite fluxes. Gut microbial shifts in T3cDM predominantly reflect EPI rather than systemic metabolic disturbances characteristic of T1DM, underscoring the central role of exocrine pancreatic dysfunction in shaping the gut microbiome and its metabolic activity.

Homeostatic control of the sphingolipid biosynthesis regulators Orm1 and Orm2 via ER retention and export.

Niklas Schomisch

ORMDL family proteins are conserved regulators of sphingolipid biosynthesis, with the main function to inhibit the rate-limiting enzyme serine-palmitoyl transferase (SPT) in the ER [1]. In humans, dysregulation of SPT activity causes a form of amyotrophic lateral sclerosis (ALS), and is genetically linked to several inflammatory diseases [2,3]. In budding yeast the ORMDL family consists of two proteins, Orm1 and Orm2. Both are embedded in a homeostatic system that adjusts sphingolipid levels to cellular demands [1].

Although Orm1 and Orm2 share about 70% sequence identity, the two proteins inhibit the SPT with different potency, Orm2 being the stronger inhibitor [4]. Their regulation is different, with Orm2 being subject to ER export and proteolytic turnover via the EGAD pathway, which is not observed for Orm1 [5]. How the specificity of ER export vs. retention of these highly homologous proteins is achieved is unknown. Here, we identified a hydrophobic sequence responsible for stably retaining Orm1 in the ER. A second, polybasic retention motif in Orm2 is controlled by phosphorylation is responsible for regulated ER export. We found this polybasic motif to be transferable onto another, constitutively exported ER protein, suggesting a more general mechanism for regulated ER to Golgi Traffic.

[1] Schomisch and Schmidt, 2024, Biospektrum

[2] Mohassel et al., 2021, Nat. Med.

[3] Moffatt et al., 2007, Nature

[4] Körner; Schäfer et al., 2024, Cell Rep.

[5] Schmidt et al., 2019, EMBO J.

Associations between the American Heart Association's Life's Essential 8 and major aging-related health outcomes: a systematic review and meta-analysis

Lisa Waltle

Waltle, Lisa(1); Kuhle, Stefan(1); Willeit, Peter(1,2,3)

1 Medizinische Universität Innsbruck, Österreich; 2 Ignaz Semmelweis Institut, Österreich; 3 Department of Public Health and Primary Care, University of Cambridge, Vereinigtes Königreich

Background: Cardiovascular disease (CVD) is the leading cause of death worldwide, with most cases attributable to modifiable risk factors. The American Heart Association's Life's Essential 8 (LE8) provides a comprehensive measure of cardiovascular health, but its associations with major health outcomes have not yet been systematically synthesized.

Methods and results: We searched PubMed, Web of Science, EMBASE, ScienceDirect, and the Cochrane Library for prospective cohort studies published up to September 2025 evaluating LE8 in relation to health outcomes. Thirty-six publications from ten cohorts met inclusion criteria. Eight studies (N = 471,397; mean age 57.4; 54.2% female) contributed to the primary all-cause mortality analysis and seven to CVD mortality. The pooled hazard ratio per 10-point higher LE8 score was 0.82 (95% CI 0.79–0.84; I^2 = 58.1%) for all-cause mortality and 0.76 (95% CI 0.70–0.82; I^2 = 86.5%) for CVD mortality. Results were robust in sensitivity analyses. Across outcomes with limited studies precluding meta-analysis, higher LE8 scores were consistently associated with lower risks of CVD, coronary heart disease, myocardial infarction, stroke, heart failure, atrial fibrillation, diabetes, and vascular dementia, while in studies on Alzheimer's dementia reported no significant associations.

Conclusion: Higher adherence to LE8 was consistently linked to lower risks of all-cause and cardiovascular mortality and several major non-communicable diseases, underscoring its value as a comprehensive framework for prevention. Future research should focus on diverse and underrepresented populations and clarify the contributions of individual LE8 components to guide targeted interventions.

PROSPERO registration: CRD420251005997

Alice Vincenzi

G-protein coupled receptors (GPCRs) are membrane proteins essential for cell signalling and can form homo- and heteromers, involved in both physiological and pathological processes. Dopamine Receptor (DR, Class A GPCR) homomerization dysfunction is linked to brain disorders like schizophrenia, drug addiction and anxiety. Detailed investigation into their heteromerization with other GPCRs could improve our basic understanding of GPCR function, disease mechanisms and potentially support the development of new treatment strategies.

This project therefore aims to systematically characterise the interactions between the long and short variants of the DR2 with different GPCRs. For this purpose, we have developed a Bioluminescence Resonance Energy Transfer (BRET)-based screening assay platform to investigate GPCRs proximity in a heterologous expression system.

Using this DR2-DR2 biosensor interaction assay, in which a reduction in BRET signal indicates disruption of DR2 biosensor proximity, we confirmed the assay with several GPCRS, which are already known to interact with DR2. In addition, we identified previously unreported GPCR interaction partners that modify DR2 proximity, including Muscarinic Acetylcholine Receptor M3 and Alpha2A-Adrenergic Receptor. We further observed differences in the interaction profile for the long and short DR2 splice variants, suggesting isoform specific interaction patterns. Ongoing work focuses on i) expanding the DR2 interaction assay to the 100 top co-expressed GPCRs across the 10 brain cell types with highest DRD2 expression, ii) confirm interaction using additional proximity and physical interaction based assays, and iii) determine how selected interaction partners modify downstream signaling, in-vitro and ex-vivo.

Differences in the assessment of rating scales in HD patients and relatives: influence of anosognosia, depression and executive dysfunction

Katarína Schwarzová

Background: The Unified Huntington's Disease Rating Scale (UHDRS) assessed motor, cognitive, neuropsychiatric and functional symptoms in Huntington's disease (HD). The Total Functional Capacity Score (UHDRS-TFC) assesses abilities in the areas of work, finances, housework, daily life and care needs on a scale from 0 (severely impaired) to 13 (fully functional). The Independence Scale (UHDRS-IS) measures overall dependence on a scale from 0 to 100, with higher scores indicating greater independence. Both scales are commonly used in clinical trials and for disease staging. The Problem Behaviours Assessment Short Form (PBA-s) assesses neuropsychiatric symptoms in Huntington's disease, such as depression, apathy, irritability and compulsive behaviour, by evaluating their frequency and severity.

Anosognosia, an impaired self-assessment of one's own symptoms, affects several areas of Huntington's disease, including motor, cognitive, emotional and functional abilities. Anosognosia varies in severity depending on the symptom area and stage. Partners or carers often report more severe symptoms than patients themselves admit to. This discrepancy affects the reliability of patient-reported outcomes, including assessments of depression and anxiety.

As these scales are important endpoints in clinical trials, it is important to examine the differences between patient and family member/caregiver assessments and the role of anosognosia, executive dysfunction, and depression in shaping these assessments.

Objectives: The primary objective of the study is to compare the results of the TFC, IS, and PBA-s scales between two groups – HK patients and their companions – to evaluate potential differences.

Methodology: Fifty patients with genetically confirmed Huntington's disease (HD) will be recruited from the Chorea Outpatient Clinic at the University Clinic for Neurology in Innsbruck. After written consent has been obtained, examinations will be carried out at baseline and after 6, 12 and 18 months as part of routine follow-up care.

Sociodemographic and disease-related data will be collected at baseline; medication will be updated at all visits. Standardised clinical scales will be used at all appointments (UHDRS-TFC, UHDRS-IS, PBA-s). Patients and relatives complete the Anosognosia Scale separately; additional scales for secondary endpoints (UHDRS-TMS, Mini-Cog, FAB bedside screening for executive functions, Hospital Anxiety and Depression Scale, Symbol Digit Modalities Test) are completed by patients only.

Expected results: There are significant differences in the assessment results of the TFC, IS and PBA-s assessments used between the responses of Huntington's patients and those of accompanying family members/caregivers. These differences are due to the presence of anosognosia and/or executive dysfunction, but not to self-reported anxiety or depression.

Conclusions: The study aims to provide insights into differences between patient and family member assessments in Huntington's disease and to shed light on the role of anosognosia and executive dysfunction in this context. The results could contribute to improved interpretation of functional and neuropsychiatric endpoints in clinical practice and research.

Julian Fenkart

Activation of Toll-like Receptor 8 (TLR8) expressed in mouse hippocampal neurons modulates neuronal excitability

Toll-like receptors (TLRs) are key components of the innate immune system. As pattern-recognition receptors (PRRs), they detect danger signals derived from pathogens (PAMPs) and from stressed or dying host cells (DAMPs), activating signaling cascades that promote pro-inflammatory cytokine production. While their functions in immune cells are well established, their roles within the central nervous system, particularly in neurons, remain poorly understood.

Previous studies have suggested that TLRs may contribute to neurodegenerative disorders such as Alzheimer's disease, where abnormal protein aggregates and DAMP release can trigger neuroinflammation. Moreover, recent evidence links TLRs to epilepsy, where dysregulated TLR signaling may enhance neuronal excitability and seizure susceptibility. Therefore, understanding the interplay between TLRs, DAMPs, and neuronal function could provide valuable insight into neurological disease mechanisms.

In this study, we investigated the function of Toll-like receptor 8 (TLR8) in neuronal excitability using mouse postnatal hippocampal cultures. TLR8 expression was analyzed by immunocytochemistry, neuronal activity was recorded via high-density multi-electrode arrays (MEAs), and downstream signaling was assessed by immunoblotting. We detected the expression of both TLR8 and the related receptor TLR7 in postnatal hippocampal neurons at DIV14. TLR8 showed broad localization in the soma and dendrites, extending beyond endosomal compartments, and was present in GABAergic parvalbumin-positive interneurons. Upon stimulation with the selective TLR8 agonist TL8-506, we observed an increase in neuronal activity in the short term, as well as enhanced neuronal synchronization in both short- and long-term recordings. Furthermore, we found that neuronal activity induced by TLR8 stimulation could be abolished by blocking NMDA receptors with the antagonist D-AP5. While short-term TLR8 stimulation resulted in MAPK phosphorylation, IkB-a degradation was not induced within the tested timeframe.

Our findings demonstrate that both TLR8 and TLR7 are expressed and functional in postnatal hippocampal neurons. Selective activation of TLR8 enhances neuronal excitability and engages MAPK signaling, potentially through modulation of NMDA receptor function or altered inhibitory control by parvalbumin interneurons. These results reveal a novel role for TLR8 in neuronal signaling and highlight new links between innate immune mechanisms and neuronal excitability.

Day 1 Poster Nr. 130

I am from clinical PhD Program presenting poster with Gender Aspect correlated to my study.

Marta Konopka

Background:

Age-related hearing loss (ARHL) is a highly prevalent sensory disorder in the elderly and is increasingly linked to vascular dysfunction, chronic inflammation, and metabolic stress. While biological sex is a major determinant of ARHL risk and progression, the underlying vascular and immune mechanisms remain incompletely understood, particularly in human tissue.

Methods:

Postmortem human arterial and cochlear tissues from elderly donors were analyzed to investigate vascular, inflammatory, and immune-related alterations associated with ARHL, with a focus on layer-specific and sex-related patterns. Endothelial coverage (CD31), macrophage infiltration (CD68), advanced glycation end products (AGE), maximal intima thickness, and cochlear immune cells (Iba1) were quantified using histological and immunohistochemical approaches.

Results:

Endothelial CD31 expression showed substantial interindividual variability but no consistent sex-related differences, suggesting predominantly age-driven endothelial remodeling. CD68-positive macrophages and AGE accumulation displayed pronounced layer specificity, with highest levels in the adventitia, highlighting this compartment as a metabolically and immunologically active vascular niche. AGE burden increased with advancing age and metabolic background but did not differ by sex. In contrast, maximal intima thickness was significantly greater in male samples compared with female samples ($p = 0.048$), indicating increased focal structural vascular remodeling in males. In the cochlea, Iba1-positive immune cells in the stria vascularis exhibited a tonotopic gradient, increasing from apical to basal turns, with higher variability observed in female specimens.

Conclusion:

These findings demonstrate that vascular and immune alterations associated with ARHL are largely driven by aging and metabolic stress, while sex-related differences emerge selectively in inflammatory burden and structural vascular remodeling. This underscores the importance of considering both spatial vascular organization and biological sex when investigating mechanisms of age-related auditory decline.

fishersci.at

: +43 800-20 88 40

: **Bestellungen:**
fisherde-at.bestellungen@thermofisher.com

Angebote:
fisherde-at.anfragen@thermofisher.com

Ihr persönlicher **Ansprechpartner:**
ping.liang@thermofisher.com
+49 15123701150

- Ihr zuverlässiger Partner: 1 Million Produkte von 17.000 Herstellern mit nur einem Klick
- Nachhaltigkeitsprogramm: Gemeinsam verändern wir die Welt
- Fisher Scientific Edge Programm: Der Versand unserer beliebtesten Produkte erfolgt noch am gleichen Tag.
- Webshopping leicht gemacht: Entdecken Sie, was möglich ist.

Distributed by Fisher Scientific

Fisher Scientific (Austria) GmbH Big Biz B |Dresdner Straße 89 | 1200 Wien, Austria

fisher scientific
part of Thermo Fisher Scientific

Sex-related differences in mechanical ventilation during an experimental animal ex vivo lung perfusion model

Manuela Ranalter

Ranalter M.1, Abram J.1, Ponholzer F.2, Neuschmid M2, Mathis S.1, Spraider P.1, Martini J.1
1 Department of Anesthesia and Intensive Care Medicine, Medical University Innsbruck, Austria
2 Department of Visceral, Transplantation and Thoracic surgery, Medical University Innsbruck, Austria

Background

Ex vivo lung perfusion (EVLP) enables extended evaluation and potential therapeutic treatment of marginal donor lungs. Mechanical ventilation during EVLP represents a relevant intervention with possible deleterious effects due to ventilator-induced lung injury (VILI). Current EVLP protocols, e.g. the Toronto Protocol, recommend standardized ventilation including a tidal volume of 7 ml/kg, independent of biological sex.

However, sex-related anatomical and physiological differences in lung structure and mechanics may not be adequately addressed by standardized ventilation strategies.

Flow-controlled ventilation (FCV) actively controls inspiration and expiration, enabling individualized ventilation within lung mechanical limits.

This analysis aimed to explore whether individualized FCV during EVLP reveals sex-related ventilation differences.

Material and methods

At the initiation of EVLP, donor lungs were ventilated either using volume-controlled ventilation according to the Toronto protocol (tidal volume 7 ml/kg, respiratory rate 7/min, positive end-expiratory pressure (PEEP) 5 mbar) or individualized FCV adjusted based on dynamic lung compliance. Biological sex of the donor animals was recorded and considered in the analysis of ventilation parameters.

Results and discussion

Due to the limited sample size (n=6, 2 female and 4 male), no statistically robust conclusions regarding sex-specific differences could be drawn. Male data are presented as mean standard deviation; female data reported descriptively because only one female animal was included.

Descriptive analysis indicated that male donor lungs showed lower peak airway pressures, PEEP levels and reduced flow rates in the FCV group, whereas female donor lungs demonstrated higher static compliance under FCV.

Previous in vivo studies have shown that individualized ventilation strategies in women are associated with lower applied tidal volumes, potentially reflecting smaller functional lung volumes. (1) Standardized ventilation approaches do not take sufficient account of such differences, exposing female lungs to excessively high tidal volumes, increasing the risk of barotrauma or volutrauma. (2) These findings highlight the importance of ventilation strategies based on actual lung mechanics and support gender- and diversity-sensitive personalized transplant medicine.

In this experimental EVLP setting, individualized FCV may have implicitly accounted for sex-related differences by adapting ventilation to lung mechanics, thereby attenuating observable disparities between sexes.

Conclusion

This pilot animal study suggests that individualized FCV during EVLP enables lower ventilation pressures, reduced flow rates, and a tendency toward smaller tidal volumes. By adapting ventilation to individual pulmonary mechanical properties, FCV may implicitly capture sex-specific differences, contributing to gender- and diversity-sensitive strategies in lung transplantation. Such approaches may ultimately improve donor lung utilization and reduce waiting-list mortality.

(1) Spraider P, et al. Sex related differences in applied tidal volume with flow-controlled ventilation: a subgroup analysis. Minerva Anestesiol. 2024;90(11):997-1003.

(2) Nijbroek SG, et al. Sex difference and intra-operative tidal volume: Insights from the LAS VEGAS study. Eur J Anaesthesiol. 2021;38(10):1034-41.

Lukas Scherer

Background:

Cardio- and cerebrovascular diseases (CVD) are the most frequent cause of death and disability worldwide, emphasizing the need for primary prevention. An analysis of patients in Tyrol with TIA or ischemic stroke from the STROKE-CARD study (Böhme, Neurology 2019) has revealed that 80% of these patients had an inadequately treated risk condition prior to acute cerebral ischemia, elucidating the high number of preventable strokes. The prevalence of unfavourable lifestyle behaviours that have an additive negative effect on potential subsequent stroke, is expected to be even higher but their effect on common vascular risk conditions has to date not been adequately assessed. Additionally, even though numerous guidelines on primary prevention exist, evidence-based intervention programs are scarce.
Through INN.HEALTH, we aim to assess the effect of a structured single time-point health examination with health counselling on the improvement on vascular health after one year in a large cohort of Tyrolian adults of the general population.

Objectives:

Primary objective is to evaluate whether a one-time health assessment and –intervention (through pre-defined protocols) will affect overall vascular health evaluated through the Life's Essential 8 overall vascular health score.

Outcomes:
Primary outcome parameter:

Changes in Life's Essential 8 overall cardiovascular health (CVH) metric between baseline and follow-up examination.
Secondary outcome parameter:
Changes in individual components of Life's Essential 8: Diet, Physical Activity, Nicotine exposure, Body weight, Blood lipids, Blood glucose, Blood pressure and Sleep.

Population:

Sample size:
1000 planned (currently at >700, recruitment ongoing)
Inclusion criteria: Signed informed consent of subject, ≥ 18 years old and main area of residence in Innsbruck and Innsbruck Land

Exclusion criteria:
Suspension upon a court order or upon other legal processes or accommodation according to the Hospitalization Act, or appointment of a custodian, impaired power of judgment and current engagement in military or community service

Study procedures:

Four in-person visits, V1 and V2 as baseline with V3 and V4 as follow-up visits. During V1, informed consent will be obtained. V1 will encompass blood draws and urine sample collection for the adjacent biobank. During V2, several assessments will be performed: anamnesis interview (demographics, family history, medical history etc.),

anthropometry and blood pressure measurement, neurovascular ultrasounds. All these measures will be taken into account for a discussion between study personnel and each individual participant resulting in a one-time in-person health promotion intervention. Several exploratory assessments will additionally be performed.
At follow-up, 12 (±2) months later, procedures performed at baseline will be mirrored to assess the potential benefit of the aforementioned intervention on vascular health.
Statistical Analysis: Statistical analyses will compare the change in the Life's essential 8 overall cardiovascular health score In subgroup analyses, we will explore potential interactions between subgroup characteristics (e.g., age and sex) and the change in Life's Essential 8 score.

Results:
Intermediate statistical analyses will be performed either after completion of the baseline assessments or shortly prior to the Life Science event, as recruitment is currently still ongoing.

Lukas Kampik

Background: Fracture-related infection (FRI) and periprosthetic joint infection (PJI) represent major complications in orthopaedic surgery and are associated with high morbidity, repeated revision procedures, and substantial healthcare costs. The current diagnostic gold standard relies on intraoperative tissue cultures, which typically require several days for definitive results and exhibit limited sensitivity and specificity. This delay restricts real-time surgical decision-making. Hyperspectral imaging (HSI) enables spatially resolved, label-free spectral analysis and therefore offers a potential approach for intraoperative detection of infection-related biochemical and structural changes in bone.

Methods: An ex vivo human bone infection model was established using 120 trabecular bone chips obtained from 40 donors. 40 samples were inoculated with Staphylococcus aureus, 40 with Staphylococcus epidermidis, and 40 served as uninoculated controls. After incubation, bacterial suspensions were standardized to 10^6 CFU/mL, and 200 µL were applied to each bone chip to induce reproducible biofilm formation. Hyperspectral images were acquired in the Vis-NIR (500–1000 nm) and SWIR (1100–1700 nm) spectral ranges. Preprocessing included PCA-based masking, spatial binning (3 for Vis-NIR, 10 for SWIR), standard normal variate (SNV) normalization, Savitzky–Golay smoothing, and first- and second-derivative transformation. Supervised machine-learning models (kNN, PLS-DA, SVM, SIMCA) were trained on pixel-wise spectra. The dataset was split at the sample level into 90% training and 10% independent test sets, with all three hyperspectral measurements from each bone sample consistently assigned to a single set. Pixel-wise predictions were aggregated to object-level classifications using majority voting.

Results: Vis-NIR spectra showed stronger class-dependent differences between inoculated and uninoculated bone than SWIR. In binary classification (inoculated vs. uninoculated), the best Vis-NIR models achieved 99.58 % validation accuracy, compared with 93.54 % for the best SWIR model. In discrimination between S. aureus and S. epidermidis, Vis-NIR PLS-DA reached 96.52 % accuracy, whereas SWIR kNN reached 81.99 %. In three-class classification (uninoculated, S. aureus, S. epidermidis), Vis-NIR kNN achieved 95.68 % accuracy compared with 88.04 % for SWIR.

On independent samples, Vis-NIR-based object-level classification achieved 100.00 % accuracy for inoculated versus uninoculated bone and 95.83 % accuracy for differentiating S. aureus from S. epidermidis. In the multiclass task, Vis-NIR kNN classified all samples correctly (100.00 %). In contrast, SWIR-based models showed lower accuracy (83.33% for binary classification and 75.00% for pathogen differentiation) and substantial misclassification of S. aureus.

Conclusion: This ex vivo study shows that hyperspectral imaging of human bone, combined with supervised machine learning, enables differentiation between inoculated and uninoculated samples and between Staphylococcus aureus and Staphylococcus epidermidis at a defined inoculum of 10^6 CFU/mL. Across pixel-wise and object-wise analyses, Vis-NIR consistently outperformed SWIR in all classification tasks, including independent test samples. The findings demonstrate that Vis-NIR-HSI captures infection-related spectral signatures in trabecular bone under highly standardized laboratory conditions. However, the homogeneous biofilm distribution in this ex vivo model, the use of majority-vote object classification, and the absence of blood, soft tissue, and other sources of intraoperative spectral and geometric variability, together with HSI's sensitivity to illumination and acquisition geometry, limit direct transferability to heterogeneous surgical environments.

Sex-specific aspects in CT-guided lung biopsy: A retrospective analysis of 100 patients

Maximilian Lutz

Background:

Intrapulmonary lesions are frequently detected in routine imaging and pose a substantial clinical challenge due to their potential malignancy. Percutaneous CT-guided lung biopsy is a well-established method for tissue acquisition, which is essential for further decision-making. However, the procedure is associated with complications, most commonly pneumothorax. Data on sex-specific differences in complication rates following CT-guided lung biopsy remain limited. This study aimed to investigate sex-specific aspects of these procedures, with a particular focus on the occurrence of postinterventional pneumothorax.

Methods:

We retrospectively analyzed 100 consecutive patients who underwent CT-guided lung biopsy under general anesthesia between August 2024 and March 2025. Baseline characteristics and comorbidities were extracted from medical records, while procedural parameters and postinterventional complications were assessed using preexisting imaging data. Standard post-biopsy imaging included a CT scan immediately after the procedure, a follow-up CT within one to four hours, and a chest radiograph on the following day. Continuous variables were compared between male and female patients using t-tests for independent-samples or Mann–Whitney U tests, depending on data distribution, while categorical variables were analyzed using chi-square tests. Multivariable logistic regression was performed to identify independent predictors of postinterventional pneumothorax.

Results:

A total of 100 CT-guided lung biopsies were analyzed, including 56 male and 44 female patients. Male patients had a significantly higher body-mass-index compared to females (median 24.9 vs. 23.9 kg/m², p = 0.022), while no significant differences were observed for age, smoking status, or pulmonary function parameters. Coronary artery disease was more frequent in male patients (26.8% vs. 11.4%), without reaching statistical significance (p = 0.056). Other comorbidities, including hypertension, emphysema, and chronic obstructive pulmonary disease, were similarly prevalent in both sexes. A history of malignancy was documented in 65.5% of male and 79.5% of female patients (p = 0.122). Lesion volume showed a non-significant trend toward larger lesions in female patients (p = 0.074). Procedural characteristics, including needle entry angle, total and intrapulmonary tract length, number of biopsy cores, and procedure duration, did not differ between sexes. Overall pneumothorax rates within 48 hours after biopsy were comparable between male and female patients (42.9% vs. 54.5%, p = 0.246), although a trend toward a higher rate of pneumothoraces requiring chest tube placement was observed in males (19.6% vs. 6.8%, p = 0.067). In multivariable logistic regression analysis, emphysema emerged as an independent predictor of pneumothorax (OR 2.93, p = 0.019), whereas sex and procedural parameters were not independently associated with pneumothorax occurrence. With respect to histopathological outcomes, malignant lesions were more frequently diagnosed than benign findings in both sexes (malignant lesions 65.5% vs. 79.5%, p = 0.122), and adenocarcinoma represented the most common diagnosis in both groups.

Conclusion:

CT-guided lung biopsy demonstrated comparable safety profiles in male and female patients. Sex was not an independent predictor of postinterventional pneumothorax, whereas emphysema emerged as the main risk factor. These findings suggest that risk stratification should primarily focus on underlying lung pathology rather than patient sex.

Dilution coagulopathy

Cristina Alomar Domínguez

Acute traumatic coagulopathy (ATC) is an endogenous coagulopathy that develops immediately after severe trauma and is an independent predictor of morbidity and mortality. Early trauma-associated coagulopathy results from both endogenous mechanisms initiated at the time of injury and acquired factors related to resuscitation. These alterations arise from the interaction of tissue injury, hemorrhage, hypoperfusion, and inflammation. Severe trauma triggers activation of the protein C pathway, endothelial dysfunction, and dysregulation of coagulation and fibrinolysis.

Increasing evidence demonstrates significant sex-based differences in coagulation responses following severe trauma. Females consistently exhibit a more hypercoagulable phenotype than males, characterized by higher thromboelastography clot strength, reduced hyperfibrinolysis, and shorter clotting times. This profile is associated with lower transfusion requirements and, in some studies, improved survival. However, studies have also demonstrated a twofold increase in mortality among women presenting with ATC.

The aim of this study was to retrospectively analyze a trauma cohort to identify significant differences in treatment and outcomes between men and women admitted to the intensive care unit at the Innsbruck Medical University Hospital.

Laura Sammarco

The transport of correctly folded secretory glycoproteins out of the endoplasmic reticulum (ER) to the Golgi apparatus is enabled by the coat protein complex type II (COPII) vesicles. Soluble secretory proteins are sorted into these COPII vesicles via cargo receptors. This work aims at a better understanding of the intracellular function of two putative cargo receptors VIP36/LMAN2 and VIPL/LMAN2L. These are transmembrane L-type lectins, which interact with the glycoproteins via their luminal domain. Although identified more than 3 decades ago, we know very little about VIP36 and VIPL with respect to the proteins they interact and how they exit the ER. The first line of research focuses on trafficking of VIP36 and VIPL within the secretory pathway. Both the proteins have a potential cytoplasmic ER exit motif (FY) on their C-termini, while they present different C-terminal ER retrieval motifs: KR in VIP36 and RKR in VIPL. I used the Retention Using Selective Hooks (RUSH) system in combination with export/retrieval deficient mutants to deepen our understanding of how the trafficking is regulated. The potential role of FY motif as an ER export motif is supported by the slowdown of the export kinetics of the construct upon its substitution by alanines. We also investigated VIP36 and VIPL dependency on SEC24, the major cargo binding module within the COPII coat. Knockdown experiments targeting its four paralogs suggest a major involvement of SEC24A and SEC24B paralogs in the trafficking of both VIP36 and VIPL. The second area of work focuses on the search for cargos for both VIP36 and VIPL. In Immunoprecipitation-based approach is unlikely to reveal new cargos because the interaction of lectins with their clients is weak and transient. We therefore used a Mass Spectrometry based analysis of the secretome from VIP36-deficient HepG2 cells. The screen identified several potential cargos for VIP36, which are currently being validated and will be discussed at the meeting

Fibrosis Burden and Recovery in Virus-negative Inflammatory Cardiomyopathy

Fabio Fugger

Background:

Virus-negative inflammatory cardiomyopathy (ICM) carries an unfavorable prognosis. Randomized trials support immunosuppressive therapy (IST), yet a clinically meaningful proportion of patients does not benefit. IST carries a relevant risk of side effects, mediated by high-dose steroids and azathioprine. Existing predictors focus on immune activation such as Toll-like receptor 4 (TLR4) or anti-heart antibodies, whereas biopsy-based myocardial fibrosis remains insufficiently studied. Adding the prognostic and predictive value of myocardial fibrosis could help generate models selecting patients with high chance of response to IST.

Objectives:

We will conduct a monocentric cohort of adults with biopsy-proven virus-negative chronic inflammatory cardiomyopathy, treated with IST. The primary aim is to develop and internally validate a multivariable pre-treatment prediction model for IST response at 6 months, defined as a ≥10-percentage-point increase in LVEF.

Archived endomyocardial biopsies undergo Masson's trichrome staining with digital fibrosis quantification and immunohistochemistry for CD3+, CD45+, CD68+, HLA-DR, and TLR4, with paired changes calculated when a follow-up biopsy is available.

We will report on change in clinical, histology, imaging parameters and outcome from baseline to 6 months. The prediction model uses clinical and imaging variables, included in a multivariable logistic regression with bootstrap internal validation. Further, we will explore the effect of adding baseline ECG data using machine-learning approaches.

Endpoints:

The main modelling endpoint will be IST responder status at ~6 months. Further endpoints are sustained responder status at ~12 and ~24 months, plus New Yeark Heart Association (NYHA) improvement at ~6 months.

Imaging endpoints include echocardiography markers (ΔLVEF, ΔLVEDVi, ΔLVESVi, ΔGLS) and cardiovascular magnetic resonance (CMR) remodeling metrics including extracellular volume (ECV), native T1, native T2, and late gadolinium Enhancement (LGE) with serial changes where available.

Histologic endpoints include baseline inflammation markers and Δfibrosis on paired endomyocardial biopsies (EMBs).

The outcome endpoint is time to first event of all-cause death, heart transplantation (HTx), or durable left ventricular assist device (LVAD) within 24 months.

Expected Impact:

If baseline histologic fibrosis and a parsimonious multivariable model reliably predict IST response, clinicians can target therapy to likely responders and reduce avoidable exposure in non-responders, improving precision care in virus-negative ICM and prevent potentially serious adverse events.

Multimodal foundation models for outcome prediction in esophageal squamous cell carcinoma treated with chemoradiotherapy: an interim analysis of sex-specific clinical outcomes

Samuel Vorbach

Background & Purpose

Esophageal carcinoma represents a major global health burden. In 2020, approximately 604,000 new cases and 544,000 deaths related to esophageal cancer were reported worldwide (1). For locally advanced tumors, a multimodal treatment approach is recommended, which has been shown to improve prognosis and may also enable organ preservation (2, 3). This study aims to analyze patients who received neoadjuvant or definitive chemoradiotherapy (CRT) for esophageal squamous cell carcinoma with the objective of developing predictive models based on multimodal imaging (peritherapeutic CT scans, endoscopic imaging, and histological images) to enable individualized tumor characterization.

Methods

Patients with esophageal squamous cell carcinoma treated at four departments of radiation oncology were retrospectively identified. Eligible patients were required to have available pre-therapeutic diagnostic CT imaging, radiotherapy planning CT scans, and tumor biopsy material. Clinical data were extracted from medical records. Histological biopsy slides were digitized, and peritherapeutic CT datasets were collected. Endoscopic image and video material were reviewed to identify and extract tumor-containing frames. The primary endpoint was pathological complete response (pCR) for patients treated with neoadjuvant CRT. Secondary endpoints included progression-free survival (PFS) and overall survival (OS). OS was defined as the time from the last day of CRT to death or censoring at the last follow-up. PFS was calculated from the last day of CRT to death or disease progression according to RECIST version 1.1 (4), with patients censored at the last oncological follow-up without documented progression. PFS and OS were estimated using the Kaplan–Meier method. Sex-based differences in pCR rates were assessed using the chi-square test, while survival outcomes were compared using Kaplan–Meier analysis and log-rank testing.

Results

A total of 91 patients were included in the neoadjuvant treatment group, of whom 28 were women (30.8%). The most commonly applied radiotherapy regimen was 41.1 Gy delivered in 1.8 Gy fractions, administered in 67.0% of patients. The most frequently used concurrent chemotherapy regimen consisted of carboplatin (doses titrated to achieve an area under the curve of 2 mg per milliliter per minute) and paclitaxel (50 mg/m² of body-surface area), administered in 64.8% of patients. A total of 31 patients (34.1%) achieved a pathological complete response. No significant difference in pCR rates was observed between men and women (chi-square test, $p = 0.393$). Progression-free survival differed significantly by sex, with a median PFS of 597 days (95% CI: 363-831) in men and 3773 days (95% CI: 742-6803) in women (log-rank $p = 0.049$). OS differed significantly by sex, with a median OS of 1716 days (95% CI: 645-2787) in men, while median OS was not reached in women (log-rank $p = 0.035$).

Outlook

Multimodal foundation model analyses integrating radiomic features from CT imaging, pathomic features from digitized histology, and tumor-specific endoscopic images are currently ongoing. Prior to model training, data harmonization and normalization across different CT scanners and imaging protocols are being performed to ensure robust and comparable feature extraction for both neoadjuvant and definitive treatment cohorts.

Early Childhood Nutrition and Cardiovascular Development in Extremely Preterm Infants: Project Progress and Gender Perspectives of the NeoVasc Study

Lena Gatterer

Background:

Prematurity is a significant influencing factor for health and survival of children. Due to incomplete development in the womb, prematurity can lead to underdevelopment of multiple organ systems, including the cardiovascular system. Consequently, extremely premature infants have a higher risk of cardiovascular and metabolic diseases. Therefore, one of the key aspects in research is to find protective factors for the development of the cardiovascular system. In the investigation of the influence of nutrition on the development of the premature body, it was found that an exclusive feeding with human milk can improve neurological development. Similar to neurological development, the working hypothesis suggests that the cardiovascular development can be positively influenced by exclusive feeding with human milk. The addition of gender-related medical aspects permits the identification of gender-specific differences and supports the development of individualized, gender-sensitive treatments for preterm infants.

Material and Methods:

The NeoVasc Study is a multicentric, prospective, randomized, open, parallel group clinical trial which is performed in the four neonatal care facilities of Innsbruck, Vienna, Salzburg and Feldkirch. The study group consists of 202 extremely preterm infants, born before 28 weeks' gestation, with a birth weight between 500 g and 1,250 g. The children were randomized into two intervention groups, one group received the human-based fortifier until 32 weeks' gestation, the other group received the human-based fortifier until 36 weeks' gestation. The control group consists of 100 term-born children without any cardiovascular diseases. Two follow-up assessments have already been performed at 1 and 2 years of corrected age. The third stage of the study is currently in data collection and involves a comprehensive examination at 5 years of age. The examination includes an echocardiography, anthropometric measurements, a blood test, a food frequency questionnaire as well as a developmental assessment.

Project progress:

As part of an interim analysis, initial results were collected for the two intervention groups. Statistical analyses were conducted for the basic data and the first two follow-up assessments and including first echocardiographic results, the feed regimen at discharge, growth measurements, maternal pregnancy complications and the number of days with parenteral nutrition, including also any adverse events resulting from parenteral nutrition. Even though there are descriptive differences between the groups, the statistical analysis does not show any previous significant differences. These are expressly preliminary results, which will be updated and re-examined as further data are collected.

Conclusion:

The previous evaluations show no significant differences between the intervention groups. It remains to be seen whether nutritional effects on cardiovascular development and gender-specific differences in the context of gender-specific medicine may emerge during the further course of the study. The final results of the 5-year follow-up will be decisive.

DUAL ICP STUDY – Fundamental principles and changes

Is ICP transmitted uniformly within the cranium? An animal porcine study

Philipp Geiger

BACKGROUND: The skull is a rigid, non-expandable container that houses intracranial contents. Intracranial pressure (ICP) has classically been presumed to be uniformly transmitted throughout the cranium. However, emerging evidence suggests that the tentorium cerebelli creates a physical and functional barrier, potentially establishing distinct pressure gradients between supratentorial and infratentorial compartments. Understanding ICP transmission across cranial compartments is essential for improving clinical management of neurosurgical pathologies, including space-occupying lesions and intracranial hypertension.

METHODS: An in vivo porcine model was employed to investigate ICP transmission under physiological and pathological conditions. Eighteen anesthetized domestic pigs (n=7 per group and 4 pilot pigs) received dual ICP monitoring probes positioned via burr holes in supratentorial (right frontal lobe) and infratentorial (right cerebellar hemisphere) locations. The physiological group underwent a systematic test battery comprising: (1) head-of-bed elevation to 20°, (2) hyperventilation, (3) hypoventilation, (4) induced hypertension, (5) induced hypotension, (6) intravenous propofol bolus (2 mg/kg), and (7) hypertonic saline bolus (10% NaCl, 100 ml). Each intervention was maintained for 10 minutes with continuous pressure monitoring. The pathological group underwent identical testing with the addition of a 3 ml saline-filled balloon catheter placed in the left infratentorial space to simulate mass effect before intervention testing.

RESULTS: Analysis of supratentorial and infratentorial pressure responses revealed a consistent pressure differential between the two compartments across both study groups. This fixed pressure difference persisted despite various physiological and pharmaceutical perturbations, suggesting that ICP transmission across the tentorium is neither uniform nor freely communicating.

CONCLUSION: These preliminary data support the hypothesis that intracranial pressure is not uniformly distributed within the cranial vault and that the tentorium creates functionally distinct pressure compartments. Further analysis of the complete dataset will elucidate the magnitude of pressure gradients under physiological and pathological conditions and may inform clinical strategies for ICP management in compartmentalized intracranial pathology.

A 3D-bioprinted Mesothelium-on-Chip to uncover Ovarian Cancer Invasion Behavior

Verena Sturmlehner

Ovarian cancer (OvCa) is the fifth-common cause of cancer death and has a 5-year survival rate of about 50%. One reason for its high mortality rate is the occurrence of multicellular aggregates in the ascites of more than 50% of OvCa patients. These spheroids are most likely a cause for metastasis and relapse. Xenograft, syngeneic and genetically engineered mouse models have been described for OvCa, but none of them allow a direct investigation of the human situation of OvCa-spheroid invasion into mesothelium.

Using 3D-bioprinting, we developed a unique in vitro system for studying OvCa-spheroid mesothelium interaction, the Mesothelium-on-Chip. Read-out methods like fluorescence imaging with measuring the area of invasion and OvCa sphere size, as well as surface profiling were implemented for this model. We investigated the invasion behavior of different OvCa cell lines and were able to show inhibition of their invasion potential with different treatment options.

This model will replace animal experiments in OvCa research and allow us to better understand the role of mesothelium and tumor spheroids in OvCa disease progression. It will assist to predict patient's therapy response using ascites-derived multicellular aggregates and has unmet potential for testing novel therapeutics in a human, organotypic system to improve patient-tailored therapy.

MitraSCORE: Enhancing Surgical Decision-Making in Secondary Mitral Regurgitation Through Mortality Risk Prediction

Ronja Lohmann

Objectives: Mitral valve (MV) disease shows sex-specific differences in morphology and outcomes. Women often present later, undergo replacement more frequently, and experience worse survival. This study investigated sex-related disparities in surgical approach, repair rates, and outcomes of MV surgery.

Methods: A total of 1531 consecutive patients undergoing MV surgery with or without concomitant tricuspid valve procedure were analysed retrospectively. Baseline characteristics, operative strategies, and outcomes were compared between sexes. Propensity score matching was used to adjust for baseline differences. Primary outcomes were 30-day and 5-year mortality. Baseline and procedural characteristics, including morphology, repair rates, use of minimally invasive MV surgery (MIMVS), and concomitant tricuspid disease, were compared between groups.

Results: Female patients (44%) were older (68 vs 62 years, $P < .001$), more symptomatic (New York Heart Association [NYHA] III: 60% vs 46%, $P < .001$), and more likely to have annular calcification (15% vs 5%, $P < .001$) or concomitant tricuspid disease (25% vs 36%, $P < .001$). Carpentier type IIIa was more prevalent in women (21% vs 4%), while type II predominated in men (75% vs 49%). MIMVS and repair were less frequent in women (49% vs 65% and 67% vs 85%, both $P < .001$). Female sex was associated with increased 30-day (HR 4.07, 95% CI 1.51-11.0; $P = .006$) and 5-year mortality (HR 1.58, 1.02-2.46; $P = .043$). After adjusting for morphology and calcification, sex was no longer an independent predictor of repair rates or long-term mortality.

Conclusions: Women present at a later stage of the disease and with more complex MV pathology, resulting in lower repair and MIMVS rates and higher perioperative mortality. These disparities are largely attributable to disease morphology rather than sex per se. Earlier referral of women is essential to improve outcomes.

Sex-Specific Differences in Intracranial Arterial Calcifications: A Retrospective Cross-Sectional Observational Study

Philipp Deisl

Authors and Affiliation
Philipp Deisl 1,2,3, Stephanie Mangesius 1,2, Astrid E. Grams 1,2, Elke R. Gizewski 1,2
[1] Department of Radiology, Medical University of Innsbruck, Anichstrasse 35, 6020 Innsbruck, Austria.
[2] Neuroimaging Research Core Facility, Medical University of Innsbruck, Anichstrasse 35, 6020 Innsbruck, Austria.
[3] VASCage, Centre on Clinical Stroke Research, 6020 Innsbruck, Austria.

Introduction
Intracranial arterial calcification (IAC) is a common finding on CT and CTA scans during routine diagnostic workups in stroke patients and has been associated with adverse cerebrovascular outcomes. Sex-related differences in atherosclerosis are well recognized, which may suggest a potential factor in the development and extent of IAC. However, data on sex-specific differences in the context of prevalence, distribution, and volume of IAC are scarce.

Patients and methods
We conducted a retrospective cross-sectional observational study including patients with at least one cerebrovascular event, such as transitory ischemic attack or ischemic stroke, admitted to the stroke unit of a tertiary center between 2010 and 2023. IAC (prevalence, distribution, volume) was analyzed on CTA images at the time of the first cerebrovascular event using open-source 3D-Slicer Software. Due to their right-skewed distribution and to deal with values of zero, volumetric measurements were transformed using the formula log10(volume + 1). Sex-specific differences in prevalence and calcification volume were assessed using the chi-square and Mann-Whitney U test, as well as univariable and multivariable models.

Results
A total of 556 eligible patients with at least one cerebrovascular event were included (36% female, median age 71.5 years). IAC prevalence in any assessed vessel, irrespective of their calcification volume, was observed in 73% (74% males, 72% females) and did not differ significantly between males and females ($p = 0.52$). However, a significant sex-specific association was observed in the vertebrobasilar territory, with males having a higher prevalence (20% vs. 12%; $p = 0.01$). In the univariable linear regression models, female sex was associated with lower vertebrobasilar calcification burden (standardized $\beta = -0.091$; $p = 0.032$). This was confirmed in the multivariable linear regression model (standardized $\beta = -0.123$; $p = 0.004$). No significant sex-specific difference was found in the anterior circulation (standardized $\beta = -0.063$; $p = 0.09$). Total IAC volume was also significantly associated with lower calcification volumes in females (standardized $\beta = -0,072$; $p = 0.049$).

Conclusion
In this retrospective cross-sectional observational study, males exhibited a significantly higher prevalence of vertebrobasilar calcifications. In territory-specific linear regression models, female sex was associated with lower vertebrobasilar calcification volume, whereas no independent sex-specific association was found in the anterior circulation. The borderline association with total intracranial arterial calcification volume appears to be primarily driven by vertebrobasilar calcification volume. These findings suggest that heterogeneous sex-related associations exist across intracranial

vascular territories, with a more pronounced contribution in the vertebrobasilar circulation.

Further studies are warranted to elucidate the underlying mechanisms and clinical implications of these territory-specific sex differences.

Anto Abramovic

Introduction

Preoperative assessment of bone quality is becoming increasingly important due to rising surgical volumes in elderly patients and their associated comorbidities. The value of the "gold standard" DXA has been questioned and may not sufficiently reflect the surgically targeted vertebral bodies. Therefore, the aim of this study was to evaluate the clinical utility of Hounsfield Units (HU) from routine CT scans in estimating the trabecular bone structure and mechanical stability of lumbar vertebrae.

Material and Methods

In an ex-vivo study, 65 lumbar vertebral bodies (L1–L5) from 53 human donors (mean age 73.0 ± 10.5 years; 22 females) were analyzed; twelve specimens were excluded based on predefined criteria. HU values were measured using routine CT (according to Schreiber et al.), followed by qCT to determine volumetric bone mineral density (vBMD). Cylindrical cores (20 mm × 15 mm) consisting of trabecular bone were extracted and embedded in PMMA. The cores were then subjected to biomechanical testing using axial loading to determine their load to failure (LOF) and linear stiffness (LS).

Results

Osteoporosis was defined using qCT (vBMD < 80 mg/cm³); 27 vertebrae (51%) met this criterion. With the used CT scan setting this corresponded to a HU value of 130. Non-osteoporotic vertebrae exhibited higher mean LOF (527 N vs. 319 N; ΔLOF ≈ 208 N; $p < 0.001$; $d > 1.5$). HU values correlated significantly with LOF ($R^2 = 0.513$; $p < 0.001$).

Stiffness of the trabecular bone was also significantly reduced in osteoporotic samples (3.06 N/mm vs. 1.86 N/mm; $p < 0.001$; $d = 1.54$). HU values showed a strong positive correlation with stiffness in regression analysis ($R^2 = 0.507$; $p < 0.001$).

Split-sample validation showed moderate generalizability of the HU-based model (R^2 training: 0.517; test: 0.366), with expected performance decline due to sample size and the simplicity of a single-parameter model.

Conclusion

HU values from standard CT scans correlate well with both mechanical strength and stiffness of lumbar vertebral bodies and represent a practical, imaging-based tool for preoperative assessment of bone quality in spine surgery.

Daniel Pavluk

Background

Periodic repolarization dynamics (PRD) is a novel ECG-derived biomarker reflecting sympathetic activity–associated oscillations in cardiac repolarization. We hypothesized that elevated PRD identifies patients after acute ischemic stroke (AIS) who are at increased risk of developing atrial fibrillation detected after stroke (AFDAS).

Methods

Between February 22, 2021, and May 5, 2023, 263 patients with AIS from the STROKE-CARD cohort were prospectively enrolled. All patients were in sinus rhythm at baseline without prior or current atrial fibrillation (AF). Within 5 days after AIS, patients underwent a standardized 30-minute high-resolution ECG to assess PRD, heart rate variability, and supraventricular premature complexes (SPCs/hour). AFDAS was identified through continuous in-hospital monitoring, 6-month follow-ups, and electronic health record review. The CHASE-LESS score served as the clinical risk model for AFDAS.

Results

During a median follow-up of 19 (IQR 14) months, AFDAS occurred in 25 of 263 patients (9.5%). Patients with AFDAS exhibited higher PRD values than those without (5.80 vs. 2.93 deg^2, $p = 0.005$). In multivariable Cox regression, PRD independently predicted AFDAS (HR 1.27, 95% CI 1.03–1.44, $p = 0.037$), alongside SPC frequency (HR 1.02, 95% CI 1.01–1.03, $p < 0.001$). A model comprising PRD and SPC per hour showed better discrimination than the CHASE-LESS score alone, with an AUC of 0.82 versus 0.67 respectively, $p = 0.005$.

Conclusions

Increased PRD and SPC frequency independently predict AFDAS and significantly improved risk prediction compared to the clinical CHASE-LESS score.

Association of Serum Ferritin with STEMI

Alex Kaser

Background: Persistent infarct core iron (PICO) after hemorrhagic ST-elevation myocardial infarction (STEMI) is associated with chronic myocardial inflammation, adverse remodeling and worse clinical outcome. However, the pathophysiology and determinants of PICO are incompletely understood.

Aim: To investigate the association between biomarkers of systemic iron status measured in the acute and chronic post-infarction phases and PICO following STEMI.

Methods: STEMI patients treated with primary percutaneous coronary intervention and enrolled in the prospective Magnetic Resonance Imaging in Acute ST-Elevation Myocardial Infarction study (MARINA-STEMI, NCT04113356) were included. Serum markers of iron metabolism (serum ferritin, iron, transferrin and transferrin saturation (TSAT)) were serially measured at hospital admission for index STEMI and at 4-months follow-up (4FU). Presence of PICO was measured on T2* magnetic resonance imaging (MRI) mapping at 4FU.

Results: In total, 442 patients (median age 59 [IQR: 53-67] years, 20% female) were analyzed. PICO was observed in 91 (21%) patients. While serum iron, transferrin and TSAT levels did not show a significant association with PICO, serum ferritin concentrations at hospital admission (271 [194-465] µg/L vs. 205 [127-365] µg/L, p<0.01) and at 4FU (221 [128-305] µg/L vs. 167 [81-256] µg/L, p<0.01) were significantly higher in patients with PICO than in those without PICO. The associations of serum ferritin concentrations with PICO remained significant after adjustment for biomarkers of inflammation, cardiac injury and wall stress both at admission (Odds ratio (OR) 1.94 [95% confidence Interval (CI), 1.03-3.64]; p=0.04) and at 4FU (OR: 2.18 [95% CI: 1.22-3.89]; p<0.01), as well as after adjustment for MRI-derived measures of cardiac function and injury at admission (OR 2.84, [95% CI: 1.48-5.47]; p<0.01) and at 4FU (OR 2.28, [95% CI: 1.36-3.83]; p<0.01).

Conclusions: In patients with STEMI, both acute and chronic serum ferritin concentrations were significantly and independently associated with PICO. These findings suggest a pathophysiological link between systemic ferritin and irreversible myocardial iron deposition following STEMI.

Pauline Alton

A novel exon 32* variant of CaV1.3 is predominantly expressed in mouse sinoatrial node and atria

Pauline Alton1, Simone Pelizzari1, Hajar El-Aouad1, Pietro Mesirca2, Matteo E. Mangoni2, Marta Campiglio1

1Institute of Physiology, Medical University Innsbruck, Innsbruck, Austria

2Institut de Génomique Fonctionnelle, Université de Montpellier, CNRS, INSERM, Montpellier, France

L-type CaV1.3 channels are unique within the high-voltage activated Ca2+ channel family, as they activate at the most negative potentials and exhibit fast activation and rapid calcium-dependent inactivation. These channels are widely expressed in the brain and peripheral organs, with their expression and regulation finely tuned to meet specific physiological demands. Post-transcriptional mechanisms, such as alternative splicing and RNA editing, contribute to their molecular and functional diversity, modulating Ca2+ signaling in various cell types. While at least 14 alternatively spliced exons of CaV1.3 have been identified, little is known about their tissue-specific expression, regulation, and impact on channel gating. In the heart, CaV1.3 channels are expressed in the sinoatrial node (SAN), atria, atrioventricular (AV) node, but are absent in adult ventricles. In the SAN, the CaV1.3-mediated L-type calcium current (ICav1.3) plays a major role in diastolic depolarization, influencing heart rate and AV conduction, while in the atrium ICav1.3 contributes to regulation of action potential duration. Here, we cloned CaV1.3 from cDNA derived from mouse atria and the SAN to identify splicing isoforms specifically enriched in each cardiac chamber. We characterized 1b8b-Δe11 as the predominant isoform in the SAN, and 1a8a-Δe11 as the predominant atrial isoform. Additionally, we identified a novel, unreported exon 32, hereby referred to as 32*, which was included in 100% of cloned SAN 1b8b-Δe11 transcripts and in the majority of 1a8a-Δe11 transcripts in the atria. Electrophysiological measurements show that the inclusion of exon 32* leads to a left-shift in both the voltage-dependence of activation and inactivation, thus leading to earlier activation during the action potential. This newly identified splice variant therefore appears to be functionally tailored for the SAN, by supporting its role in spontaneous activity and maintain reliable pacing at rest.

Mateus Enzenberg

Design and Preliminary Validation of an In-Vitro Elbow Joint Simulator for Quantitative Assessment of Injury-Related Kinematics

Introduction:

Elbow injuries can alter joint motion and affect upper limb function. Understanding these effects supports decisions on the need for surgical intervention and rehabilitation planning. Existing test setups that aim to identify such changes often lack the ability to produce repeatable physiological motions or to assess joint behavior under controlled, dynamic loading. In vitro simulators that apply controlled muscle-driven actuation offer a platform to study elbow kinematics under defined and reproducible conditions.

Methods:

An active elbow joint simulator was developed to reproduce elbow flexion and extension by applying physiologically driven muscle forces. Fresh-frozen human cadaveric upper extremities were prepared with preservation of the joint capsule, collateral ligaments, and interosseous membrane. Tendons were connected to electromechanical actuators via high-strength braided suture strands routed along anatomical paths. Actuators were controlled using a cascaded strategy based on estimated muscle forces and activation profiles, with integrated elastic elements to more closely mimic physiological muscle behavior. The humerus was rigidly mounted, while the ulna and radius were free to articulate. Joint kinematics were captured using an angle sensor attached to the wrist. Dynamic flexion/extension cycles from 0° to 120° were performed at defined forearm rotations and under different external loading directions. Following intact testing, a standardized radial neck osteotomy was performed to simulate a proximal radial head/neck fracture and enable preliminary evaluation of injury-related kinematic changes.

Results:

The simulator reproduced controlled elbow flexion between 0° and 120° while maintaining forearm orientations at neutral, pronated, and supinated targets. Rotational positioning remained within ±3° of the intended angles. Muscle force trajectories were highly repeatable across cycles. After radial neck osteotomy, specimens demonstrated comparable flexion profiles, while increased rotational deviations were observed, suggesting that the system can detect changes in forearm motion associated with the simulated injury state.

Discussion:

The designed and constructed simulator was capable of producing consistent, repeatable elbow motion while enabling continuous measurement of joint kinematics and muscle forces under dynamic conditions. Intact testing demonstrated stable control of flexion and forearm orientation. The injured configuration showed altered rotational behavior, indicating sensitivity of the setup to changes in joint mechanics. Ongoing work focuses on testing multiple specimens and applying controlled injury scenarios and external loading conditions to further investigate clinically relevant elbow pathologies.

Dagmar Morell Hofert

Previous research has demonstrated suboptimal correlation between surgical and MRI #ENZIAN classification scores across different anatomical compartments, particularly in compartment T, as well as compartments A and B. This limitation highlights the need for alternative approaches to enhance preoperative MRI assessment accuracy in endometriosis evaluation in these compartments. MRI offers the potential for indirect detection of pelvic adhesions through systematic assessment of organ displacement and asymmetric anatomical positioning.

The primary objective of this investigation was to establish correlations between both pelvic MRI and operative findings (dichotomized mr#ENZIAN and op#ENZIAN scores) and specific imaging parameters indicative of adhesive disease (asymmetric ovarian positioning within the pelvis, uterine retroflexion/-version and lateral deviation of the uterus). The secondary objective was to investigate volumetric effects caused by larger and/or infiltrative endometriotic lesions, examining how space-occupying endometriotic masses influence surrounding organ positioning and pelvic anatomy. Finally, we analysed ovarian size variations and intra-pelvic positioning patterns in relation to endometriotic involvement, recognizing that ovarian endometriosis can alter both ovarian dimensions and their spatial relationships within the pelvis.

This comprehensive approach may provide valuable supplementary information to traditional #ENZIAN scoring methods.

EVIDENT

Faster, Smarter, Clearer Imaging

FLUOVIEW™ FV5000 Confocal and Multiphoton Laser Scanning Microscope

Push the boundaries of microscopy further than ever before. Built on Evident's renowned optical expertise, the FLUOVIEW FV5000 is redefining the boundaries of confocal and multiphoton imaging with extraordinary clarity, speed, and reliability.

For more information, visit:
EvidentScientific.com/FV5000

Emanuel Vogel

Background: Acute myeloid leukemia (AML) shows a significant gender-specific differences in incidence, pathobiology, and survival. While modern medicine relies mostly on molecular markers, biological sex and socioeconomic factors often remain unconsidered as independent variables. The aim of this abstract is to draw attention to and compile current data on molecular profiles and healthcare realities in order to evaluate the need for gender-specific risk stratification.
Methodology: A literature review of epidemiological registry data (including HCUP NIS, French longitudinal studies), large-scale genomic studies (Alliance, AMLCG, Beat AML, TCGA), and pharmacokinetic reviews was conducted. The focus was on the correlation of gender and socioeconomic status (SES) with mutation profiles, treatment response, and hospitalization rates.
Results: Epidemiology and socioeconomic factors: There is a global "male disadvantage" with significantly higher hospitalization rates among men (up to 33.8 per 10,000 in the 60–79 age group), with the difference being most pronounced in young adults (18–39 years). Socioeconomic analyses show that low SES correlates with poorer overall survival. However, this is not mainly due to a lack of access to intensive care, but rather to the circumstance that patients with low SES are more likely to present with unfavorable biological tumor characteristics (e.g., secondary AML) and advanced stages of disease, as well, suggesting structural barriers to early diagnosis. In addition, women are diagnosed significantly later due to more nonspecific symptoms. Molecular divergence: Biologically, men and women show different leukemogenesis pathways. Women show a dominance of mutations in the NPM1-DNMT3A-FLT3 cluster and WT1. Specifically, the FLT3-ITD mutation has a significantly worse prognostic effect in women than in men, which necessitates gender-adjusted weighting of this marker. Men, on the other hand, show an accumulation of high-risk mutations in ASXL1, RUNX1, KIT, and spliceosome genes (SRSF2, U2AF1). In particular, TP53 mutations, which are associated with complex karyotypes, chromothripsis, and altered telomere maintenance, occur more frequently in men and are characterized by a particularly aggressive course. SF3B1 mutations have also been specifically identified as bad prognostic factors in men (<60 years).
Pharmacology and outcome: Despite less favorable genetics, women undergoing standard therapies suffer more frequently from severe side effects (e.g., cardiotoxicity, mucositis) due to systematic overdose based on body surface area (BSA) dosing, which neglects pharmacokinetic differences in distribution volume and clearance. Paradoxically, they often show better overall survival, which is attributed to more sensitive tumor biology.

Novel therapies such as CD33 CAR-T cells face the challenge that the aggressive kinetics of (more frequently male) relapsed AML complicate the time-critical production of autologous cell products.
Conclusion: AML is a bio-socially dimorphic disease. The male predominance in highrisk gene profiles (TP53, spliceosome) and female susceptibility to chemotoxicity, as well as specific drivers such as FLT3-ITD, require a transition from gender-neutral to genderadapted precision oncology. Clinical procedures must also take socioeconomic factors into account in order to minimize mechanisms that delay diagnosis in disadvantaged groups.

CGRP and PACAP in aneurysmatic subarachnoid hemorrhage

Lena Gufler

CGRP and PACAP in aneurysmatic subarachnoid hemorrhage

Background:

Aneurysmal subarachnoid hemorrhage (aSAH) is a severe form of acute brain injury associated with high mortality and long-term neurological morbidity. Among secondary complications, delayed cerebral ischemia (DCI) represents a major determinant of unfavorable outcome. DCI is defined as a primarily clinical syndrome characterized by secondary cerebral ischemia that cannot be fully explained by angiographic vasospasm alone, reflecting additional contributions from microvascular dysfunction and impaired cerebrovascular autoregulation. Early detection of DCI remains challenging, as neurological assessment is often limited in critically ill or sedated patients, and current diagnostic approaches show variable sensitivity and considerable inter-operator variability. This leads to a substantial unmet need for reliable, blood-based biomarkers that reflect cerebrovascular alterations and support early risk stratification after aSAH.

Calcitonin gene-related peptide (CGRP) and pituitary adenylate cyclase-activating polypeptide (PACAP) are neurovascularly active peptides involved in the regulation of cerebral blood flow and vascular tone. Alterations in circulating levels of these peptides have been reported after aSAH; however, systematic longitudinal data in human patients and their association with clinically defined DCI are limited. The objective of this study is therefore to characterize longitudinal CGRP and PACAP profiles during the acute and subacute phases after aSAH and to assess their association with the occurrence of DCI.

Methods:

This prospective biomarker study is conducted as a substudy of the TROYJA registry (Disease trajectories of acutely brain injured patients), an observational cohort and biobanking initiative at the Department of Neurology, Medical University of Innsbruck. Approximately 200 adult patients with confirmed aSAH will be enrolled consecutively. Arterial and venous blood samples will be obtained daily for up to 14 days after hemorrhage and again at a standardized 3 month follow up. CGRP and PACAP concentrations will be measured using validated laboratory assays following standardized protocols.

DCI will be defined according to established consensus criteria as a primarily clinical diagnosis; cerebral infarction on follow up imaging will be considered a radiological manifestation where applicable. The primary analysis will evaluate associations between longitudinal CGRP and PACAP trajectories and the occurrence of clinical DCI. Statistical analyses will include linear mixed effects models to characterize longitudinal changes in CGRP and PACAP concentrations over time. Associations with the occurrence of DCI will be assessed using multivariable logistic regression adjusted for established DCI risk factors. Secondary analyses will include group comparisons between patients with and without DCI, evaluation of associations with hemorrhage severity and cerebral infarction, exploration of sex specific effects, and assessment of relationships with short and long term functional outcomes.

Conclusion:

This study will generate a comprehensive longitudinal dataset on circulating CGRP and PACAP levels after aSAH in a well characterized clinical cohort. By integrating biomarker dynamics with detailed clinical and radiological data and focusing on clinically defined DCI, the findings may improve understanding of neurovascular alterations after aSAH and support the development of biomarker based strategies for risk stratification in future clinical studies.

Paul Petermann

The PIDDosome-p53 axis dictates cell fate after cell-cell fusion

In pathological cell-cell fusion events induced by viral or bacterial infections, asynchronous cells form multinucleated syncytia. These fusion events may contribute to pathogenesis and induce chromosomal instability, potentially promoting tumorigenesis. The cellular mechanisms preventing this are incompletely understood. Exploiting the ability of the vesicular stomatitis virus glycoprotein (VSV-G) to induce cell fusion of VSV-G-expressing cells in a pH-dependent manner, we provide evidence that the fusion of asynchronous cells triggers the activation of the PIDDosome multiprotein complex, resulting in caspase-2-mediated cleavage of MDM2, stabilization of p53, and upregulation of p21, which contributes to a reduced syncytial cell cycle progression. This process depends mainly on the recruitment of PIDD1 to clustered mature centrioles present after cell fusion, as centriole depletion, the application of centrosome declustering agents, and knockout of the centrosomal distal appendage protein ANKRD26 abrogate PIDDosome activation in this context. Moreover, the majority of multinucleated cells die within 72 h post-fusion, which is significantly delayed upon pan-caspase inhibition and in scenarios of caspase-9 deficiency and BCL2 overexpression, indicating that syncytial death is primarily induced by a MOMP-driven apoptosis. Interestingly, PIDDosome-deficient syncytia exhibit reduced survival rates, indicating a partially protective effect for PIDDosome signaling. In a second model, we studied infection events of Burkholderia thailandensis, a gram-negative bacteria that after invasion hijacks the host actin machinery to spread into neighboring cells, thereby inducing cell-cell fusion. By impairing bacterial growth using the bacteriostatic chloramphenicol to promote syncytial endurance, we could confirm the clustering of centrosomes, activation of the PIDDosome, and PIDDosome-dependent reduction in syncytial cell cycle progression also in B. thailandensis-mediated fusion events. Taken together, our results indicate that PIDDosome signaling can act as an important player in shaping the cellular fate after pathological cell-cell fusion events, allowing cells to arrest instead of die.

Robert Barket

Background: Since its first description in 2014, anti-IgLON5 disease has been recognized as a complex and heterogeneous neurological disorder combining sleep disturbances, movement disorders, and neuroimmunological as well as neurodegenerative features. With the continuously expanding spectrum of clinical manifestations, classification and recognition of the disease have become increasingly challenging. Therefore, the aim of this systematic review and meta-analysis was to comprehensively summarize the clinical spectrum of anti-IgLON5 disease, including laboratory findings, therapeutic approaches, and reported outcomes.

Methods: A systematic literature search was conducted in the electronic databases PubMed/MEDLINE, Web of Science, and Semantic Scholar. Case reports and case series describing patients with anti-IgLON5 disease were included. For quantitative synthesis in the meta-analysis, only case series comprising at least ten patients were considered.

Results: In total, 285 patients from 85 case reports and case series were included in this systematic review. A marked heterogeneity in clinical presentation was observed. Sleep-related abnormalities (N = 218; 76.5%) and bulbar dysfunction (N = 175; 61.4%) were the most frequently reported clinical features. Additional manifestations included movement disorders, cognitive impairment, autonomic symptoms, and other neurological signs. The meta-analysis demonstrated that IgLON5 antibodies were detectable in serum in up to 98% of patients.

Conclusion: Based on the findings of this systematic review, anti-IgLON5 disease should be considered in patients presenting with sleep disorders accompanied by additional neurological symptoms, particularly when the clinical picture mimics other neurological conditions but does not fully meet their diagnostic criteria or shows atypical features. Serum testing for IgLON5 antibodies shows high sensitivity in this disorder, suggesting that lumbar puncture is not necessarily required as an initial diagnostic step.

Post-stroke epilepsy

Luisa Delazer

Background: Post-stroke epilepsy (PSE) occurs in 2–14% of ischaemic stroke survivors and is associated with increased mortality and poorer functional recovery. Stroke incidence, severity, and aetiology differ by age and sex, potentially influencing PSE outcomes, yet demographic differences within PSE cohorts remain insufficiently explored.

Aim: To assess age- and sex-related differences in seizure presentation, stroke characteristics relevant to PSE risk, and mortality within a well-characterised PSE cohort.

Methods: We included consecutive people with ischaemic stroke at the University Hospital Innsbruck between 2014–2017 and 2020–2025 who developed PSE during a median follow-up of 40 months (range 1–146). Data on PSE onset (latency, seizure type), stroke severity, stroke aetiology, SeLECT score, and mortality were extracted from electronic medical records and analysed via univariable and multivariable regression models.

Results: Eighty-four individuals (46 men, 38 women; median age 72.4 years) with PSE were included. Latency to first unprovoked seizure (median 266 days) and seizure type did not differ by demographics. Women had more severe strokes and predominantly of cardioembolic aetiology (47%). Overall mortality was 33%; women showed 3.8-fold higher odds of mortality than men (OR 3.80; 95% CI 1.31–11.95; p=0.017), independent of age. Status epilepticus and focal to bilateral tonic-clonic seizure markedly elevated mortality risk (OR 4.23; 95% CI 1.38–14.81; p=0.016).

Conclusion: Age and sex are associated with distinct stroke characteristics and mortality in PSE. Women had more severe and predominantly cardioembolic strokes and substantially higher mortality, underscoring the need for sex-specific risk assessment and optimised prevention strategies.

Katharina Wagner

Impaired mitochondrial respiration in peripheral blood mononuclear cells of Post-COVID patients

Wagner K1, Kurz K1, Engl S1, Srinivasan N1, Weiss G1, Volani C1

1 Department of Internal Medicine II, Medical University of Innsbruck, Anichstrasse 35, 6020 Innsbruck, Austria

Background:

Post-COVID condition is characterized by persistent symptoms such as fatigue and post-exertional malaise (PEM), while its pathogenesis remains incompletely understood. Mitochondrial dysfunction has been proposed as a potential contributing mechanism. Therefore, mitochondrial respiration was assessed in peripheral blood mononuclear cells (PBMCs) from Post-COVID patients and healthy controls.

Methods:

PBMCs were isolated from 21 Post-COVID patients and 9 healthy controls. Mitochondrial respiration was assessed using the Seahorse XF Mito Stress Test, including basal and maximal respiration. In addition to cellular bioenergetic measurements, an extensive laboratory characterization was performed. Clinical assessment included standardized patient-reported measures of fatigue, post-exertional malaise, and somatic symptom burden.

Results:

Basal and maximal mitochondrial respiration were significantly lower in Post-COVID patients compared with healthy controls. In addition, mitochondrial respiratory parameters were significantly associated with symptom severity. Higher mitochondrial respiratory function was observed in patients with lower overall symptom burden, including less severe fatigue, post-exertional malaise, and somatic symptoms.

Conclusion

These findings indicate impaired mitochondrial respiration in PBMCs of Post-COVID patients, with respiratory parameters associated with symptom severity. Reduced basal and maximal oxygen consumption points to altered cellular bioenergetics and suggests a potential role of mitochondrial dysfunction in the pathophysiology of Post-COVID condition, with possible implications for the development of biomarkers and targeted therapeutic strategies.

Stefan Hardy Lung

Unbiased Long-Read Nanopore Sequencing Enables Scalable, End-to-End Quality Control and Capsid Library Profiling of Recombinant AAV Vectors

Recombinant adeno-associated viruses (rAAVs) are among the most widely used vectors for gene therapy, requiring stringent quality control to ensure vector integrity, safety, and therapeutic performance. Oxford Nanopore Technologies (ONT) sequencing enables unbiased, real-time analysis of native DNA and RNA and offers unique advantages for comprehensive rAAV characterization through long-read sequencing.

Here, we established ONT sequencing as a scalable, end-to-end platform for rAAV quality management and capsid library assessment. Genomic DNA from purified individual rAAV vectors and large, technically non-equimolar rAAV capsid libraries was directly sequenced using ONT native barcoding on MinION and PromethION P2 Solo devices. Following transduction of multiple cell lines, rAAV-derived transcripts were analyzed by ONT direct RNA sequencing as well as by cDNA sequencing using the PCR-cDNA Barcoding Kit V14, enabling a direct comparison of RNA- and cDNA-based approaches. All genomic DNA datasets were analyzed using the dedicated wf-aav-qm bioinformatic pipeline.

Long-read sequencing revealed no detectable backbone contamination from production plasmids and only minimal genome truncations, with a remarkably high proportion of full-length (ITR–ITR) rAAV genomes. Both direct RNA and cDNA sequencing confirmed accurate and reproducible transcription of the gene of interest across multiple cell lines. Importantly, ONT sequencing enabled precise quantification of inherently non-equimolar rAAV libraries, allowing high-resolution determination of capsid variant distributions and reliable identification of the desired rAAV capsid candidate.

In summary, ONT sequencing provides a robust, scalable, and comprehensive solution for rAAV quality control, transcript validation, and library screening, supporting accelerated vector development from discovery to production.

Lena Denk

Chronic cocaine use can lead to ischemic damage, osteonecrosis, and defects of the nasal and palatal regions. Because patients often conceal substance use, diagnosis may be delayed or complicated. We report the case of a patient who presented with a newly developed palatal defect accompanied by an oronasal fistula. Regular cocaine use was only disclosed after targeted questioning. Functional rehabilitation was achieved with a custom-made palatal obturator to close the defect, resulting in a marked improvement in quality of life. Although surgical reconstruction represents the definitive treatment option, it is not advisable without sustained abstinence. Cocaine-associated palatal defects are rare but should be considered in patients presenting with unexplained palatal lesions. Thorough medical history taking is essential, and prosthetic rehabilitation offers an effective interim solution. In addition, the repeated offer of addiction treatment during follow-up visits is of great importance.

Identification of the origin and fate of azole

Olayinka Ruth Bamidele

Background

Azole compounds are extensively used as antifungal compounds in both agricultural and pharmaceutical applications, yet data on their use and occurrence in Tyrol remain limited. To fill this gap, workflows employing targeted and non-targeted liquid chromatography-mass spectrometry (LC-MS) are being developed to detect, identify and quantify azoles across various matrices, with a particular focus on assessing potential human use and exposure.

Objectives / Aims:

Generate information on human use and exposure to azoles and other pesticides in Tyrol for the analysis of human and wastewater samples.

The specific aims of my work are:

- Compile a comprehensive list of compounds representing potential suspects/targets for LC-MS/MS analysis.
- Develop non-targeted and targeted LC-MS/MS workflows for the qualitative and quantitative analysis of azoles and other pesticides in human and wastewater samples.
- Analyse human and environmental samples.

Methods:

Information on the azoles used as pesticides, biocides, pharmaceuticals, and cosmetic ingredients were obtained from publications of the Fungicide Resistance Action Committee, from the Austrian Biocides Helpdesk, the Austrian Plant Protection Products Register, and the Austrian Medicinal Product Index. Pesticide sales data for Austria for the years 2022 and 2023 were kindly provided by the Bundesamt für Ernährungssicherheit.

Reference standards were purchased from certified suppliers (Sigma, LGC and Merck) and stored at -20 °C. Mixtures of reference compounds (10 µg/ml each) and serial dilutions thereof (0.2-100 ng/mL) were prepared from the obtained stock solutions and analysed with an established non-targeted LC-MSMS method.

Plasma samples and (waste)water samples were processed either with protein precipitation or solid-phase extraction. Spiked samples were used to evaluate the efficiency of the sample preparation methods tested.

Results:

More than 400 reference compounds, including all kinds of azoles used as pesticides, biocides, pharmaceuticals, and cosmetic ingredients, were analyzed with an established non-targeted LC-MS/MS method to verify their detectability. The observed retention times were used to establish a suspect list for screening applications.

The analysis of serial dilutions was further used to evaluate the limits of identification (LOI) of the non-targeted LC-MS/MS method. The observed LOI-values ranged from 0.2 to 20 ng/ml. The detection sensitivity should be sufficient to apply non-targeted LC-MS/MS for the analysis of clinical samples. For screening of pesticides in human and wastewater samples, however, targeted LC-MS/MS, which usually enables to reach lower limits of quantification, seems to be more appropriate.

Sample preparation will represent an integral step of the envisioned analytical workflows, serving as a means for the purification and concentration of analytes. The performance of established sample preparation workflows was evaluated. Protein precipitation is the method of choice for plasma samples, whereas solid-phase extraction will be applied for (waste)water samples.

Finally, the general usability of the screening workflow applied by the forensic casework unit for the detection of illegal drugs and pharmaceutical compounds was evaluated with regard to azole compounds. Although low recoveries were observed for some of the targeted analytes, retrospective analysis of already acquired data of already screened plasma appears to be a valuable additional source of information for gaining insights into local use and exposure to azoles.

Conclusion: Azoles used in Tyrol as pesticides, biocides, pharmaceuticals, and cosmetic ingredients have been identified and their principal detectability with non-targeted LC-MS/MS has been demonstrated. Furthermore, sample preparation methods for the efficient processing of plasma and (waste)water samples were identified. Thus, suitable workflows for screening analyses are available.

Keywords: Suspect screening, Solid-phase extraction, liquid chromatography-mass spectrometry

OUR SPONSORS

LIFE SCIENCE PHD MEETING 2026
08.-10. April

Promega

EVIDENT

SZABO SCANDIC
Part of Europa Biosite

Leica MICROSYSTEMS

fisher scientific
part of Thermo Fisher Scientific

OROBOROS INSTRUMENTS

THQ MEDICAL PRODUCTS

Microsynth AUSTRIA

SIEMENS Healthineers

XPseq Analytics

Miltenyi Biotec

MED EL

ZEISS

MACHEREY-NAGEL
www.mn-net.com

NEW ENGLAND Biolabs

eurofins

QIAGEN

Nikon